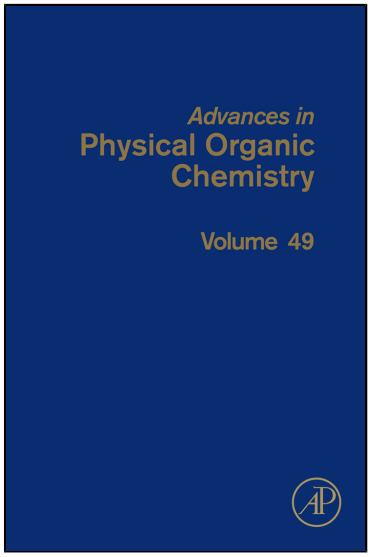




From Hayes CJ, Burgess Jr DR, Manion JA.
Combustion Pathways of Biofuel Model Compounds:
A Review of Recent Research and Current Challenges Pertaining to First-, Second-, and Third-Generation Biofuels. In: Williams IH, Williams NH, eds. *Advances in Physical Organic Chemistry*. 2015:103–187.
ISBN: 9780128022283

Academic Press

CHAPTER THREE

# Combustion Pathways of Biofuel Model Compounds: A Review of Recent Research and Current Challenges Pertaining to First-, Second-, and Third-Generation Biofuels

**Carrigan J. Hayes*[,1], Donald R. Burgess, Jr.[§], Jeffrey A. Manion[§]**
*Department of Chemistry, Otterbein University, Westerville, OH, USA
[§]Division of Chemical Sciences, National Institute of Standards and Technology, Gaithersburg, MD, USA
[1]Corresponding author: E-mail: chayes@otterbein.edu

## Contents



*Advances in Physical Organic Chemistry*, Volume 49
ISSN 0065-3160
http://dx.doi.org/10.1016/bs.apoc.2015.09.001





Advances in Physical Organic Chemistry, First Edition, 2015, 103–187

## Abstract

In this chapter, we present a review of recent research of interest to biofuel combustion. An overview of chemical kinetic mechanism development as it pertains to combustion chemistry is provided. We then discuss experimental and computational studies of the pyrolytic and oxidative pathways of model compounds of interest to the first-generation biofuels ethanol and biodiesel, along with an overview of current challenges in modeling these oxygenated compounds. We also describe experiments and calculations regarding reaction pathways of the small cyclic and bicyclic oxygenated systems used to model lignocellulosic (second-generation) biofuel chemistry, along with a summary of challenges in modeling these functionalized compounds. A general theme is the impact of the functional groups commonly found in first-generation and second-generation biofuels on thermochemistry and reaction pathways, compared with those of hydrocarbon fuels. We discuss recent progress with respect to third- and fourth-generation biofuels, as well as to biofuel combustion engineering challenges.

## 1. INTRODUCTION

Biofuels constitute an area of complex interest and intense debate from a variety of perspectives, including societal, economic, and environmental ones. Tilman et al.[1] acknowledged the "food, energy, and environment trilemma," calling for full consideration of production and combustion pathways in implementing policies related to biofuels, while Bryan[2] cited "the four horsemen of the biofuels apocalypse: sustainability, technology, profitability, and politics" in a recent American Chemical Society plenary lecture. Biofuels can be produced domestically, they are renewable fuels, and they have the potential for decreasing several harmful emissions, such as soot, carbon monoxide, and carbon dioxide. While hydrocarbon (HC) fuels such as gasoline and oil are still predicted to dominate energy needs in the transportation sector for the immediate future,[3,4] the uses of oxygenated biofuels as blends with these petroleum-based fuels and as fuels in their own right have seen an enormous increase in research interest recently.[5]

From the perspective of a physical organic chemist, some key topics of interest related to alternative fuels involve the impacts that different

functional groups have on different types of biofuels and their combustion reactions. Petroleum-based fuels consist of saturated HC species; for instance, the primary reference fuel mechanism commonly used to model gasoline chemistry relies on mechanisms of *n*-heptane[6] and *iso*-octane.[7] Alternative fuels, conversely, are typically functionalized species; for instance, the two main alternative fuels currently in use[5] are ethanol (derived from biomass) and biodiesel (generally produced from the transesterification of vegetable oils and animal fats, and consisting of a mixture of long-chain methyl esters). Representative compounds are shown in Figure 1. Moreover, a number of other biomass-derived fuels are in development and contain a variety of functional groups; reactive intermediates derived from these fuels will differ in chemical makeup as well.

Graboski and McCormick[8] published a seminal review on biodiesel combustion in 1998. In the nearly two decades since, many reviews have investigated several current perspectives on biofuels. For instance, Huber et al.[9] reviewed overall progress in converting biomass to transportation fuels, while Naik et al.[10] provided an overview of production pathways to first- and second-generation biofuels. Kohse-Hoinghaus et al.[11] have provided a thorough overview of biofuels from ethanol to biodiesel; they acknowledged the extreme variability of the word "biofuel," noting the impact of a fuel's chemical structure on its reactivity and potential emissions. Lai et al.[12] reviewed advances in modeling biodiesel via the use of smaller methyl esters, while Tran et al.[13] reviewed several oxygenated biofuel models and proposed reaction classes and properties likely to be of interest

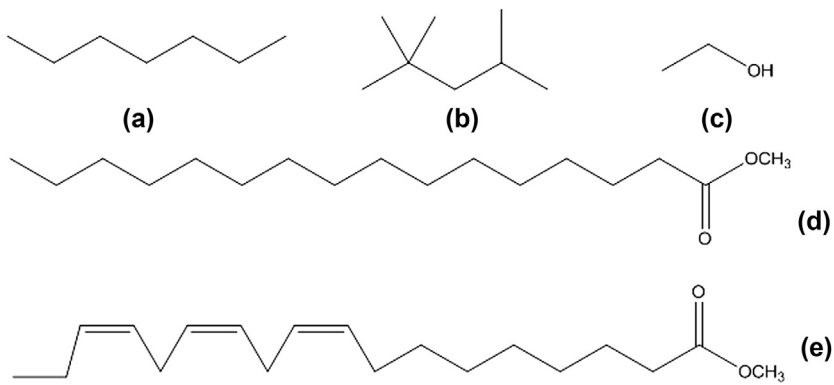


**Figure 1** Compounds seen in gasoline combustion (a,b) and alternative fuel combustion (c,d,e): (a) *n*-heptane, (b) *iso*-octane, (c) ethanol, (d) methyl palmitate, (e) methyl linolenate.

in subsequent studies. Nigam and Singh[14] reviewed production pathways to liquid biofuels. Battin-Leclerc et al. reviewed chemical kinetic mechanisms of interest to improving engine performance.[15] Westbrook[5] reviewed biofuel combustion in different types of combustion engines. Bergthorson and Thomson[16] reviewed the impact of biofuels on possible emissions and engine performance. Dryer recently discussed historical and current fuel combustion concerns and provided an overview of useful diagnostics for evaluating alternative fuels relative to HC fuels.[17]

## 1.1 Kinetic Mechanisms

Detailed chemical kinetic mechanisms provide the link between discrete experiments or computational studies and overall behavior of a given fuel; they allow simulation of fuel performance and combustion behavior. These mechanisms are files of enormous use to combustion chemists and differ from the electron-pushing mechanisms of traditional organic chemistry. It will be useful to first define a detailed chemical kinetic mechanism in the specific context of combustion chemistry.

Senkan[18] more than two decades ago provided what is still a useful overview of mechanism development, delineating how experiment and theory are used to compile the thermochemical and kinetic data that contribute to a detailed chemical kinetic mechanism. While more automated methods have since become available, the underlying principles remain the same. More recently, Frenklach in 2007 has provided an excellent discussion of the pertinent vocabulary.[19] For instance, in the case of methane, the *general mechanism* of combustion is well established; the general process by which methane reacts with oxygen to form carbon dioxide and water is accomplished via several steps. Methane first loses hydrogen atom via reaction with a flame species such as OH to form methyl radical ($CH_3$). Methyl radical is oxidized to formaldehyde ($CH_2O$), which is converted to carbon monoxide (CO) and finally oxidized to carbon dioxide ($CO_2$). The *detailed mechanism* for methane combustion is then the set of specific elementary reactions, which together describe the general mechanism. When combined with their parameterized rate coefficients and species thermochemical information (enthalpies of formation, entropies, heat capacities), these elementary reactions allow one to describe the physical (e.g., temperature and pressure) and chemical evolution of the system: this is the *mathematical model*. Finally, the mathematical model can be used with a set of initial and boundary conditions to yield a *predictive model* that can describe how a fuel will perform within the range of conditions defined by the parameters.

Detailed chemical kinetic mechanisms describe the *chemistry* of the system at a *microscopic* level. When used in tandem with a transport model, a simulation of *macroscopic* behavior (such as fuel performance in an engine or a similarly complex combustion environment) can be obtained. Advances in computational software[20] now allow efficient mathematical and predictive modeling of engine/fuel performance, given the detailed mechanism,[31] which can be used with modeling software to simulate the performance of an engine with a given fuel. To return to the terms from Frenklach's review, once a detailed mechanism is obtained for a fuel, engine performance (or performance of a reactor) with that fuel can be simulated; the software package generates the mathematical model necessary to provide the predictive model.

Kinetic information in a detailed mechanism is summarized via three Arrhenius parameters: $A$, the preexponential factor; $n$, a temperature dependence factor; and $E_A$, the activation energy. Together these yield a rate coefficient $k$ (Eqn (1)) for a given elementary reaction:

$$k(T) = AT^n e^{(-E_A/RT)} \tag{1}$$

Thermochemical information is also included in a detailed mechanism to compute the reverse reactions of those provided in the mechanism, and transport coefficients are used to model the diffusion of species in the flame or reactor.

No single, universally accepted detailed mechanism exists for most fuels. In part this is because mechanisms are often created and validated for particular combustion regions: those focused on ignition will be sensitive to chemistry that is different from that of high-temperature oxidation under lean conditions, models designed to describe heat release may not require a description of soot formation, and so forth. In addition, model development is usually iterative, and it is common for new reactions to be added and rate constants refined as knowledge of a system expands. This complexity can lead to difficulties in selecting the "best" model of a fuel system. Efforts such as the Process Informatics Model[19] are intended to address this problem by facilitating comparisons and useful evaluations of data and existing detailed mechanisms. A further obstacle arises from the multiscale nature of combustion, which requires contributions from multiple research groups and institutions and a range of scientific disciplines; a complementary challenge thus becomes effective and timely communication. Many collaborative efforts are underway to address these issues. In particular, the communication efforts useful in chemical kinetics mechanism development

are facilitated via both the development of shared databases and combustion resources,[21–26] as well as by the creation of a systematic and standardized nomenclature.[27–30]

This particular review will report mainly on recent efforts to obtain the data necessary to generate detailed chemical kinetic mechanisms: that is, cataloging the experiments and computational studies that yield the kinetic and thermodynamic parameters for detailed mechanisms for oxygenated biofuels. Before we describe these research efforts, we will define a few additional terms that may be useful in understanding specific experiments, mechanism development, and combustion chemistry.

## 1.2 Experimental Techniques

In terms of understanding fuel combustion, several experimental approaches are commonly used for evaluating combustion processes and species, including static reactors, stirred reactors, plug-flow reactors, shock tubes, laminar flames, and rapid compression machines (RCMs).[31,32] *Static, stirred, and plug-flow reactors* usually involve the introduction of the mixture to be studied into a metal or quartz reactor at a specified time. Kinetic and mechanistic information are then determined by following time histories of product formation at various temperatures. In static systems there is no flow; stirred reactors can utilize an impeller in a static system but more commonly utilize the rapid flow of a gas mixture through a bulb, with the flow pattern designed to create a homogenous mixture within the bulb, as in a *jet-stirred reactor* (JSR).[33] Product formation at various average residence times and temperatures is used to determine the kinetic and mechanistic information. Plug-flow reactors use narrow-bore tubes and flow rates such that there is a correspondence of distance and reaction time. Timescales in reactor studies are typically in the range of a few tenths to perhaps a few hundred seconds.

A general drawback of reactors is that the molecules have time to migrate to the hot surfaces of the reactor and undergo heterogeneous reactions, thus preventing isolation of the gas-phase processes. This problem is avoided in *shock tubes*, which use a shock wave to nearly instantaneously compress and heat a reaction mixture of interest to temperatures in the range of 800–2000 K. Reexpansion of the gas, after typically 300–1000 μs, then recools the system and quenches reaction. Timescales are so short that the material does not have time to diffuse to the cold walls of the reactor, thus allowing gas-phase reactions to be isolated. Shock tubes are in some cases used to isolate individual reactions for study, but they are also ideal for determining global properties of interest, such as ignition delay times

of mixtures at various temperatures, pressures, and fuel equivalence ratios. An RCM[34] is used to simulate under controlled conditions the pressure and temperature changes in an engine. RCMs are similar in some respects to shock tubes, but compress the mixture more slowly and lead to lower reaction temperatures. They are most often used for the complementary study of ignition delay times at temperatures lower than those possible with shock tubes. Flames are also studied directly. *Laminar flames* are often used to determine the flame speed of a combustible mixture, which is the rate at which a flame will propagate. A flame is operated at low-pressure conditions and a reaction mixture of interest flows through it; the burning velocity and temperature can be monitored.[31] Finally, speciation data are also obtainable in various types of flames, including *Low Pressure Flat Flames*, *Low Pressure Diffusion Flames*, and *Opposed Flow Diffusion Flames*. These flames are all designed to present stable temperature and species concentration profiles that typically vary only along a single dimension, which is then probed using optical or micro-probe sampling techniques.[101,351]

Detection methods vary with the timescales of the reactions of interest and include pressure measurements, spectroscopy, gas chromatography, and mass spectrometry.[35] Both real-time and postreaction methods are used; real-time detection is particularly useful for short-lived intermediates and can enable a very direct probe of the reaction kinetics, but, compared with postreaction methods, is often quite limited in the number and types of species that can be detected and identified with certainty. Of particular interest in biofuel mechanistic studies are methods capable of discerning between reactive isomers, such as photoionization molecular beam mass spectrometry.[36]

## 1.3 Computational Techniques

With advances in computational speed, theoretical methods[37,38] are often used to explore specific reactions of interest; certain composite ab initio methods and density functional theory (DFT) achieve a good balance of computational expense and quantitative accuracy and have often been proved to be useful in investigating the model systems summarized in this review. In general, an appropriate computational method for a given investigation is selected via consideration of what techniques have previously worked with similar systems and calibration against known experimental data. A useful resource is the National Institute of Standards and Technology (NIST) Computational Chemistry Comparison and Benchmark Database,[39] which provides direct comparisons of computed and experimental data for a variety of species and methods. *Ab initio methods*[40] are those that utilize the Schrödinger equation

and some level of approximation to solve the wave function of a chemical species and obtain the energy; composite ab initio methods in particular approach this challenge via a set of stepwise corrections to a computationally efficient geometry optimization. In *DFT methods*,[41] the properties of a molecule are calculated via extrapolation from its electron density; the experimentally observable electron density is itself a function of position [ρ(x,y,z)], and the energy is a functional of the electron density (E[ρ]).[37]

Briefly, via an electronic structure calculation, the minimum energy conformation of a chemical species can be identified, and its electronic energy and vibrational frequencies can be calculated. Thus, thermodynamic quantities such as enthalpy ($H$), entropy ($S$), and Gibbs free energy ($G$) can be extrapolated. If such analyses are repeated for the reactant, transition state, and product for a discrete reaction step, a reaction coefficient [$k(T)_{\mathrm{TST}}$] can be generated (Eqn (2)) via transition state theory (TST),[42] as a function of the free energy reaction barrier ($\Delta G_0^{\neq}$), Planck's constant ($h$), Boltzmann's constant ($k_B$), temperature ($T$), and the Wigner approximation [$\Gamma(T)$],[43] which itself depends on the imaginary vibrational frequency ($\nu_i$) corresponding to the transition state (Eqn (3)).

$$k(T)_{\mathrm{TST}} = \Gamma(T)\frac{k_B T}{h} e^{\left[-\Delta G_0^{\neq}/(k_B T)\right]} \tag{2}$$

$$\Gamma(T) = 1 + \frac{1}{24}\left(\frac{h\nu_i}{k_B T}\right)^2 \tag{3}$$

TST calculations apply in the high-pressure limit; pressure-dependent reactions can be analyzed via more complex kinetic analyses such as Rice–Ramsperger–Kassel–Marcus (RRKM) theory. The RRKM theory is used to model the energy transfer in the transition state (or activated complex) of a molecule, using statistical mechanical methods that describe the density of energy states, which depend upon the vibrational and rotational partition functions for the molecule.[44]

When rate coefficients are analyzed as a function of temperature, two- and three-parameter Arrhenius expressions can be obtained (Eqns (1) and (4)); as seen previously (Eqn (1)), the parameters from the latter are the data most commonly summarized in detailed mechanisms. In Arrhenius theory, the rate coefficient $k(T)$ is expressed as a function of activation energy ($E_A$), preexponential factor ($A$), temperature dependence factor ($n$), the gas constant ($R$), and the temperature ($T$).

$$k(T) = Ae^{(-E_A/RT)} \tag{4}$$

In addition to kinetic parameters, thermodynamic quantities can also be calculated via electronic structure methods. In particular, isodesmic reactions (in which the same numbers and types of bond are conserved) and isogyric reactions (in which the total number of electron pairs is conserved) are often used to determine reliable enthalpies of formation for previously unexplored species.[38]

## 1.4 Simplifying Detailed Mechanisms

Detailed chemical kinetic mechanisms quickly become large and unwieldy. Hudgens et al.[45] illustrated how increasing the complexity of a fuel increases the corresponding complexity of that fuel's chemical kinetic mechanism: to model the oxidation of hydrogen, eight species and 27 reactions are used; for the oxidation of methane, 34 species and 210 reactions are needed; and for the oxidation of *iso*-octane, 860 species and 3600 reactions are required. Furthermore, of interest to biofuel chemistry, Dryer[17] addressed the likelihood that the complex chemical makeup of alternative fuels will lead to significantly different chemical and physical properties of these fuels. Westbrook[5] noted that the presence of the ester functionality and the double bonds common in the long side chains of fatty acid methyl esters have impacts on biodiesel combustion. Moreover, the possibility of isomeric fuels and intermediates are likely to have significant impacts in terms of their properties and reactivity for alternative fuels; Kohse-Hoinghaus et al.[11] provided an instructive example in comparing two simple compounds: ethane, in which abstraction of any hydrogen atom yields the same ethyl radical, and ethanol, in which three isomeric radicals are possible from hydrogen atom abstraction: 1-hydroxyethyl, 2-hydroxyethyl, or ethoxy radical.

Methods exist to simplify mechanism development. As described by Westbrook and Dryer,[46] this process can be systematized by acknowledging the hierarchical nature of fuel combustion. For instance, in the combustion of ethanol, several smaller species are involved, such as $H_2$, CO, formaldehyde, methane, ethane, ethene, and acetylene. The combustion mechanisms of these species can thus be used to build the detailed mechanism of ethanol combustion. Sensitivity and reaction path analyses are tools that allow key reactions in a detailed chemical kinetic mechanism to be identified.[31] The former highlights the reactions most likely to dictate overall fuel reaction rate, whereas the latter identifies key reactions by which a chemical species of interest is formed and consumed. As needed, these analyses are sometimes used to generate skeletal mechanisms, in which species and reactions unlikely to play a major role are removed from consideration, and reduced

mechanisms, which are further simplified via application of steady-state assumptions.[31]

Perhaps most pertinent to this review, model compounds play an integral role in the development of detailed chemical kinetic mechanisms. For instance, *n*-propylperoxy,[47] 1-butoxy radical,[48] and *n*-pentyl[49,50] radical are, respectively, the simplest alkylperoxy radical, alkoxy radical, and alkyl radical capable of undergoing facile 1,5-H atom transfers (each via a favorable six-membered-ring transition state, as illustrated in Figure 2). Thus, these smaller systems are commonly used as models to investigate the comparable isomerizations possible in the larger radical, oxy radical, and peroxy radical species that are involved in HC fuel combustion.

It is evident that species involved in biofuel combustion will require different model compounds than those involved in HC fuel combustion. An important topic of investigation for the combustion chemistry community is how much the available data pertinent to HC combustion will overlap with the data necessary for modeling alternative fuel combustion. In the past few years, model compounds for alternative fuels have seen significantly increased interest from computational and experimental perspectives; Lai et al.[12] and Tran et al.[13] have provided informative reviews in this regard. Within the past few years, in particular, a variety of model compounds have been investigated in the hope of better understanding first- and second-generation biofuels.

As representative examples, Tables 1 and 2 provide a small portion of a detailed mechanism[51] for ethanol combustion: ethanol is the simplest biofuel species explored in this review. The kinetic parameters for reactions pertaining to the chemistry of ethanol in a flame (the ethanol submechanism) are shown in Table 1, while the thermochemical quantities for species involved in this submechanism are included in Table 2. As can be seen, accurately describing the chemistry of even a few chemical species requires dozens of elementary reaction steps. Moreover, as described above, a full detailed chemical kinetic mechanism for ethanol[51] will also involve hundreds of other reactions for hydrogen/oxygen species; C1, C2, and C3 HC chemistry; and oxidative reactions involving C1, C2, and C3 HCs.

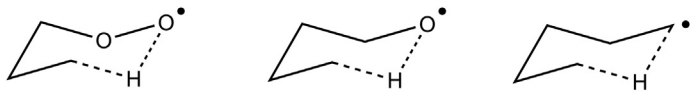


**Figure 2** The figure shows 1,5-H atom transfers in (from left) *n*-propylperoxy radical, 1-butoxy radical, and *n*-pentyl radical, used to investigate the corresponding isomerizations in larger alkylperoxy radicals, alkoxy radicals, and alkyl radicals, respectively.

**Table 1** Ethanol subset of reaction mechanism rate coefficients [$k = A\,T^n \exp(-E_A/RT)$]. Units are expressed in mol, $cm^3$, s, K, and kJ $mol^{-1}$

| | *A* | *n* | $E_A$ |
|---|---|---|---|
| ***Ethanol reactions*** | | | |
| $C_2H_5OH(+M) = CH_2OH + CH_3(+M)$ | 5.94E+23 | −1.68 | 21.8 |
| $C_2H_5OH(+M) = C_2H_5OH(+M)$ | 1.25E+23 | −1.54 | 22.9 |
| $C_2H_5OH(+M) = C_2H_4 + H_2O(+M)$ | 2.79E+13 | 0.09 | 15.8 |
| $C_2H_5OH(+M) = CH_3CHO + H_2(+M)$ | 7.24E+11 | 0.095 | 21.8 |
| $C_2H_5OH + OH = C_2H_4OH + H_2O$ | 1.74E+11 | 0.27 | 0.1 |
| $C_2H_5OH + OH = CH_3CHOH + H_2O$ | 4.64E+11 | 0.15 | 0 |
| $C_2H_5OH + OH = CH_3CH_2O + H_2O$ | 7.46E+11 | 0.3 | 0.4 |
| $C_2H_5OH + H = C_2H_4OH + H_2$ | 1.23E+07 | 1.8 | 1.2 |
| $C_2H_5OH + H = CH_3CHOH + H_2$ | 2.58E+07 | 1.65 | 0.7 |
| $C_2H_5OH + H = CH_3CH_2O + H_2$ | 1.50E+07 | 1.6 | 0.7 |
| $C_2H_5OH + O = C_2H_4OH + H_2O$ | 9.41E+07 | 1.7 | 1.3 |
| $C_2H_5OH + O = CH_3CHOH + H_2O$ | 1.88E+07 | 1.85 | 0.4 |
| $C_2H_5OH + O = CH_3CH_2O + H_2O$ | 1.58E+07 | 2 | 1.1 |
| $C_2H_5OH + CH_3 = C_2H_4OH + CH_4$ | 2.19E+02 | 3.18 | 2.3 |
| $C_2H_5OH + CH_3 = CH_3CHOH + CH_4$ | 7.28E+02 | 2.99 | 1.9 |
| $C_2H_5OH + CH_3 = CH_3CH_2O + CH_4$ | 1.45E+02 | 2.99 | 1.8 |
| $C_2H_5OH + HO_2 = C_2H_4OH + H_2O_2$ | 1.23E+04 | 2.55 | 3.8 |
| $C_2H_5OH + HO_2 = CH_3CHOH + H_2O_2$ | 8.20E+03 | 2.55 | 2.6 |
| $C_2H_5OH + HO_2 = CH_3CH_2O + H_2O_2$ | 2.50E+12 | 0 | 5.7 |
| ***Ethoxy reactions*** | | | |
| $CH_3CH_2O + M = CH_3CHO + H + M$ | 1.16E+35 | −5.89 | 6.0 |
| $CH_3CH_2O + M = CH_3 + CH_2O + M$ | 1.35E+38 | −6.96 | 5.7 |
| $CH_3CH_2O + CO = C_2H_5 + CO_2$ | 4.68E+02 | 3.16 | 1.3 |
| $CH_3CH_2O + O_2 = CH_3CHO + HO_2$ | 4.00E+10 | 0 | 0.3 |
| $CH_3CH_2O + H = CH_3 + CH_2OH$ | 3.00E+13 | 0 | 0 |
| $CH_3CH_2O + H = C_2H_4 + H_2O$ | 3.00E+13 | 0 | 0 |
| $CH_3CH_2O + OH = CH_3CHO + H_2O$ | 1.00E+13 | 0 | 0 |
| ***1-Hydroxyethyl reactions*** | | | |
| $CH_3CHOH + O_2 = CH_3CHO + HO_2$ | 4.82E+14 | 0 | 1.2 |
| $CH_3CHOH + CH_3 = C_3H_6 + H_2O$ | 2.00E+13 | 0 | 0 |
| $CH_3CHOH + O = CH_3CHO + OH$ | 1.00E+14 | 0 | 0 |
| $CH_3CHOH + H = CH_3 + CH_2OH$ | 3.00E+13 | 0 | 0 |
| $CH_3CHOH + H = C_2H_4 + H_2O$ | 3.00E+13 | 0 | 0 |
| $CH_3CHOH + HO_2 = CH_3CHO + OH + OH$ | 4.00E+13 | 0 | 0 |
| $CH_3CHOH + OH = CH_3CHO + H_2O$ | 5.00E+12 | 0 | 0 |
| $CH_3CHOH + M = CH_3CHO + H + M$ | 1.00E+14 | 0 | 6.0 |
| ***Ethanal reactions*** | | | |
| $CH_3CHO + OH = CH_3CO + H_2O$ | 9.24E+06 | 1.5 | −0.2 |
| $CH_3CHO + OH = CH_2CHO + H_2O$ | 1.72E+05 | 2.4 | 0.2 |

(*Continued*)

**Table 1** Ethanol subset of reaction mechanism rate coefficients [$k = A\,T^n \exp(-E_A/RT)$]. Units are expressed in mol, $cm^3$, s, K, and kJ $mol^{-1}$—cont'd

| | *A* | *n* | $E_A$ |
|---|---|---|---|
| $CH_3CHO + OH = CH_3 + HCOOH$ | 3.00E+15 | −1.076 | 0 |
| $CH_3CHO + O = CH_3CO + OH$ | 1.77E+18 | −1.9 | 0.7 |
| $CH_3CHO + O = CH_2CHO + OH$ | 3.72E+13 | −0.2 | 0.8 |
| $CH_3CHO + H = CH_3CO + H_2$ | 4.66E+13 | −0.35 | 0.7 |
| $CH_3CHO + H = CH_2CHO + H_2$ | 1.85E+12 | 0.4 | 1.3 |
| $CH_3CHO + CH_3 = CH_3CO + CH_4$ | 3.90E - 07 | 5.8 | 0.5 |
| $CH_3CHO + CH_3 = CH_2CHO + CH_4$ | 2.45E+01 | 3.15 | 1.4 |
| $CH_3CHO + HO_2 = CH_3CO + H_2O_2$ | 2.40E+19 | −2.2 | 3.4 |
| $CH_3CHO + HO_2 = CH_2CHO + H_2O_2$ | 2.32E+11 | 0.4 | 3.6 |
| $CH_3CHO + O_2 = CH_3CO + HO_2$ | 1.00E+14 | 0 | 10.1 |
| ***2-Ethanoyl reactions*** | | | |
| $CH_2CHO + H = CH_3 + HCO$ | 5.00E+13 | 0 | 0 |
| $CH_2CHO + H = CH_2CO + H_2$ | 2.00E+13 | 0 | 0 |
| $CH_2CHO + O = CH_2O + HCO$ | 1.00E+14 | 0 | 0 |
| $CH_2CHO + OH = CH_2CO + H_2O$ | 3.00E+13 | 0 | 0 |
| $CH_2CHO + O_2 = CH_2O + CO + OH$ | 3.00E+10 | 0 | 0 |
| $CH_2CHO + CH_3 = C_2H_5 + CO + H$ | 4.90E+14 | −0.5 | 0 |
| $CH_2CHO + HO_2 = CH_2O + HCO + OH$ | 7.00E+12 | 0 | 0 |
| $CH_2CHO + HO_2 = CH_3CHO + O_2$ | 3.00E+12 | 0 | 0 |
| $CH_2CHO = CH_3 + CO$ | 1.17E+43 | −9.83 | 10.5 |
| $CH_2CHO = CH_2CO + H$ | 1.81E+43 | −9.61 | 11.0 |

Data excerpted from Ref. 51.

## 1.5 High- and Low-Temperature Oxidation Pathways

Combustion chemistry is commonly classified in three temperature regimes: low temperature ($T \sim 298$−$550$ K), the negative temperature coefficient (NTC) range (550−700 K), and high temperature ($T > 1000$ K). Different reaction pathways dominate in each range. As combustion temperatures are reduced, reaction pathways increasingly merge with the low-temperature oxidation chemistry of the atmosphere, whereas as one enters the NTC

**Table 2** Thermochemical quantities for species seen in the excerpted ethanol mechanism in Table 1. Enthalpies of formation at 298.15 K [$\Delta H_f(298)$, kJ $mol^{-1}$], standard-state entropies at 298.15 K [$S_m^\circ$, (J $mol^{-1}$ $K^{-1}$)], and heat capacities as a function of temperature [$C_p(T)$, (J $mol^{-1}$ $K^{-1}$)]

| Species | $\Delta H_f(298)$ | $S(298)$ | $C_p(300)$ | $C_p(400)$ | $C_p(500)$ | $C_p(600)$ | $C_p(800)$ | $C_p(1000)$ | $C_p(2500)$ |
|---|---|---|---|---|---|---|---|---|---|
| $C_2H_5OH$ | −234.9 | 280.5 | 65.6 | 80.8 | 95.6 | 108.6 | 128.0 | 142.9 | 165.4 |
| $CH_3CH_2O$ | −17.2 | 260.3 | 58.9 | 74.1 | 87.2 | 98.4 | 116.1 | 128.9 | 147.8 |
| $CH_3CHOH$ | −43.1 | 262.3 | 61.3 | 73.8 | 85.2 | 95.6 | 112.9 | 126.1 | 145.3 |
| $CH_2CHO$ | 25.1 | 267.8 | 55.1 | 63.4 | 71.0 | 77.8 | 89.1 | 97.7 | 110.2 |

Data excerpted from Ref. 51.

and high-temperature regions, the chemistry progressively involves species and higher-energy reactions that are not accessible at low temperatures. Reaction pathways from all three regimes are typically included in detailed chemical kinetic mechanisms.

At low temperatures, when an alkyl radical (R) is formed, it can add molecular oxygen to form an alkylperoxy radical (ROO), opening up several reaction pathways (Figure 3), including isomerizations, eliminations, and bond scissions. Rules for estimating kinetic parameters for these reactions in HC fuels were recently refined by Villano et al.,[52,53] using composite CBS-QB3 calculations; they cited the advance of new fuels and new engine technologies as likely to require increasing mechanistic explorations and insights.

As temperature increases past 550 K, increasing the combustion temperature actually decreases the reaction rate; the range in which this occurs is the NTC regime. This happens because of the complicated temperature dependence of reactions involving alkylperoxy radicals (ROO), which are themselves formed through the reaction of HC radicals (R) with oxygen ($R + O_2 = ROO$). The stability and reactivity of peroxy radical species strongly depend on temperature and pressure effects.[54]

Finally, at high temperatures (over 1000 K), oxidation typically begins with hydrogen atom abstraction by oxygen atom, hydroxyl radical, or hydrogen atom (all of which are common species in flames). As described by Glassman, a simplified scenario can be considered for high-temperature methane oxidation (Eqns (5)–(13)).[55]

$$CH_4 + M \rightarrow CH_3 + H + M \tag{5}$$

$$CH_4 + X \rightarrow CH_3 + XH \tag{6}$$

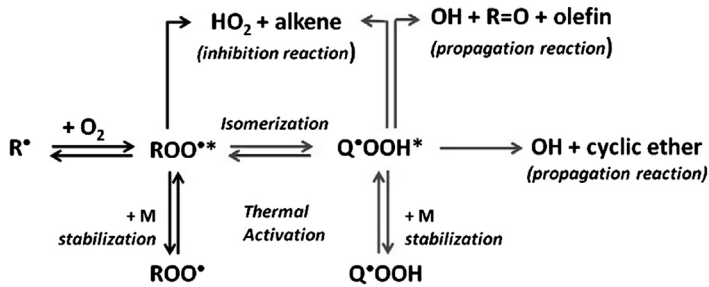


**Figure 3** Low-temperature combustion pathways available to a reactive radical species R, itself formed by hydrogen atom abstraction from parent molecule RH. Both the resulting peroxy radical (ROO) and isomerization product radical (QOOH) are capable of undergoing subsequent reaction pathways with implications for combustion processes. *Reprinted with permission from Villano et al.[52] Copyright 2012 American Chemical Society.*

$$CH_3 + O_2 \rightarrow CH_3O + O \quad (7)$$

$$CH_3 + O_2 \rightarrow H_2CO + OH \quad (8)$$

$$CH_3O + M \rightarrow H_2CO + H + M \quad (9)$$

$$H_2CO + X \rightarrow HCO + XH \quad (10)$$

$$HCO + M \rightarrow H + CO + M \quad (11)$$

$$CH_3 + CH_3 \rightarrow C_2H_6 \quad (12)$$

$$CO + OH \rightarrow CO_2 + H \quad (13)$$

The chemistry is clearly complex; most pertinently, a methyl radical can be oxidized by flame species to formaldehyde either directly or via a methoxy radical intermediate (Eqns (7)–(9)). Subsequent hydrogen atom abstraction yields formyl radical (Eqn (10)); once collisionally stabilized, formyl radical can form CO (Eqn (11)) and, presuming complete combustion, it ultimately reacts to form $CO_2$ (Eqn (13)). The methyl radical intermediate, alternatively, can combine with another methyl radical to form ethane (Eqn (12)), which can then yield ethyl radicals by chemically activated C–H bond fission or via H atom abstraction, opening up a wide variety of side reactions. (In unsaturated systems common to HC fuel combustion, another common initiation step involves addition of a reactive flame species to a double bond to yield a radical center.)

As a fuel becomes larger and/or more functionalized, the properties and reaction pathways of the resulting radicals and peroxy radicals are likewise more varied. For instance, comparing the cyclic ether tetrahydropyran (THP) to its HC analog cyclohexane (Figure 4), it is evident that three isomeric radicals are possible from the former, relative to only one in the latter; moreover, each of these three THP-derived radicals can proceed to

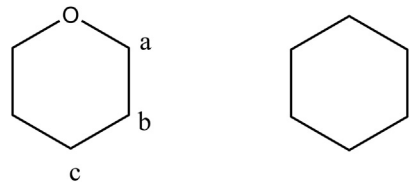


**Figure 4** Impact of a heteroatom on initial fuel reactivity. Three isomeric radicals can be formed via hydrogen atom abstraction from THP, at positions a, b, or c. In the HC analog, cyclohexane, abstraction of hydrogen atom from any position would yield cyclohexyl radical.

its own distinct set of radical pathways. Combustion pathways are of interest for biofuel model compounds, and the presence of a functional group increases significantly the number of possible isomeric reactive radicals and subsequent reactions.

## 1.6 Atmospheric Chemistry

Topics of interest to low-temperature combustion overlap with those of interest to atmospheric chemistry, given the oxidative environment of the troposphere. A number of general resources are available. The NIST Chemical Kinetics Database[24] provides a compilation of gas phase kinetic data, including both atmospheric and combustion chemistry. Specific to atmospheric chemistry are comprehensive reviews and resources by Monks,[56] Atkinson and Arey,[57] and Finlayson-Pitts and Pitts,[58] as well as the National Aeronautics and Space Administration/Jet Propulsion Lab database on chemical kinetics and atmospheric chemistry,[59] the International Union of Pure and Applied Chemistry Task Group on Atmospheric Chemical Kinetic Data Evaluation,[60] and the Master Chemical Mechanism[61] at Leeds.

Alternative fuels are expected to have different environmental impacts than HC fuels, in terms of common emissions. For instance, soot arises via incomplete combustion processes leading to the formation of polycyclic aromatic HCs; it has a variety of adverse environmental and health effects.[62,63] Oxygenated biofuels have been shown to decrease soot relative to HC fuels: the presence of an oxygen atom in the fuel leads to the availability of less carbon for sooting pathways.[64] Omidvarborna et al.[65] reviewed specific sooting pathways in diesel and biodiesel. However, biofuels also have been shown to lead to greater $NO_x$ formation; these emissions lead to acid rain formation and have been shown to have many adverse health effects. Mueller et al.[66] have explored the mechanism of increased $NO_x$ formation in biofuels and suggested that it is due to a complex interplay of coupled mechanisms, which can be investigated from many perspectives.[16] Early formation of carbon dioxide[64] in biodiesel combustion has been noted and attributed to the methyl ester moiety, which can decompose to methoxyformyl radical and subsequently to $CO_2$. Biofuels are also likely to lead to greater emissions of aldehydes,[67] which have been implicated in the formation of peroxyacetyl nitrate[58]; this species can transport $NO_x$, act as a lachrymator, and contribute to smog formation. From even this cursory overview, it is evident that the presence of a functional group can have complex beneficial and harmful effects on the atmospheric chemistry of a given biofuel, relative to a HC fuel. These pathways likewise constitute a relatively new area of investigation for the combustion community.

We have focused thus far on the general pathways and challenges of combustion chemistry, which are most well understood in the context of HC fuel combustion. The remainder of this chapter will focus on recent research exploring biofuel combustion chemistry. In particular, we will document recent work toward understanding reactive pathways of first- and second-generation biofuels and their model compounds, to better understand the chemical and physical properties of these species, along with their reactions with implications for fuel combustion and atmospheric chemistry. In the context of the introduction, we will summarize recent experiments and calculations that will be of use in generating detailed chemical kinetic mechanisms for oxygenated biofuels. We will also provide an overview of third- and fourth-generation biofuels, and we will close with an overview of the environmental, practical, and engineering aspects of these fuels.

## 2. OVERVIEW OF FIRST-GENERATION BIOFUELS AND THEIR MODEL COMPOUNDS

The so-called first-generation biofuels are those that compete with the food cycle for land, water, and other resources. Ethanol and biodiesel are the main examples, although in both cases there are efforts to develop methods for obtaining the same fuels from sources that would not impact the food chain. Several excellent previous reviews that address the chemistry of first-generation biofuels are available; these include, for ethanol and other alcohols, the 2014 review of Sarathy et al.,[68] and, for biodiesel, reviews by Lai et al.[12] in 2011, and by Coniglio et al.[69] and Westbrook[5] in 2013.

### 2.1 Combustion Pathways of Ethanol

#### *2.1.1 Unimolecular Decomposition of Ethanol*

Ethanol is one of the smallest fuel molecules, and its unimolecular decomposition has been studied both experimentally and theoretically by many researchers. The early literature has been thoroughly reviewed in the late 1990s and the early 2000s by Marinov,[51] Park et al.,[70] Li et al.,[71] and Tsang.[72] Baulch et al.[73] have also reviewed and evaluated data through 2001 on many of the relevant reactions in their series on evaluated kinetic data for combustion modeling.

Egolfopolous et al.[74] developed an early combustion model for ethanol in 1992, and Marinov[51] assembled a more comprehensive version in 1999. Park et al.[70] looked in detail at ethanol decomposition reactions, computing

potential energy surfaces for 11 possible pathways, suggesting that no more than four were of any importance under combustion conditions. Most researchers have subsequently concluded that only three paths are likely to play a role under typical conditions:

$$C_2H_5OH \rightarrow C_2H_4 + H_2O \quad (14)$$

$$\rightarrow CH_3 + CH_2OH \quad (15)$$

$$\rightarrow C_2H_5 + OH \quad (16)$$

The primary initial thermal process is a four-center molecular elimination of water, although the C−C and C−O bond fissions cannot be entirely neglected at high temperatures. With only three heavy atoms in ethanol, pressure effects on the rate constants are significant under many conditions. In 2004, Li et al.[71] provided parameterized pressure-dependent rate constants for the first two channels, and Tsang[72] reported a detailed analysis of energy transfer effects and provided assessments for all three of the above channels. Updated combustion models validated for various conditions are given by Li et al.,[71] Saxena and Williams,[75] Haas et al.,[76] Leplat et al.,[77] Lee et al.,[78] and Metcalf.[79]

### 2.1.2 Bimolecular Radical-Induced Decomposition of Ethanol

Decomposition induced by bimolecular reactions revolves around abstraction of H by active radicals present in combustion systems (generally represented by X): predominantly OH and H, with smaller contributions from O, $HO_2$, and alkyl radicals under some conditions. Three channels are available:

$$X + C_2H_5OH \rightarrow CH_3CHOH + XH \quad (17)$$

$$\rightarrow CH_2CH_2OH + XH \quad (18)$$

$$\rightarrow C_2H_5O + XH \quad (19)$$

Experimental work to date has mostly focused on the case where X = OH, where there are measurements of the total reaction rate at low temperatures relevant to atmospheric chemistry, and at temperatures up to about 1300 K. Meier et al.[80] in 1985 determined from experiment that abstraction from the $CH_2$ group represents 75% ± 15% of reaction at 300 K. The reaction with OH has also been heavily studied by theoretical methods. Xu and Lin[81] performed a computational study in 2007 and

derived branching ratios, suggesting that abstraction of the hydroxyl hydrogen is minor even at combustion temperatures. In 2010, Sivaramakrishnan et al.[82] reported new experimental data on the total $OH + C_2H_5OH$ rate constant from 857 to 1297 K; they used high-level computations and literature data to derive recommended branching ratios and rate expressions for all three channels over the temperature range of 200–2500 K. In agreement with Xu and Lin,[81] they concluded that abstraction from the hydroxyl group is minor. In 2011, Carr et al.[83] studied the reaction of OH with $C_2H_5OH$ and $C_2D_5OH$ between 298 and 523 K, deriving site-specific rate constants on the basis of kinetic isotope effects. Abstraction from the $CH_2$ group was derived to be 92% ± 8% at 298 K, decreasing to 76% ± 9% at 523 K. They obtained additional data requiring a more complex treatment at temperatures of 658–864 K. Contrary to other researchers, Carr et al. suggested that abstraction of the hydroxyl hydrogen is significant at high temperatures, reaching around 50% of reaction at 864 K. In 2012, Zheng and Truhlar[84] reported multipath variational transition-state calculations and derived rate constants between 200 and 2400 K. As with other theoretical studies, they predicted that abstraction of the hydroxyl hydrogen remains minor, reaching a contribution of just over 10% at their highest temperatures. Overall, there is general consensus that the $CH_2$ group is more reactive than the methyl group and that abstraction of the hydroxyl hydrogen is minor at low temperatures. There remains, however, significant uncertainty in the branching ratios at high temperatures, particularly with respect to the reactivity of the hydroxyl group.

Kinetic data on $H + C_2H_5OH$ are more limited than those with OH. Aders and Wagner[85] experimentally measured the total rate constant between 295 K and 700 K in 1973. Theoretical work by Park et al.[70] in 2003 suggested that abstraction of H from the hydroxyl group is negligible and that attack on the $CH_2$ group is faster than attack at the $CH_3$ position. Sivaramakrishnan et al.[82] in 2010 measured the rate of $D + C_2H_5OH$ at 1054–1359 K and carried out additional high-level calculations for abstraction by H/D. They then slightly tuned the theoretical results to better match available experimental data and to derive rate expressions for the three abstraction channels covering 300–2250 K. Their theoretical results are qualitatively similar to those of Park et al.[70]

While OH and H are the main attacking radicals under most combustion-related conditions, other radicals also have some impact, and limited data are available for their reactions. The overall rate constant for reaction of $O(^3P)$ with ethanol has been measured by several researchers. In 2007,

Wu et al.[86] reported a theoretical study of the branching fractions. They suggested that abstraction from the $CH_2$ group would dominate at low temperatures, with abstraction from the $CH_3$ position increasing and reaching about 40% at 2000 K. Abstraction of the hydroxyl H was predicted to be minor, reaching only 11% at 2000 K. In 2011, Carr et al.[87] reported experimental branching fractions at temperatures of 650–860 K, finding abstraction from the $CH_2$ position to account for about 75% of reaction under these conditions.

Overall rate constants for the reaction of methyl radicals with $C_2H_5OH$ are available at low temperatures and the reaction has been studied theoretically by Xu et al.[88] in 2004. Theoretical results for the overall rate constant are in reasonable agreement with experiment. As with other reactive radical species, the dominant reaction is predicted to be abstraction from the $CH_2$ group, with a smaller contribution from the $CH_3$ position, and little involvement of the hydroxyl group.

### 2.1.3 Reactions of Radical Intermediates Derived from Ethanol

#### 2.1.3.1 Unimolecular Processes

Abstraction of hydrogen from ethanol results in three possible $C_2H_5O$ radicals: 1-hydroxyethyl, 2-hydroxyethyl, or ethoxy radical. These species decompose primarily by β-scission reactions (breaking a bond that is two bonds from the radical site) at high temperatures. Most of the available data pertain to ethoxy radical, which decomposes by β-scission of a C–H or C–C bond. Curran[89] reviewed in 2006 the experimental and computational work pertaining to this species and derived recommended high-pressure rate expressions. In 2007, Matus et al.[90] used high-level methods to compute the heats of formation of the three $C_2H_5O$ radicals and computed rate constants for the β-C–C scission pathway in the ethoxy radical, suggesting that heavy atom tunneling may be important. The effect of anharmonicity on the rate constants for C–C and C–H scission in ethoxy radical was examined by Shao et al.[91] in 2010; significant effects were seen only at temperatures above 2000 K or for molecules with high excitation energies.

In 2009, Xu et al.[92] completed a comprehensive study of the $C_2H_5O$ potential energy surface, reporting on the decomposition and isomerization reactions of all three $C_2H_5O$ radicals and reviewing the previous literature. Multiple decomposition paths were found for all species, with a main channel accounting for >75% of reaction for each species at moderate to high pressures and temperatures below about 800 K; the secondary processes were predicted to increase in importance at higher temperatures and lower

pressures. Xu et al. also used an RRKM/master equation analysis to derive rate expressions covering 300−3000 K at selected pressures of helium, ranging from 1 torr to 100 atm. More recently, Dames[93] carried out an RRKM/master equation analysis of the decomposition of ethoxy and the 1-hydroxyethyl radical in nitrogen and reported pressure-dependent rate constants in the Troe format suitable for combustion modeling.

#### 2.1.3.2 Bimolecular Processes

The $C_2H_5O$ radicals formed by H atom abstraction from ethanol decompose by rapid unimolecular processes at typical combustion temperatures. However, bimolecular processes can be important during the initial ignition phase, where temperatures are lower and corresponding radical lifetimes are much longer, and in certain other situations, such as low-pressure flames. Zador et al.[94] in 2009 reviewed the previous literature and reported the results of a high-level computational study of the reaction of $O_2$ with 1-hydroxyethyl and 2-hydroxyethyl, as well as an experimental investigation of the reaction products. Rate constants and product branching ratios were computed at temperatures from 250 K to 1000 K and pressures of 1 torr−100 atm. Reaction of oxygen with 1-hydroxyethyl yields primarily $HO_2$ and acetaldehyde (Eqn (20)), while reaction with 2-hydroxyethyl yields a distribution of formaldehyde and OH (Eqn (21)), ethenol and hydroperoxy radical (Eqn (22)), and peroxy radical $OOCH_2CH_2OH$ (Eqn (23)):

$$O_2 + CH_3CHOH \rightarrow CH_3CHO + HO_2 \quad (20)$$

$$O_2 + CH_2CH_2OH \rightarrow 2H_2C{=}O + OH \quad (21)$$

$$\rightarrow CH_2{=}CHOH + HO_2 \quad (22)$$

$$\rightarrow OOCH_2CH_2OH \quad (23)$$

Zador et al. found qualitative agreement between experiment, theory, and existing model estimates, but noted that uncertainty remains in the product branching ratios and rate constants.

Labbe et al.[95] recently considered the importance of "well-skipping" reactions in radical + fuel radical recombination processes. Bond formation in the initial association leads to a chemically activated intermediate with an internal energy well above the thermal background; in multichannel systems, rather than thermalizing or redissociating, this intermediate can proceed directly to other products. Labbe et al. thus concluded that a major

source of ethene and propene in low-pressure ethanol flames are the reactions shown in Eqns (24) and (25). They further suggested that similar processes involving relatively stable fuel radicals and common flame radicals such as H, OH, O, and $CH_3$ may need to be generally considered.

$$H + CH_3CHOH \rightarrow [CH_3CH_2OH]^* \rightarrow C_2H_4 + H_2O \quad (24)$$

$$CH_3 + CH_3CHOH \rightarrow [(CH_3)_2CHOH]^* \rightarrow C_3H_6 + H_2O \quad (25)$$

## 2.2 Combustion Pathways of Biodiesel

The other first-generation biofuel currently in use, biodiesel, is composed of fatty acid esters obtained from animal and plant oils after transesterification with methanol or ethanol. Animal sources include beef tallow and pork lard, and recycled cooking oils and greases. Existing plant-derived sources include soybean, coconut, palm, rapeseed, and cottonseed oils. (As we will discuss subsequently, algae may embody third- and fourth-generation routes to some chemically similar fuels, but production technology is not yet in place. Because of high energy costs and inefficiency in the growth of livestock, animal-derived biodiesel is expected to arise primarily from waste streams in the food production cycle, and thus remain in rather modest supply, whereas algae and plants represent potentially much larger and more attractive sources, particularly when using non-food-competitive technologies.)

Most biodiesel is composed of $C_{16}$ to $C_{22}$ monoesters. Common compounds include methyl oleate, methyl linoleate, methyl palmitate, methyl stearate, and methyl linolenate (Table 3).

Chemically, the structures are long-chain HCs modified by an ester functionality at one end, with varying degrees of unsaturation, typically zero to three double bonds. The portion of the molecule that is far removed from the ester group behaves similarly to HC fuels: that is, C—C and C—H bond strengths distant from the ester functionality are essentially identical to those in pure HCs, as are rates of radical attack by OH, H, and other flame radicals; rates of β-scission reactions of radical intermediates; etc. This gives a strong basis for development of a significant portion of the chemistry required for combustion models.

On the other hand, compared with conventional saturated HC fuels, new chemistry is introduced by the presence of the ester group and sites of unsaturation. The subsequent discussion will focus on these aspects of the chemistry; the reader is referred to reviews by Simmie[97] and Battin-Leclerc[98] for overviews of the underlying HC chemistry.

**Table 3** Structures of methyl esters and average composition in rapeseed and soybean biodiesels

| Ester | Structure | Average composition (mass %) | |
|---|---|---|---|
| | | Rapeseed | Soybean |
| Methyl palmitate, $C_{17}H_{34}O_2$, (C16:0) | 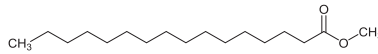 | 4.3 | 6–10 |
| Methyl stearate, $C_{19}H_{38}O_2$, (C18:0) | 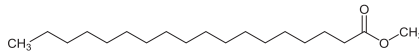 | 1.3 | 2–5 |
| Methyl oleate, $C_{19}H_{36}O_2$, (C18:1) | 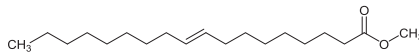 | 59.9 | 20–30 |
| Methyl linoleate, $C_{19}H_{34}O_2$, (C18:2) | 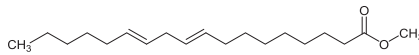 | 21.1 | 50–60 |
| Methyl linolenate, $C_{19}H_{32}O_2$, (C18:3) | 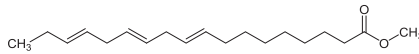 | 13.2 | 5–11 |

Adapted from Westbrook et al.[132] who used data from Van Gerpen et al.[96]

### 2.2.1 Biodiesel Model Compounds

#### 2.2.1.1 Methyl Butanoate and Related Small Esters

Methyl butanoate (MB) has been widely used as a useful model compound for understanding the chemistry of methyl ester biofuels: it is small enough to result in models of tractable size, yet large enough to realistically probe at least some of the chemistry associated with the ester group and its possible interactions with the HC chain.

The first detailed chemical kinetic model of MB oxidation was constructed by Fisher et al.[99] in 2000. The model was developed by following rate rules used in HC combustion models, with some modifications, and inclusion of additional reactions specific to the ester moiety. Some initial comparisons of this model with MB oxidation in a flow reactor were presented by Marchese et al.[100] in 2004, and reasonable overall agreement was noted for major species. The model has since been utilized and updated by a number of researchers as knowledge of MB chemistry has advanced.

In 2007, Gail et al.[101] studied MB oxidation in several global-type experiments, reporting profile data for 20 product species in a JSR, six species in a variable pressure flow reactor, and 14 species in an opposed flow diffusion flame (OFDF). They revised the Fisher et al.[99] model to better fit their data, but noted that the mechanism for early formation of $CO_2$ remained unclear.

Also, in 2007, El-Nahas et al.[102] reported a computational study of the thermochemistry and decomposition kinetics of MB and its $C_5H_{10}O_2$ isomer, ethyl propanoate (EP). For each compound, they identified six unimolecular decomposition paths, both molecular and homolytic, finding that concerted six-center eliminations were the lowest energy paths:

$$\mathrm{EP} \rightarrow \mathrm{H_2C{=}CH_2 + CH_3CH_2COOH} \quad (26)$$

$$\mathrm{MB} \rightarrow \mathrm{H_2C{=}CH_2 + CH_2{=}C(OH)OCH_3} \quad (27)$$

The decomposition barrier for the ethyl ester was found to be significantly lower, by about 75 kJ $mol^{-1}$, than that for the methyl compound, with the consequence that carboxylic acid species play a prominent role in the decomposition of ethyl esters, but not in their methyl cousins.

That same year Metcalfe et al.[103] measured ignition delay times of MB and EP in shock tube studies, and modeled both systems using a revised version of the Fisher MB model. Their revisions included incorporation of results from the computations of El-Nahas et al.,[102] replacement of the $H_2/O_2$ submechanism with that of O'Conaire et al.,[104] changes to fuel radical decomposition rates based on Curran,[89] the inclusion of falloff effects on unimolecular reactions, and small adjustments to thermochemistry and other rate constants. The resulting simulations were in good agreement with reflected-shock temperature and pressure data, and reproduced effects of varying fuel and oxygen concentrations.

In 2008, Dooley et al.[105] studied ignition delay times of MB at 1250–1760 K in shock tubes and at 640–949 K using an RCM. The 2007 model of Metcalfe et al.[103] was used as a basis and extensively updated, including changes to the $C_3$ submechanism based on the work of Petersen et al.,[106] development of a new $C_4$ submechanism, use of revised H abstraction rates from MB by fuel radicals, and changes to the decomposition rates of a number of fuel radical intermediates. The new model was used to simulate the new ignition delay time data, as well as the earlier results of Gail et al.[101] Analysis of the model showed that the reactions important in predicting behavior varied significantly with temperature, pressure, and fuel equivalence ratio. They noted the importance of unimolecular decomposition of MB at high temperatures, reactions involving $HO_2$ radicals in the low to mid temperature regime, and the decomposition kinetics of alkyl fuel radicals under fuel-rich conditions.

In 2009, Walton et al.[107] used an RCM to investigate ignition delays of MB and EP at 935–1117 K and simulated the results with a slightly

modified version of the 2007 Metcalfe et al. model.[103] They reported excellent agreement for both compounds and suggested the importance of H abstraction reactions from the fuel by $HO_2$ and $CH_3OO$ radicals in determining the ignition delay behavior.

In 2008, Huynh and Violi[108] used quantum chemical methods to carry out an extensive investigation of radical-induced pyrolytic pathways in MB decomposition. Thirteen pathways, shown in Figure 5, were explored. Rate constants for abstraction of H from the various positions of MB by H, OH, and $CH_3$ were computed along with those for the subsequent unimolecular processes. Rate expressions covering the 300−2500 K temperature range were derived. In a subsequent paper, using their results and additional data from the literature, Huynh et al.[109] updated the Fisher et al.[99] model of MB chemistry to describe MB and methyl acetate (MA) pyrolysis. The model was then further extended by Farooq et al.[110] in 2009 to describe methyl propionate (MP) pyrolysis and compared with experimental $CO_2$ yields obtained in shock tube studies of MB, MA, and MP pyrolysis at 1260−1663 K. The Farooq et al. model was found to better predict $CO_2$ yields for MB than those of Fisher et al.,[99] Gail et al.,[101] and Metcalfe et al.[103] In a follow-up study in 2012, Farooq et al.[111] reexamined MB pyrolysis in a shock tube at temperatures of 1200−1800 K, but used improved laser diagnostics to simultaneously monitor time histories of CO, $CO_2$, $CH_3$, and $C_2H_4$. Experimental results were compared with the predictions of the models of Huynh et al.[109] and Dooley et al.[105] Although both models showed qualitative agreement with experiment, the Huynh et al. model generally performed better. However, both models underpredicted $CH_3$ and $C_2H_4$ formation, and neither was able to capture CO and $CO_2$ yields over the full range of conditions. Important reactions controlling the distributions were identified as unimolecular bond fissions in MB, in competition with abstraction of H from MB by active radicals, primarily H atoms. The authors concluded that the high-temperature pyrolysis of all linear methyl esters should be expected to yield CO:$CO_2$ ratios of about 2:1, with one CO produced per ester molecule.

Simulations performed in the above works were all based on modifications to the MB model of Fisher et al proposed in 2000.[99] A different approach was adopted by Haaka et al., who reported in 2010 the use of the automated mechanism generation software EXGAS[112−114] to independently derive an alternate model of the oxidation of MB and ethyl butanoate. They tested their models with shock tube-based ignition delay data at temperatures of 1250−2000 K and species profile data obtained in a

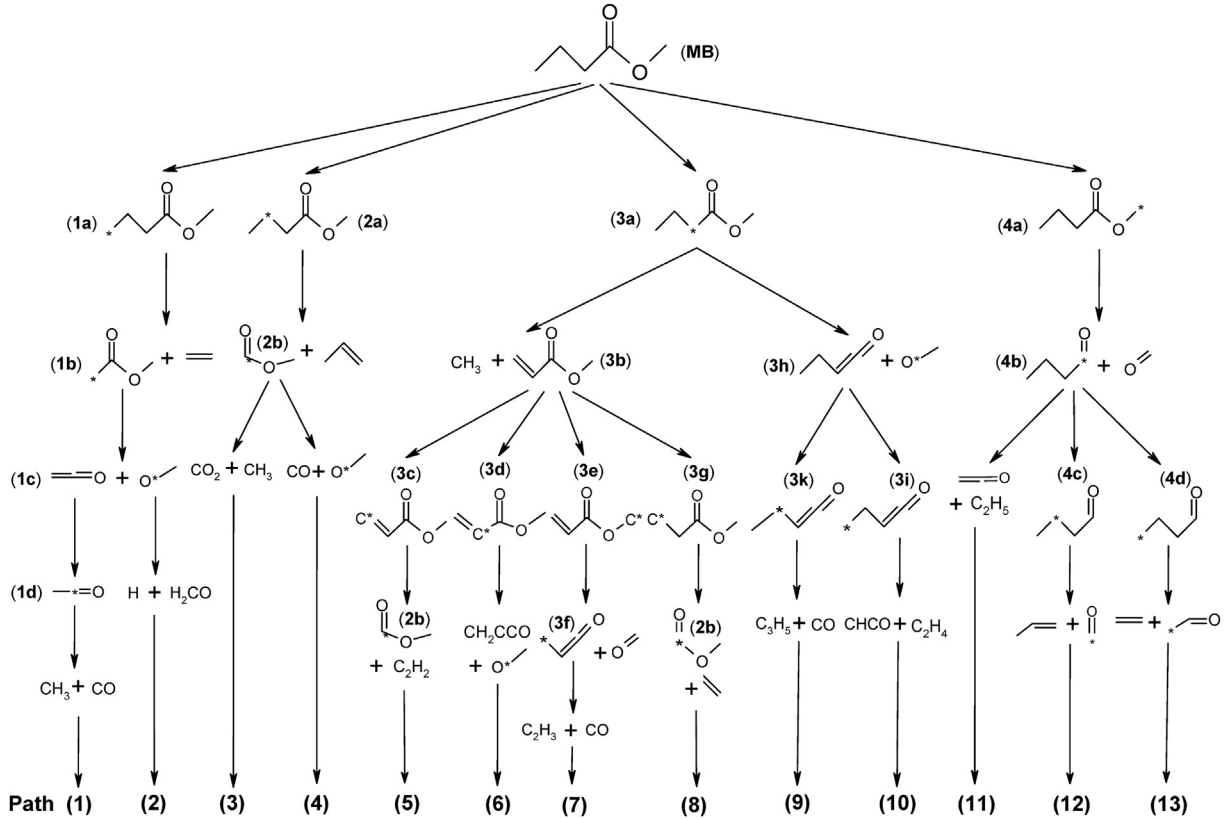


**Figure 5** Pathways proposed for the radical-induced pyrolytic decomposition of MB. *Reprinted with permission from Huynh et al.*[108] *Copyright 2008 American Chemical Society.*

JSR at 800 and 850 K. Ignition delay times were well predicted by the EXGAS model. Monitored in the MB JSR experiments were 10 species: $O_2$, CO, $CO_2$, $CH_4$, $C_2$ HCs, methyl acrylate, methyl crotonate (MC), and MB. The experimental species profile results were compared with predictions from the EXGAS model, as well as with the models of Fisher et al.,[99] Gail et al.,[101] and Dooley et al.[105] While there was some variation in the predictions, all models were found to overestimate MB reactivity and underestimate ethene formation compared with the JSR data, but the authors were unable to discern if this was due to incorrect model chemistry or other difficulties (e.g., wall reactions in the JSR experiments).

Several researchers have applied models to experimental data pertaining to flames. Westbrook et al.[115] in 2009 measured species profiles in laminar flames for the small alkyl esters methyl formate, MA, ethyl formate, and ethyl acetate, developing detailed kinetic models. Yang et al.[116] in 2011 used photoionization mass spectrometry, using monochromated synchrotron radiation, to measure species profiles, including those of radical intermediates, in low-pressure flat flames of MB and two other $C_5H_{10}O_2$ esters. Significant differences in the intermediate species were noted for the three fuels. The authors built hierarchical models, taking submechanisms from the literature and adding additional chemistry when necessary, and achieved good agreement with experiment. They emphasized the importance of decomposition of the fuels by unimolecular and H abstraction reactions, as well as by β-scission reactions of fuel radical intermediates. Wang et al.[117] in 2014 determined laminar flame speeds of seven small methyl and ethyl esters, including MB, and simulated the results using a number of models. Flame speeds were generally overpredicted by all models, although the qualitative ordering was reproduced. The authors found that simulations could be significantly perturbed by changes in several rate constants for fuel-specific reactions, and noted that improved accuracy in the kinetic parameters is needed.

#### 2.2.1.2 Large Methyl Esters

Studies of MB and related small esters have provided great insight into the important new chemistry associated with the introduction of the ester moiety to the HC backbone. Actual biofuels are much larger compounds, however, typically in the range of $C_{16}$ to $C_{22}$. Parallel to development of the MB mechanism, researchers were also investigating the behavior of larger esters and developing detailed chemical kinetic models of these species. These models all used in some form the chemistry and knowledge gained from the MB studies.

In 2008 Dayma et al.[118] experimentally studied the oxidation of methyl hexanoate in a JSR at 500–1000 K, obtained speciation data, and developed a kinetic mechanism by modifying that used for MB. Similar JSR studies[119] on methyl heptanoate oxidation from the same group were reported in 2009, and their model was extended to this compound. HadjAli et al.[120] in 2009 examined methyl hexanoate autoignition in an RCM, discussed reaction pathways, and discussed the importance of esteralkyl radicals and esteralkylperoxy radicals in low-temperature autoignition.

Dayma et al.[121] in 2012 studied the oxidation of ethyl pentanoate in a JSR at 560–1160 K, measuring profiles of 19 species, and also determined laminar burning velocities in a spherical combustion chamber. Results were simulated after adding an ethyl pentanoate submechanism to a previously developed combustion model, and good agreement was found. In a separate paper that same year, Dayma et al.[122] reported laminar burning velocity data on a series of $C_4$ to $C_7$ ethyl esters and extended their model to include the new compounds. They compared their model with the new data, as well as with a variety of data from the literature: species profile data from low-pressure laminar flames and JSR experiments, as well as ignition delay times from shock tubes and RCMs. Good agreement between model and experiment was found. On the basis of sensitivity analyses, they concluded that laminar burning velocities were primarily sensitive to the small species chemistry.

Even larger esters have been considered. Herbinet et al.[123] in 2008 developed an oxidation mechanism for methyl decanoate (MD) oxidation, by combining models for *n*-alkanes and MB, and then adding additional reactions specific to MD. This model was compared with results from engine experiments and a JSR. That same year, Seshadri et al.[124] looked at extinction and ignition of MD in laminar nonpremixed flows and used a skeletal version of the Herbinet et al.[123] model to simulate the results. In 2010, Sarathy et al.[125] obtained new species profile data for MD in an OFDF and used these data to develop an improved skeletal mechanism from the earlier Herbinet et al. model.[123]

Also, in 2010, Glaude et al.[126] studied methyl hexanoate, methyl heptanoate, and MD oxidation in a JSR from 500 to 1100 K, developing a new mechanism using the EXGAS software that had previously been applied to MB oxidation. They found that predictions of the EXGAS model and the 2008 model of Herbinet et al.[123] were similar. They also concluded that the combustion behavior of large saturated esters is similar to that of *n*-alkanes. Shortly thereafter, Herbinet et al.[127] used the EXGAS software to extend

their model to the $C_{11}$ to $C_{19}$ saturated methyl esters. They found generally good agreement with experimental data; however, they also noted that the model was unable to predict certain specific products such as unsaturated esters, since EXGAS was at that time unable to account for the chemistry of double bonds present in the ester side chains.

#### 2.2.1.3 Unsaturated Methyl Esters

Typical biofuels from plant oils contain a degree of unsaturation in the methyl esters, and researchers have examined such compounds as well. MC [$CH_3CH{=}CH(C{=}O)OCH_3$] is a $C_5$ intermediate formed in MB oxidation. Sarathy et al.[128] reported JSR and OFDF studies of MC oxidation in 2007, and this work was then extended in 2008 by Gail et al.,[129] who compared results with MB in similar experiments. These studies noted higher levels of unsaturated compounds formed by MC in comparison with MB, and discussed the mechanistic pathways that control the product distributions.

Actual biodiesel fuels contain unsaturated esters much larger than MC, however. As indicated earlier in Table 3, soy and rapeseed oils are mainly composed of five methyl esters: methyl stearate (C18:0), methyl oleate (C18:1), methyl linoleate (C18:2), methyl linolenate (C18:3), and methyl palmitate (C16:0), where the parenthetic notation following each molecule has the form (C$x$:$y$) where $x$ denotes the length of the main carbon backbone (thus excluding the methyl portion of the ester), and $y$ is the number of double bonds in the chain.

Dagaut et al.[130] in 2007 obtained JSR speciation data for rapeseed oil oxidation and proposed a surrogate model based on *n*-hexadecane. This model did not, however, contain chemistry directly associated with the alkenyl ester structures. In 2010, Herbinet et al.[131] developed a model containing alkenyl ester chemistry for a rapeseed oil surrogate mixture containing methyl-5-decenoate, methyl-9-decenoate, MD, and *n*-alkanes. They compared their simulations with the Dagaut et al.[130] data. Westbrook et al.[132] in 2011 developed a detailed kinetic model of the five alkenyl ester components of soy and rapeseed oil shown in Table 3. The mechanism was constructed by bringing together submechanisms relevant to HC fuels, together with the use of thermochemical kinetic estimation techniques for various reactions specific to the esters. In their analysis, they pointed to the need for more information on isomerization reactions of radical species containing double bonds and on the chemistry of allylic radical + $O_2$ reactions. The influence of the double bonds on the low-temperature

chemistry, ignition delay times, and cetane numbers (numbers indicating combustion speed of the fuel) was later expounded on by Westbrook et al.,[133] and the importance of allylic sites was emphasized.

### 2.2.2 Elementary Reaction Kinetics for Biodiesel Fuels

The above modeling efforts have mostly sought to match global experiments using rule-based mechanisms and kinetics, with some limited computational efforts. This has resulted in a much improved understanding of the general features of small ester oxidation and pyrolysis, yet there are numerous difficulties reported in quantitatively matching experimental observations. Often the uncertainties are traceable to the kinetics of specific reactions. Recent efforts have accordingly focused on the application of higher levels of theory and direct experimental measurements to better quantify key elementary reactions.

Pathways and reaction barriers for the unimolecular decomposition of MB were explored with CBS-QB3 methods by El-Nahas et al.[102] in 2007. Ali and Violi[134] have recently used ab initio and DFT methods to reexamine MB decomposition. Their bond energies and reaction barriers were generally in good agreement with those of El-Nahas. They have used the computations to compute high-pressure and pressure-dependent kinetics for 10 possible decomposition pathways. They noted the importance of entropic factors in addition to the energetics in determining the kinetics.

Abstraction of H from MB by H and OH radicals has been identified as a key reaction. Abstraction by H atoms has been examined at various levels of theory by a number of researchers, including Huynh and Violi,[108] Akih-Kumgeh and Bergthorson,[135] Liu et al.,[136] and Zhang et al.[137] The more recent work[136,137] using higher levels of theory gives rate constants that are significantly smaller than the earlier studies[108,135] at temperatures below about 1000 K, as well as differences in the branching ratios. Differences were attributed to both barrier heights and the treatment of hindered internal rotors in the calculation of thermodynamic properties.

For OH + MB, there are several experimental measurements[138–140] of the total rate constant at ambient and low temperatures. At high temperatures, Lam et al.[141] have measured in 2012 the overall rate for MB and several other small esters at 876–1371 K in shock tube studies by following decays of the OH signal using ultraviolet laser absorption. Theoretical rates for OH + MB are available from Huynh and Violi[108] and Zhang et al.[137] and include information on the abstraction sites that is not available from

experiment. Substantial differences in the predicted rate constants and site selectivities are derived from the two theoretical works. With respect to overall rates, the 2008 values of Huynh and Violi are in fair accord with the 2012 high-temperature measurements of Lam et al. above 1000 K, but badly underpredict the rate constants measured at ambient and low temperatures. In contrast, the 2015 values of Zhang et al. are in excellent accord with experiments at lower temperatures, but appreciably underpredict the high-temperature measurements of Lam et al.

Low-temperature ignition is known to depend strongly on the chemistry of peroxy radical intermediates and their isomerization and decomposition products. The ignition chemistry of alkyl species is highly related and is a useful starting point. An excellent review by Zador et al.[142] in 2011 summarizes the relevant chemistry. In a series of articles, Villano, Carstensen, Dean, and coworkers have used electronic structure calculations performed at the CBS-QB3 level of theory to develop rate rules for many of these reaction classes. In 2011, Villano et al. looked at alkyl + $O_2$, reactions,[52] and developed rate rules for dissociation, concerted eliminations, and isomerization channels of alkylperoxy radicals. In 2012, they considered[53] the isomerization, cyclic ether formation, and β-scission reactions of hydroperoxyalkyl radicals, and in 2013, they investigated the $HO_2$ + olefin addition reactions,[143] again developing rate rules, and considering branching ratios and the pressure dependence of the reactions.

There are additionally a few studies that directly address biodiesel-related esters. Hayes and Burgess[144] in 2009 explored hydrogen transfer reactions of the alpha peroxy radicals of MB and methyl pentanoate. Such reactions had been suggested by Herbinet et al.[123] to be important in the early $CO_2$ formation seen in methyl ester combustion. Hayes and Burgess were able to derive high-pressure rate expressions and considered a number of competing reactions as well. They also reported that composite G3B3 calculations matched available benchmark data on related reaction barriers with better accuracy than DFT approaches.

In 2014, Tao and Lin[145] reported a subsequent detailed investigation of the chemistry associated with MB ignition at the G3MP2B3 level of theory, determining mechanisms, reaction thermochemistry, and kinetics for the decomposition of methyl ester peroxy radicals formed from MB. They particularly focused on the intramolecular H atom transfers in peroxy radicals ROO, the unimolecular dissociations of ROO and QOOH species, and the reactions of ROO and $HO_2$. A new submechanism with 114 pathways was developed. In very recent work from 2015, Jiao et al.[146] explored this

same chemistry at the CBS-QB3 level of theory. They found activation barriers for some of the reactions to be significantly ($\geq$12.5 kJ mol$^{-1}$) different when computed with CBS-QB3 and G3MP2B3. In many cases, the relative rates remain similar, but in some instances, substantially different branching ratios for competing reactions are predicted. For the related MA system, Mai et al.[147] reported in 2015 a CBS-QB3 study of the reaction of MA radicals with $O_2$, deriving pathways and pressure-dependent rate constants suitable for combustion modeling. Also, in 2015, Le et al.[148] used CBS-QB3 methods to examine the pathways stemming from the reaction of methyl propanoate radicals with $O_2$; they derived pressure- and temperature-dependent rate constants.

There is a general paucity of computational data on the specific molecules present in biofuels, in part because of the large size of the molecules and the corresponding computational expense. Zhang and Zhang[149] in 2015 suggested the value of the hybrid two-layer ONIOM[150] approach, wherein one applies a higher level of theory near the reactive site, and a lower level for uninvolved portions of the molecule. They used this technique to investigate the hydrogen abstraction reactions of large alkyl esters, obtaining good results when employing a QCISD(T)/CBS method for the high-level layer and a DFT method for the low-level layer. They suggested that the procedure is an affordable and computationally accurate means for high-level theoretical studies of the chemical kinetics of large biodiesel molecules.

## 2.3 General Challenges in Modeling First-Generation Biofuels

While detailed chemical kinetic mechanisms have long been developed for the combustion of HC fuels (gasoline, diesel), biofuels are by nature functionalized (alcohols, esters, etc.), and their resultant chemistry is rich and complex. Conversely, HC fuels contain hundreds of compounds and dozens of different types of HCs, each with their own chemical behavior. This contrasts with biofuels, which have only on the order of tens of compounds with very similar chemistry, differing only by alkyl chain lengths and degrees of unsaturation.

In short, biofuel chemistry is *less* complex because there are fewer types of components, but *more* complex because the reactions are more diverse. An example of additional complexity in biodiesel is the large variation in hydrogen saturation, which depends on the type of oil. Sunflower and corn oil are high in polyunsaturated fatty acids, coconut and palm oil are

high in saturated fatty acids, and canola and lard are high in monounsaturated fats. Saturated fats yield biofuels with high cetane numbers, whereas polyunsaturated fats yield biofuels with lower cetane numbers.[151] The unsaturation in alcohols and other oxygenated HCs significantly changes their reactivity, especially at low temperatures (the ignition regime).[152,153] It also affects their stability in long-term storage, since olefins have higher oxidation rates.

Biofuels contain oxygen in addition to carbon and hydrogen; furthermore, there are different classes of oxygenated HCs (alcohols, ethers, esters, etc.) used as biofuels, and each class has particular chemistry associated with it.[154–156] Some characteristics and factors that are important in biofuel chemistry do not play as large a role in pure HC fuels (i.e., gasoline, diesel, and jet fuel). Operating conditions and ignition behavior can also be different, since ignition mechanisms can be somewhat different with oxygenated species. As discussed in the introduction, fuels can exhibit an NTC regime, where at intermediate temperatures, ignition delays may increase with temperature, because of the temperature dependence of isomerization pathways for alkylperoxy (ROO) radicals.[157,158] The NTC regime affects peroxy radicals arising from oxygenated species such as alcohols and alkyl esters as well; the extent to which this behavior parallels that of alkylperoxy radicals is a topic of interest.

Most current studies of biodiesel chemistry, and the detailed chemical kinetic mechanisms derived therefrom, are based on surrogate molecules and mixtures: the proxies contain the same or similar chemical functionalities as actual fuels, but are simplified systems designed to isolate particular aspects of the chemistry or behavior. Biodiesels in current use are alkyl esters of saturated and unsaturated fatty acids, with lipid chain lengths that range from about C14 to C22 (most typically C16 to C18), with the chemical composition varying from oil to oil. The surrogates used in the models are often smaller saturated and unsaturated lipids such as MB (and methyl butenoate),[129] methyl hexanoate,[126] or MD (and methyl decenoate).[131] A detailed chemical kinetic mechanism has also been developed for typical oils (methyl stearate and methyl oleate).[159]

Of the first-generation biofuels, ethanol and larger alcohols have been modeled most extensively and can thus be used to explore complex chemistry of interest. Branching in alcohols and the position of branching[160] can impact ignition delays, overall conversion, and the distribution of intermediates, incomplete products of combustion, and emissions (aldehydes, unsaturated HCs).[161] For alcohols, reaction of alkyl radicals with $O_2$ molecules results

in peroxy intermediates, leading to isomerizations of alkylperoxy radicals to hydroperoxyalkyl radicals (ROO → QOOH) and to water elimination from hydroperoxyalkyl species; this impacts radical chemistry at low temperatures and hence ignition characteristics.[162] This chemistry is also applicable to other oxygenated species such as ketones. Hydroperoxyalkyl radicals can also readily undergo isomerizations leading to cyclic ether formation (e.g., hydroperoxybutyl → tetrahydrofuran (THF) + OH) with different ring sizes depending on the location of the radical site.[163] NTC behavior for alcohols is strongly impacted by this chemistry and depends upon pressure, the size of the molecule, and other factors.[164] It has been determined through modeling aided by ab initio calculations that product branching ratios during decomposition of alcohols through abstractions and subsequent β-scissions are sensitive to bond strengths, which are impacted by functional (and structural) substitutions.[165] In addition, it is believed that fine details in the thermochemical partition functions for conformations and torsional modes in hydroxyl and alkoxy radicals may influence the chemistry.[166]

## 3. OVERVIEW OF SECOND-GENERATION BIOFUELS AND THEIR MODEL COMPOUNDS

Second-generation biofuels are so named due to they being developed after the first-generation biofuels (such as biodiesel), which are those derived from conventional feedstocks.[167] First-generation biofuels are not ideal; they compete with the food cycle and require a significant amount of water to generate.[168] A major benefit of second-generation fuels is their derivation from nonfood portions of plants (stalks, stems, grasses, wood, etc.).[169]

Second-generation biofuels are also referred to as lignocellulosic biofuels, since they derive from cellulose, hemicellulose, and lignin. These three components each consist of large, complex structures, made up of repeating cyclic units with varying functional groups. Cellulose (Figure 6) is a carbohydrate polymer consisting of D-glucose monomers connected by β-1,4′-glycosidic bonds. It has a rigid structure and is found in the primary cell wall of plants.[170] In contrast, hemicellulose has a branched, random structure consisting of a variety of carbohydrate monomers; its molecular structure varies by the type of plant in which it is found, and it serves to connect the cellulosic structure of a plant.[171]

Finally, lignin (Figure 7) is a highly complex polymer with a noncarbohydrate, irregular structure. It consists of three main types of monomeric

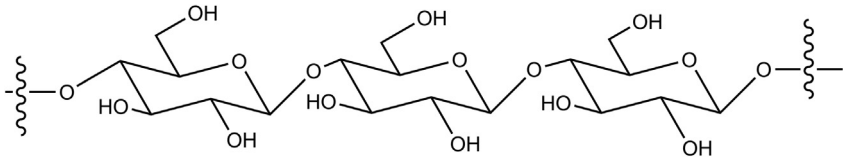


**Figure 6** Structure of cellulose,[172] consisting of glucose monomers regularly linked by β-1,4′-glycosidic bonds. (In contrast, hemicellulose consists of varying types of saccharide monomers and has a branched structure overall; see Ref. 171.)

subunits, each derived from an aromatic alcohol: the syringyl group, abbreviated S in the relevant literature, derived from sinapyl alcohol; the guaiacyl group, abbreviated G, derived from coniferyl alcohol; and the *p*-hydroxyphenyl group, abbreviated H, derived from *p*-coumaryl alcohol (Figure 8).[173] In addition to the characteristic monomers, several characteristic linkages[174] bond these lignols together (as can be seen in Figure 7). The most widely studied has been the β-O-4 linkage, as it is the most prevalent.

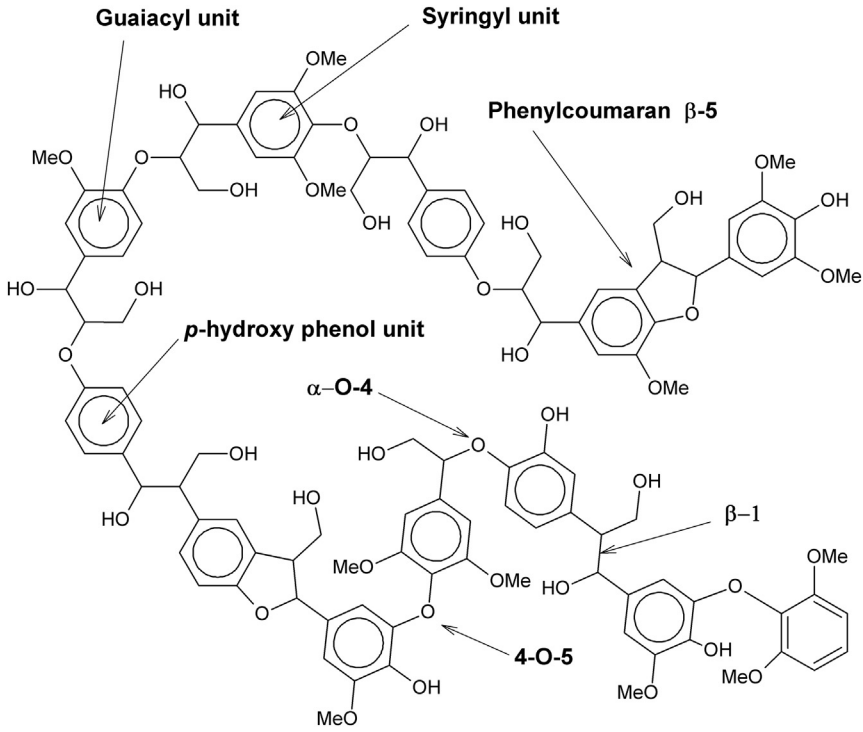


**Figure 7** Schematic representation of lignin including syringul (S), guaiacyl (G), and *p*-hydroxyphenyl (H) phenylpropanoid moieties, and lignin—lignin linkages. *Adapted from Lupoi et al.*[173]

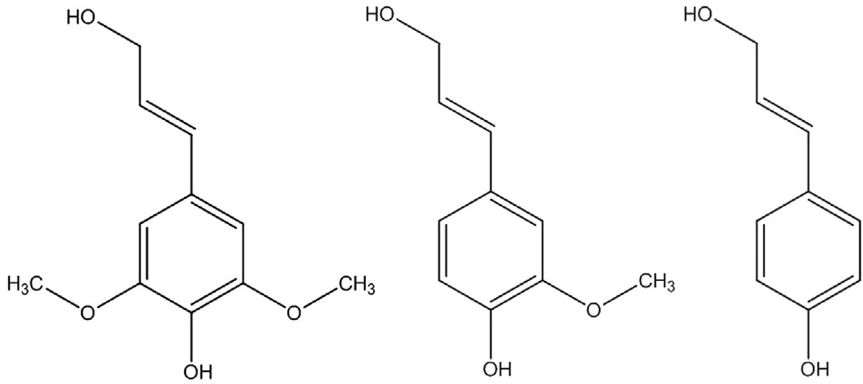


**Figure 8** The characteristic monomeric subunits found in lignin: sinapyl alcohol (left), coniferyl alcohol (center), and *p*-coumaryl alcohol (right). *Reprinted from Lupoi et al.*[173] *Copyright 2015 with permission from Elsevier.*

Biomass reactivity has been an area of interest for several years. In early papers, Evans and Milne compiled perspectives on biomass and the many compounds observed in its pyrolysis,[175] while Diebold proposed a global mechanism for cellulose decomposition.[176] Both lignin and cellulose systems are of increasing interest recently, given the pertinence of these systems to sustainability. Biomass is converted to useful fuels via pyrolysis, gasification, or hydrolysis; the products of each of these three primary conversion processes are subjected to several secondary processing routes. For instance, cellulose and hemicellulose can be subjected to hydrolysis to cleave their polymeric structures into the monosaccharides glucose, fructose, and xylose (Figure 9); these sugars can subsequently be dehydrated to form the platform molecules furfural (2-furfuraldehyde) and 5-hydroxymethylfurfural (5-HMF).[169]

Conversions of biomass to platform molecules[177] (which themselves can be converted to a wide variety of useful molecules) constitute an intense area of interest. Nimlos et al.[178] modeled the decomposition of xylose, a common component of hemicellulose, to furfural. Caratzoulas et al.[179] recently reported progress in the dehydration of fructose to 5-HMF. Lange et al.[180] summarized the potential of furfural for developing lignocellulosic biofuels. Yan et al.[181] reviewed the many pathways possible to furfural in terms of synthesizing fuel additives and value-added chemicals. Furfural and 5-HMF can be converted to molecules with promise as conventional HC fuels or to potential biofuels.[169,182] Comprehensive reviews of the catalytic conversion of lignocellulosic biomass to liquid fuels have been provided by

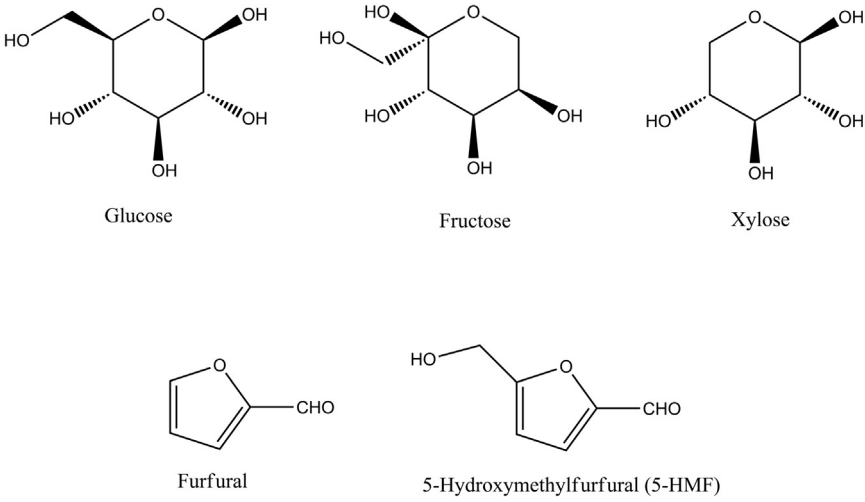


**Figure 9** Compounds relevant to biomass conversion. Common monosaccharides glucose, fructose, and xylose are shown in their pyranose forms in the top row. Platform molecules furfural and 5-hydroxyfurfural (5-HMF) are shown in the bottom row.

Corma et al.,[183] Chheda et al.,[184] and Lin and Huber,[185] while Bohre et al.[186] recently reviewed catalytic pathways between furfural and drop-in biofuels, highlighting the particular promise of 2-methylfuran (2-MF) and 2,5-dimethylfuran (2,5-DMF), given the similarities of their fuel properties and those of gasoline (Table 4).

Within the past decade, researchers have reported the direct conversion of biomass to small monocyclic compounds with potential as fuels. Roman-Leshkov et al.[187] developed a catalytic pathway from fructose, itself obtained directly from biomass, to 2,5-DMF (this and other species named in this paragraph can be seen in Figure 10), which exhibits several desirable alternative fuel properties such as high energy density, high boiling point, and water insolubility, when compared to the renewable fuel ethanol. Yang and Sen reported a one-step pathway from biomass to 2,5-dimethyltetrahydrofuran (2,5-DMTHF), which demonstrates many similar properties to 2,5-DMF and, as a saturated molecule, additionally has the potential for increased storage and transportation stability.[188] The subsequent chemistry and environmental impact of these compounds is still very much under investigation. Phuong et al.[189] noted the mutagenic capability of some intermediates implicated in 2,5-DMF combustion. Simmie and Wurmel[190] used 2,5-DMF as a test compound in an exhaustive case study exploring the environmental impact of this possible alternative fuel; they noted

**Table 4** Properties of 2-MF, DMF, and ethyl 5-ethoxymethylfurfural (EMF) compared to gasoline and ethanol

| Properties | Gasoline | Ethanol | DMF | 2-MF | EMF |
|---|---|---|---|---|---|
| Chemical formula | $C_6$–$C_9$ |  | 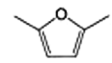 |  | 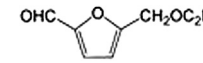 |
| H/C ratio | 1.795 | 3 | 1.333 | 1.2 | 1.27 |
| O/C ratio | 0 | 0.5 | 0.17 | 0.2 | 0.37 |
| Density @ 20 °C (kg $m^{-3}$) | 745 | 791 | 890 | 913 | 1100 |
| Reach octane number | 97 | 107 | 101 | 103 | – |
| Motor octane number | 85.7 | 89 | 88.1 | 86 | – |
| Energy density (MJ $L^{-1}$) | 31.9 | 21 | 29.3 | 28.5 | 30.3 |
| Initial boiling point (°C) | 32.8 | 78.4 | 92 | 64.7 | 274 |

Reprinted with permission from Bohre et al.[186] Copyright 2015 American Chemical Society.

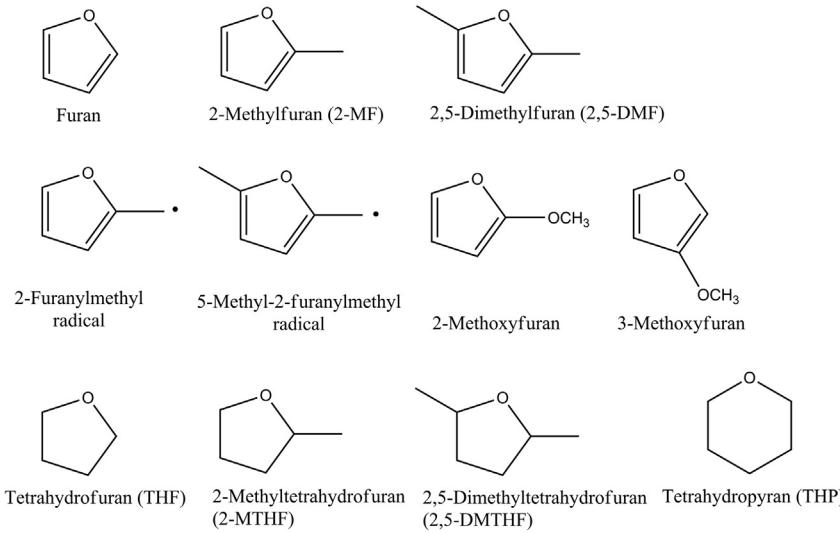


**Figure 10** Cyclic ethers and related species commonly considered in the combustion processes of second-generation biofuels.

intermediates likely to be formed in atmospheric reactions, highlighted environmental concerns, and summarized the need to better understand the chemistry of these species. However, few such studies have been completed.

The chemistry of lignin has been investigated for several decades given its pertinence to the paper industry and its overlap with aspects of coal chemistry, and several previous reviews summarize aspects of its general reactivity. Amen-Chen et al.[191] have reviewed the pyrolytic production pathways of monomeric phenols from biomass. Elder and Fort[192] reported the use of computational methods to model aspects of lignin chemistry. In recent years, interest in lignin has increased given its specific pertinence to potential biofuels; Zakzeski et al.[193] provided a comprehensive review of the catalytic pathways from lignin to renewable chemicals, and Lupoi et al.[173] recently provided a thorough account of lignin assessment techniques.

Given the cyclic, functionalized structures of cellulose and lignin, it is evident that the resulting chemistry of these units and of second-generation biofuels as a whole could differ markedly from both HC-based fuels and from first-generation biofuels. In 2012, Tran et al.[13] provided an excellent overview of reaction pathways likely to be significant for carbohydrate-derived cyclic oxygenates. They highlighted three specific ways in which the chemistry of cyclic ethers will differ from those of cyclic HCs: unimolecular initiation reactions involving the breakage of C−O bonds (rather than C−C bonds), the role that an alkyl substituent can play in β-scissions of oxygenated radicals, and the unusual bicyclic transition states available to peroxy radicals of these ethers. They also noted that while other reaction classes will overlap somewhat with those of HC fuels, kinetic parameters were generally lacking in the literature and likely to differ from those of HC analogs given the presence of the heteroatom.

This section will thus highlight recent mechanistic studies of monocyclic and bicyclic compounds that can (1) be derived from biomass or (2) serve as model compounds for overall behaviors of second-generation biofuels. We will first report on furan, its methyl-substituted derivatives, and its saturated derivatives. As stated above, 2-MF and 2,5-DMF are increasingly of interest as biofuels; more generally, furanic compounds have been highlighted as useful models[13] and subjected to increasingly significant study as model compounds for cellulose and fuels derived from cellulose over the past few years. Likewise, an overview of the chemistry of 2-phenethyl phenyl ether (PPE) (a simplified model containing the β-O-4 linkage) will be provided, as this species has been consistently used to understand reactions

of lignin. Explorations of a variety of other models will also be summarized for lignocellulosic biofuels. Studies of thermodynamic properties, pyrolytic processes, and atmospheric oxidation pathways will be examined. This section will close with a brief summary of general challenges in modeling lignocellulosic biofuels.

## 3.1 Cellulose Model Compounds

### *3.1.1 Combustion Pathways of Furan and Methylfurans*

Furan and its derivatives have been subjects of interest for several years, given their roles in several combustion processes, and this interest has expanded significantly in the past decade as attention to biomass-derived fuels has increased. This section will summarize mechanistic studies of the pyrolytic and oxidative chemistry of furan and its substituted derivatives (Figure 10). Studies of the combustion pathways of furan and its methyl-substituted derivatives are particularly intertwined; together, these studies provide a comprehensive case of following initial mechanistic studies through the development of a full chemical kinetic mechanism.

In 1985, Grela et al.[194] examined low-pressure pyrolysis of furan, 2-MF, and 2,5-DMF in the 1050−1270 K temperature range. They used a molecular flow reactor with mass spectrometry detection and observed that carbon monoxide loss played a significant role in the decomposition processes. They proposed that a biradical mechanism resulting from scission of the C−O bond, followed by isomerization, was ultimately responsible for the products seen. They also noted a likely commonality between the decomposition mechanisms of furan, 2-MF, and 2,5-DMF. Soon thereafter, Lifshitz et al.[195] examined the pyrolysis of furan over the 1050−1460 K range via a shock tube study. They noted that the major reaction products (Figure 11) were methyl acetylene and carbon monoxide, in roughly equal amounts, proposing a ring-opening initiation step. Acetylene was another major product seen; the authors proposed that it could be directly formed from furan with the concomitant formation of ketene; however, the ketene was not directly observed in the reaction mixture, which was attributed to its high reactivity with water. In 1991, Organ and Mackie[196] studied the pyrolysis of furan via a comparable shock tube study, monitoring the decomposition reaction via Fourier transform infrared spectroscopy (FTIR) spectroscopy. They noted the production of carbon monoxide, propyne, allene, and acetylene; furthermore, they detected ketene via FTIR spectroscopy. They proposed that C−O bond scission formed a reactive biradical intermediate that could decompose along each of the four common channels (Figure 12).

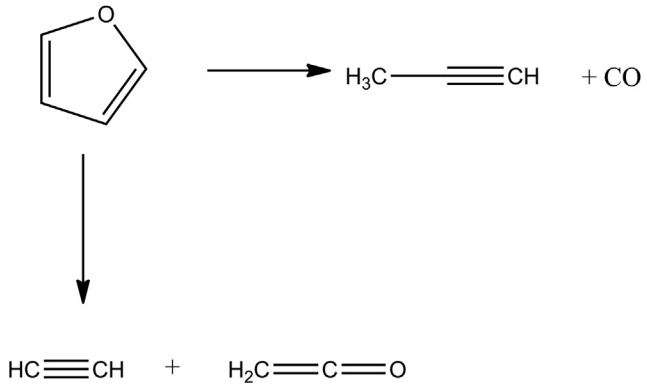


**Figure 11** Decomposition pathways of furan. *Adapted from Lifshitz et al.*[195] *Copyright 1986 American Chemical Society.*

From 1997–1998, Lifshitz et al. also completed shock tube studies of the methylated derivatives 2-MF[197] and 2,5-DMF,[198] suggesting a chemical kinetic model for the decomposition of each species and noting that the wide range of products formed rely in each case on the initial hydrogen atom and methyl group migrations.

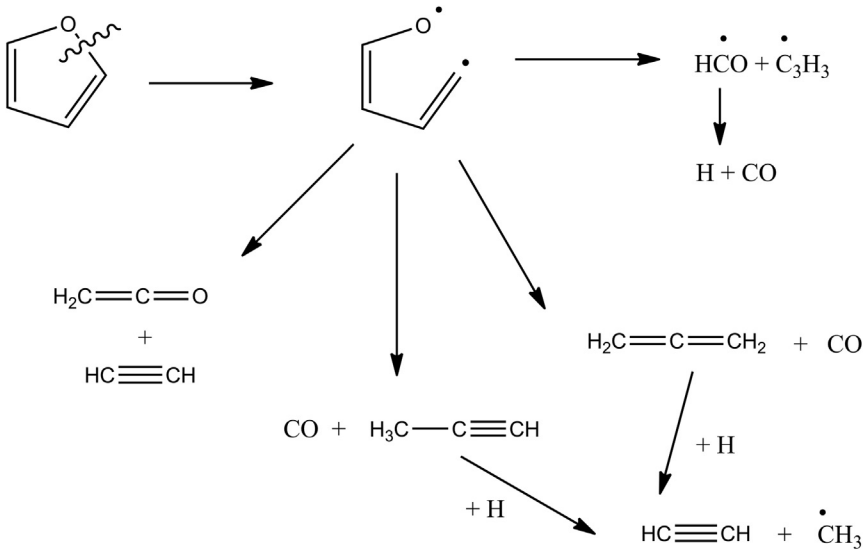


**Figure 12** Four decomposition pathways for furan via a common biradical intermediate. *Adapted from Organ and Mackie.*[196] *Adapted with permission from Phys Chem Chem Phys. Owner Societies.*

In two nearly concurrent studies in 2000, Sendt et al.[199] and Liu et al.[200] revisited the initial mechanisms for furan decomposition via computational chemistry techniques; each group suggested that different pathways were more likely than the biradical mechanism initially proposed, due to the high energetic requirements of direct ring scission. Sendt et al. used CASSCF, CASPT2, and G2(MP2) calculations to model the carbene pathways seen in Figure 13 and to demonstrate that they could account for the known experimental kinetics of furan and the major products. Liu et al. explored alternative mechanisms via G2(MP2) calculations.

In 2009, Vasiliou et al.[201] used a silicon carbide reactor with time-of-flight mass spectrometry detection to identify the early decomposition products of furan, lending further insight into the immediate decomposition of this species. Their experimental work supported the calculations of Sendt et al., as they identified products proposed via their mechanism and also confirmed the hypothesized formation of propargyl radical at higher temperatures, leading to implications for sooting behavior.

Computational studies of furan decomposition reactions have increased significantly in recent years and lend further insights to the pyrolytic

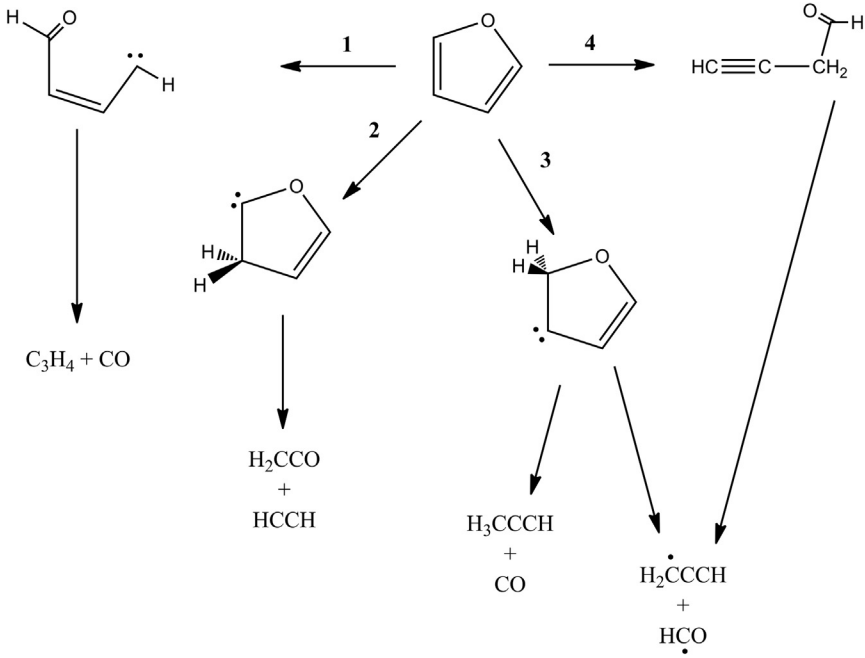


**Figure 13** Unimolecular decomposition pathways of furan. *Reprinted with permission from Sendt et al.[199] Copyright 2000 American Chemical Society.*

mechanisms of furan and its derivatives. In 2009, using CBS-QB3, CBS-APNO, and G3 composite calculations with a wide array of isodesmic reactions, Simmie and Curran[202] provided formation enthalpies and bond dissociation energies (BDE) for a variety of substituted alkylfurans, to better serve chemical kinetic models of these species. They noted that ring C—H bonds in furans and ring C—$CH_3$ bonds in alkylated furans have particularly high BDE values, due to the inability of the resulting radicals to either effectively delocalize their spin density or distort the aromatic network, while the methyl groups on alkylated furanyl species have lower C—H bonds than those in alkylated HC species (Figure 14). Thus, the furanylmethyl radicals are particularly important radical intermediates to consider. Vogulhuber et al.[203] supported these findings in 2011 via an experimental determination of the $C_\alpha$—H bond dissociation energy of furan.

In 2011, using composite methods (CBS-QB3, CBS-APNO, G3, and G3MP2B3), Simmie and Metcalfe[204] modeled the decomposition of 2,5-DMF, looking at three initiation steps: a 3,2-H shift to form β-carbene; a 2,3-methyl shift to form α-carbene (Figure 15); and the loss of H atom from the methyl group. They noted that the $CH_2$—H scission and β-carbene pathways were dominant and that several subsequent ring-opening reactions could result in a variety of little-studied intermediates. They identified likely mechanistic pathways between 2,5-DMF and 2-MF and explored addition and abstraction pathways available to 2,5-DMF. Similarly, high-level calculations have since been used to explore enthalpies of formation of furan, 2-MF, and 2,5-DMF,[205] as well as of several substituted furans and furan derivatives.[206]

Given the relatively low bond dissociation energies of the $CH_2$—H bonds in MFs, the reactions of the resulting methyl radicals are particularly important. In 2012, Sirjean and Fournet[207] explored the decomposition of 5-methyl-2-furanyl radical and noted that its most likely reaction path

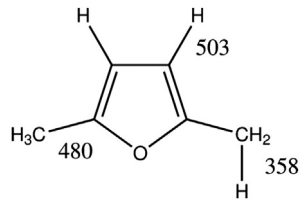


**Figure 14** Bond dissociation energies (kilojoules per mole) in 2,5-DMF for a typical $C_{ring}$—H bond, methyl group $CH_2$—H bond, and $C_{ring}$—$C_{methyl}$ bond. *Reprinted with permission from Simmie and Metcalfe.[204] Copyright 2011 American Chemical Society.*

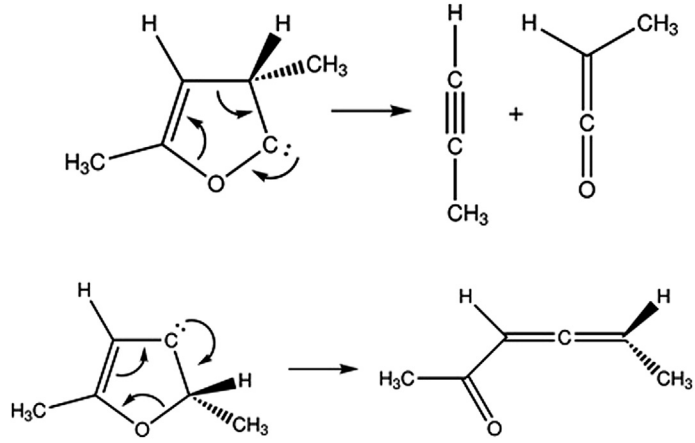

**Figure 15** α-Carbene (top) and β-carbene (bottom) formed from 2,5-DMF, and selected products formed from each carbene. *Adapted with permission from Simmie and Metcalfe.*[204] *Copyright 2011 American Chemical Society.*

involved ring opening and enlargement to form cyclohexadienone. They subsequently expanded on this work in developing a potential energy surface for the unimolecular decomposition of 2,5-DMF via CBS-QB3 calculations, observing that the most likely reaction was a 3,2-H atom transfer yielding hexa-3,4-dien-2-one, followed by C—H bond fission at the methyl group (with an ~70%:~30% product distribution between these two paths).

Oxidation pathways of furans are also of interest. In 2000, Fadden and Hadad modeled the rearrangements possible for the formation of peroxy radicals derived from five- and six-membered heteroaromatic rings,[208,209] including the peroxy radicals derived from furan. More recently, in 2013, Davis and Sarathy[210] examined several reactions with relevance to the atmospheric chemistry (oxidative) pathways of 2-MF (one such reaction scheme is illustrated in Figure 16). They used CBS-QB3 and G4 composite methods to investigate the reactions available to species formed following OH addition to the 2-MF ring and $O_2$ addition to the radical derived from that ring. They saw that general reaction preferences varied depending on whether $O_2$ added *cis* or *trans* to the product of initial OH addition to the ring. Many different pathways of the resulting peroxy radicals were then explored; 1,4-H atom shifts in which the peroxy group abstracted the H atom substituted *ipso* to OH were particularly favorable (Figure 17). They also noted a new reaction, deemed a Waddington concerted elimination, available to some peroxy radicals, wherein H atom transfer occurs concurrently

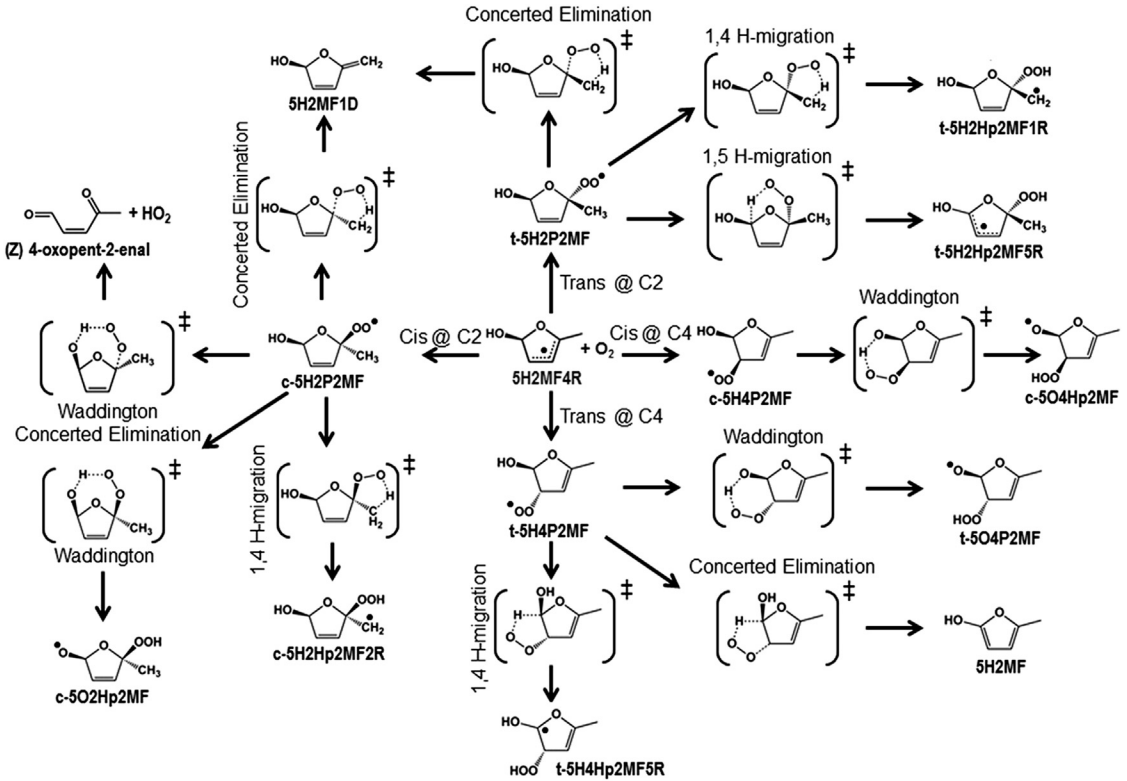


**Figure 16** Reaction mechanism diagram for the 5-hydroxy-2-methyl-furan-4-yl radical (5H2MF4R) + $O_2$ reaction and subsequent pathways. In the naming scheme employed by the authors, each species name takes the form n(H/O)m(P/Hp)2MF, where n and m represent the positions of the hydroxy/oxy or peroxy/hydroperoxy groups, respectively. In the authors' numbering scheme, the methyl carbon is designated as position 1, the methyl-substituted carbon as position 2, and so on around the ring. Moreover, c and t designate cis and trans addition of the peroxy group relative to the initial hydroxyl radical addition, while R denotes position of a carbon-centered radical and D designates a double bond. *Reprinted with permission from Davis and Sarathy.*[210] *Copyright 2013 American Chemical Society.*

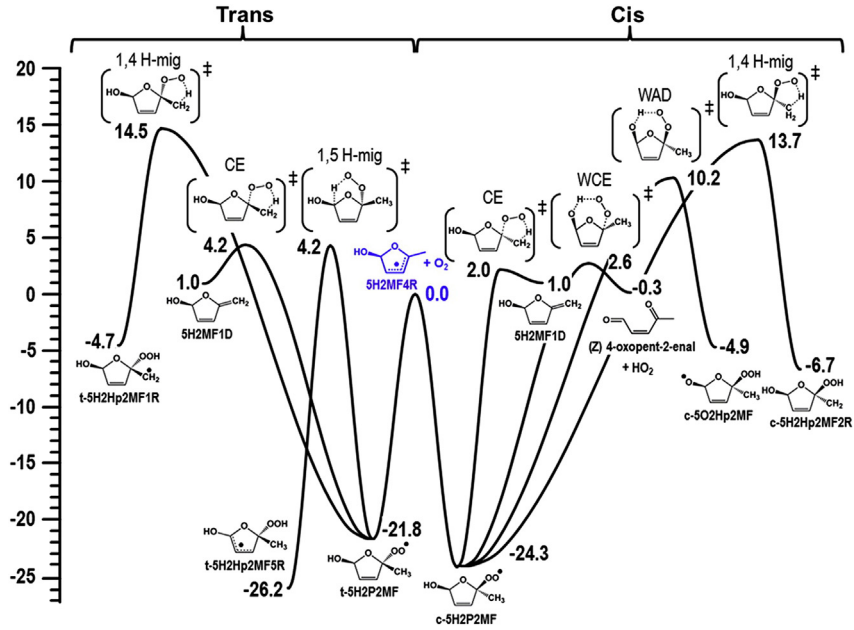


**Figure 17** Diagram comparing the potential energy surfaces of the possible reactions initiated from the 5-hydroxy-2-methyl-furan-4-yl radical (5H2MF4R) + $O_2$ reaction, when $O_2$ adds to the radical at the 2-position (methyl-substituted position). Values are in kilocalories per mole at 298 K. *Reprinted with permission from Davis and Sarathy.*[210] *Copyright 2013 American Chemical Society.*

with the breakage of the C—OO bond, ultimately yielding $HO_2$ and a ring-opened carbonyl species. The highly functionalized nature of these peroxy radicals affords a wide variety of possible reaction pathways.

Somers et al.[211] reported in 2014 a thorough exploration of the pyrolysis of 2-MF via composite-level calculations and kinetic modeling. In parallel with the most crucial initiation pathways identified for 2,5-DMF, three pathways were identified as most significant: two involving β-carbene intermediates that could undergo ring opening to ultimately form several HC and functionalized species and a third involving 2-furanylmethyl radical, ultimately yielding a variety of species including *n*-butadienyl radical and carbon monoxide (Figures 18—20).

Less studied than the methyl-substituted furans but pertinent to the study of biomass-related species are methoxy-substituted furans. These species were first identified as unusually reactive more than 15 years ago, after a coiled-tube flow reactor study on 2-methoxyfuran by Bruinsma et al.[212] In 2010, Hudzik and Bozzelli[213] used DFT and composite methods to

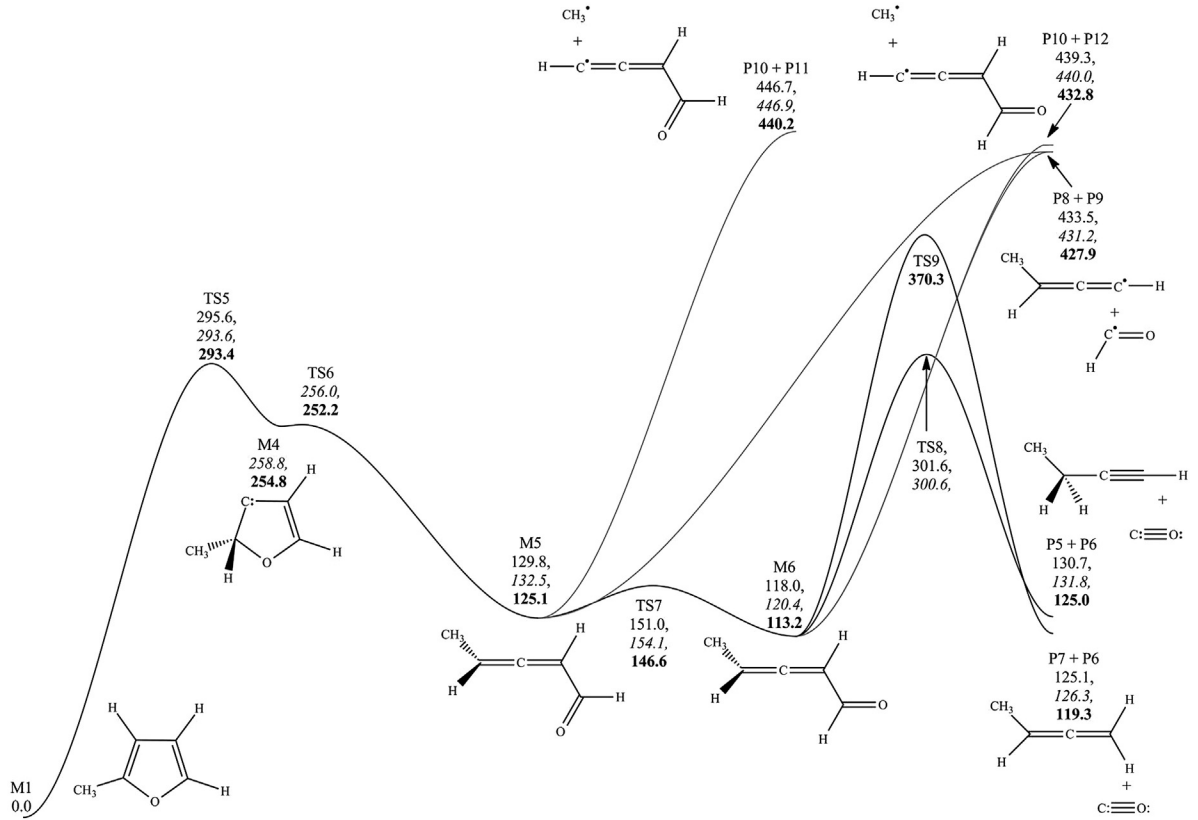


**Figure 18** Potential energy surface for the formation and decomposition of β-carbenes formed from a 3 → 2 hydrogen shift. CBS-QB3, CBS-APNO, and **G3** energies in kilojoules per mole at 0 K relative to 2-MF. Variational processes in gray scale. *Reprinted with permission from Somers et al.*[211] *Copyright 2014 Royal Society of Chemistry.*

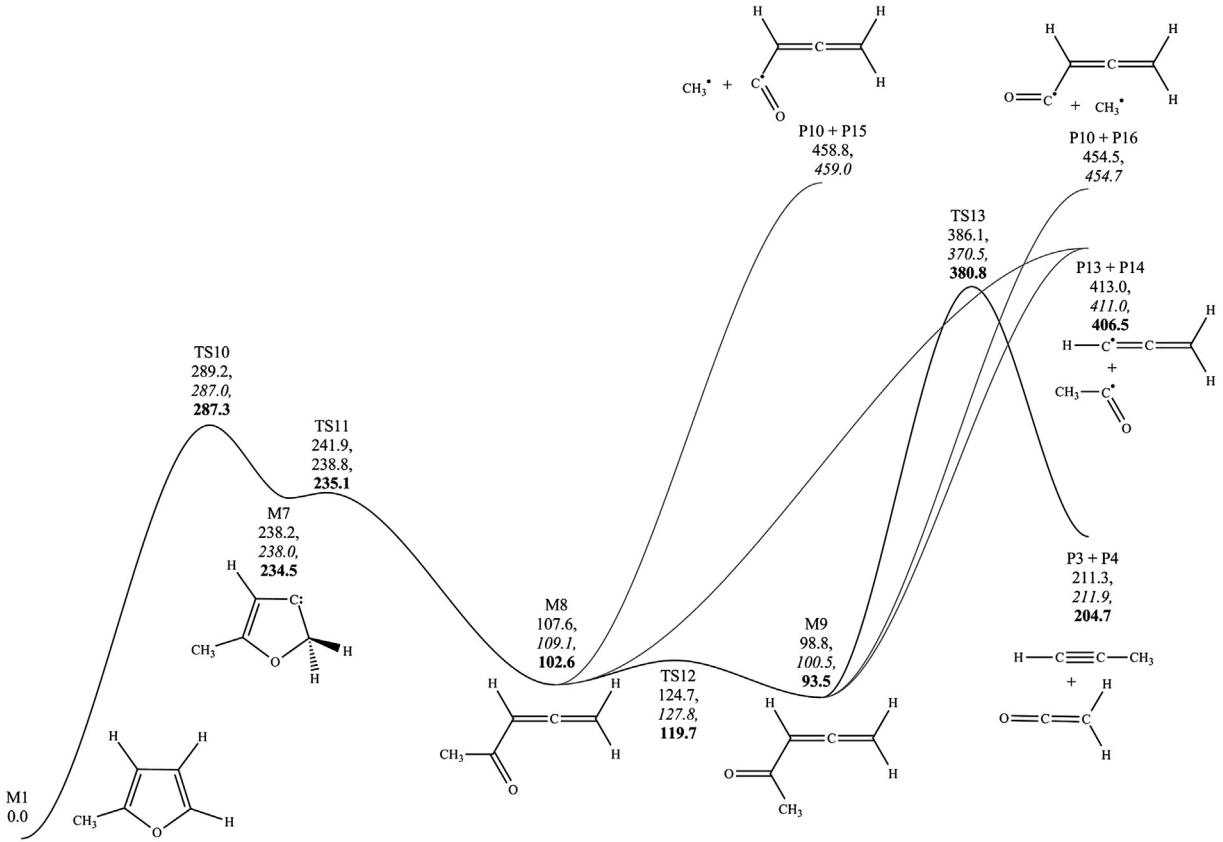


**Figure 19** Potential energy surface for the formation and decomposition of β-carbenes formed from a 4 → 5 hydrogen shift. CBS-QB3, CBS-APNO, and **G3** energies in kilojoules per mole at 0 K relative to 2-MF. Variational processes in gray scale. *Reprinted with permission from Somers et al.*[211] *Copyright 2014 Royal Society of Chemistry.*

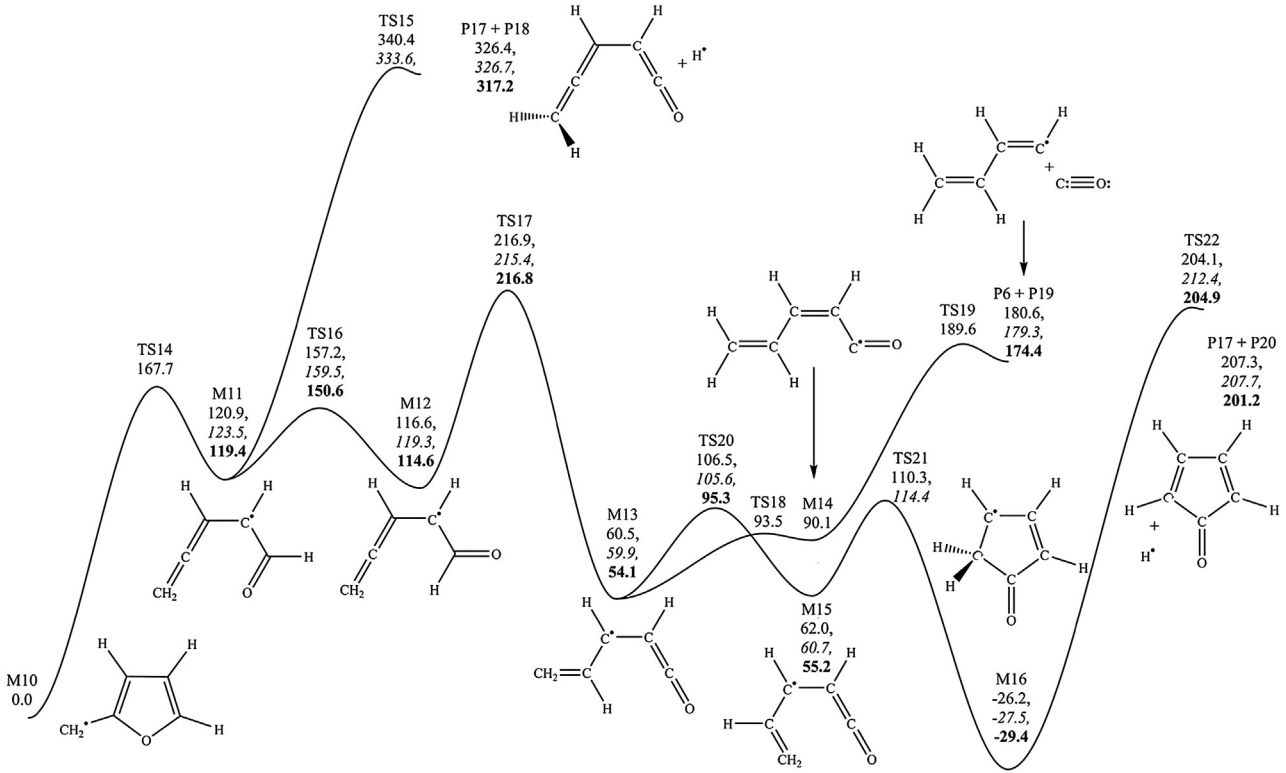


**Figure 20** Potential energy surface for the decomposition of the 2-furanylmethyl radical. CBS-QB3, CBS-APNO, and **G3** energies in kilojoules per mole at 0 K relative to 2-furanylmethyl. *Reprinted with permission from Somers et al.*[211] *Copyright 2014 Royal Society of Chemistry.*

characterize the structure of 2- and 3-methoxyfuran, as well as to calculate enthalpies of formation and bond dissociation energies in these species; they saw BDEs of $\sim$500 kJ mol$^{-1}$ for C–H bonds in the furan ring itself (in keeping with earlier experimental and computational observations of the unlikely reactivity at these positions), whereas the methoxy methyl group had C–H BDEs of 410 kJ mol$^{-1}$. In 2013, Simmie et al.[214] noted that the O–C bond dissociation energy for the bond between the methoxy oxygen and methyl carbon was significantly lower, at roughly 190 kJ mol$^{-1}$, leading to the overall high reactivity of the 2-methoxyfuran; they suggested that the resulting 2-furanyloxy radical is likely to be particularly long lived, analogous to the case of phenoxyl radical.

Recently, the comprehensive combustion pathways of furan and alkylated furan biofuels have also been explored. In 2013, Somers et al. explored the pyrolysis and oxidation pathways of 2,5-DMF,[215] as well as the oxidation of 2-MF.[216] Studying 2,5-DMF decomposition, the authors developed a chemical kinetic mechanism supplementing known, relevant submechanisms with recent high-level calculations and compared the results of this model to a shock tube study completed over a 1200–1350 K temperature range and 2–2.5 atm pressure range. They noted several important reactions worthy of further investigation: the reactions of 2,5-DMF with oxygen and with hydroperoxyl radical, the reactions of 5-methyl-2-furanylmethyl radical with hydroperoxyl radical and methyl peroxy radical, and the addition of OH to 2,5-DMF. They also highlighted the need for further study of ethylfurans and formylfurans, which were proposed to be important intermediates in the oxidation pathways of 2,5-DMF.

Likewise, a thorough three-part study of the combustion chemistry of furan group biofuels was recently completed; in 2014, the combustion chemistry and flame structure were explored by Liu et al. for furan,[217] by Tran et al. for 2-MF,[218] and by Togbe et al. for 2,5-DMF,[219] using the same reaction model for all three to better compare the reactivity of each fuel. The authors emphasized several trends of environmental concern: acetylene production played a major role in all three flames, most notably in furan; conjugated HC species that could serve as soot precursors (namely, 1,3-cyclopentadiene, benzene and phenol) were most likely to form in 2,5-DMF; and multiple carbonyl species were detected in each of the three flames, but to a lower extent in 2,5-DMF flames than in furan and 2-MF. Different pollutants were seen to different extents in each of several fuels, some HC based and some oxygenated. Generally speaking, the lowest amount of soot precursors was seen in acyclic

oxygenated fuels, while cyclic oxygenated fuels generated soot precursors in amounts similar to HC fuels.

### 3.1.2 Combustion Pathways of Saturated Ethers (Tetrahydrofuran, Tetrahydropyran, and Derivatives)

While saturated cyclic ethers such as THF have seen less attention than furanic species, they have been the subjects of increasing exploration in the past few years. In addition to their role in biomass combustion, cyclic ethers often are seen as intermediate products in combustion reactions of HC fuels.

In 1946, Klute and Walters[220] provided the first exploration of the pyrolysis of THF, observing the formation of ethene, methane, and CO as major products during pyrolysis over a temperature range of 802–842 K and a pressure range of 50–300 torr. They proposed that the main breakdown pathway of THF involved formation of ethene and acetaldehyde (which ultimately decomposed to methane and carbon monoxide); a secondary pathway involved formation of propene and formaldehyde (which then formed carbon monoxide and $H_2$). Their work was followed several decades later by Lifshitz et al.,[221] in a 1986 study exploring initiation pathways available via a shock tube study of isotopic derivatives of THF over the temperature range 1070–1530 K. These authors noted that two pathways were possible: the first yielded ethene and a biradical [$(CH_2)_2$–O], while the second yielded propene and formaldehyde.

Very recently, Verdicchio et al.[222] provided a computational study of the unimolecular decomposition reactions possible for THF, focusing on biradical, carbenic, and pericyclic pathways via CBS-QB3 calculations. Of note for THF compared to pyrolytic pathways of analogous HC species, the presence of the oxygen atom leads to asymmetry in the molecule, leading to the possibility of more distinct radical pathways than in cyclohexane. Carbenes do not play a major role in HC decomposition but had been previously seen to play a major role in furan decomposition; conversely, biradicals in furans were not plausible intermediates due to the high endothermicity of the relevant bond scissions, but biradical species have been seen in HC combustion fuel pathways. Thus, a wide variety of pathways were explored, and four were seen to be particularly significant: C–O bond scission to form a biradical species, α-carbene formation and concomitant ring opening, a pericyclic reaction yielding 3-butenol, and a pericyclic reaction in which $H_2$ is lost to form a biradical intermediate that can ultimately decompose to form propene and carbon monoxide. The authors proposed that the stability of some of the α-carbene species might make

them significant intermediates to consider and also noted that it will be difficult to experimentally differentiate between biradical and carbene mechanisms experimentally, given the similar product distributions from each intermediate.

2-Methyltetrahydrofuran (2-MTHF) has itself demonstrated potential as a biofuel, in addition to its role as a model compound.[181,188] In 2012, Simmie[223] explored the kinetics and thermochemistry of THF, 2-MTHF, and 2,5-DMTHF via CBS-QB3, G3, and CBS-APNO methods, noting that these data were not only useful in terms of understanding alternative fuels but also would likely prove instructive in modeling the cyclic ethers formed in low-temperature HC combustion. This work noted the relative lack of thermochemical or kinetic data about these species and highlighted some key commonalities and differences between HC chemistry and the chemistry of the cyclic heteroatomic fuels. For instance, the carbon–carbon bond dissociation energy for methyl group loss was seen to be comparable among methylcyclopentane[224] (358.2 kJ $mol^{-1}$), MTHF (361.6 ± 2.4 kJ $mol^{-1}$), and DMTHF (360.8 ± 2.1 kJ $mol^{-1}$). These saturated species saw significantly lower values than did the unsaturated furans (which demonstrated carbon–methyl bond energies around 480 kJ $mol^{-1}$). While ring-opening combustion pathways yielded some intermediates comparable to those seen in HC combustion, eliminations to form partially unsaturated dihydrofurans were also seen to occur, meriting further consideration of these relative-unexplored species in mechanism development.

In 2013, Moshammer et al.[225] examined the reactivity of 2-MTHF via an experimental flame (low-pressure, fuel-rich) study and developed a kinetic model for its combustion, building on Simmie's work and other studies. They reported generally good agreement between experimental observations and most of the model's predictions, highlighting the underprediction of THF production via the mechanism as an exception. Emissions of interest to environmental chemistry were explored: aldehydes and soot precursors were identified. They noted less potential for benzene production than in the unsaturated ethers.[211,217,218] Reaction pathways reflected the importance of hydrogen atom loss and ring-opening pathways, as well as demonstrated the range and variety of HC and functionalized products.

Chakravarty and Fernandes[226] examined the kinetics of the reactions of 2-MTHF and 2,5-DMTHF with hydroperoxyl radical, looking at hydrogen atom abstractions via CCSD(T)/cc-pVTZ//B3LYP/cc-pVTZ and CBS-QB3 calculations; they also completed a parallel study on methylcyclopentane. They noted that H atom abstraction at C2 was most likely

and H atom abstraction at the methyl group was least likely, for both 2-MTHF and 2,5-DMTHF; they also reported a faster overall reaction for the dimethyl-substituted species. Comparing their work to other mechanistic studies available in the literature, they noted generally different activation barriers and thus rate constants for linear alkanes, cyclic alkanes, and cyclic ethers.

Labbe et al.[227] explored the chemistry of THP via a flame study, developing a skeletal mechanism for THP combustion by comparisons to the mechanism of the HC analog cyclohexane[228] and supplemental calculations via CBS-QB3. Three sites for hydrogen atom loss are available in THP, each of which leads to its own set of decomposition pathways, primarily via β-scission. Benzene formation was noted and proposed to form via molecular weight growth, since the presence of oxygen prohibits the direct dehydrogenation of THP to a benzene ring.

### 3.1.3 Mechanistic Studies of Other Functionalized Monocycles

Interest in biomass-derived fuels has correspondingly led to increased attention to a variety of other functionalized monocyclic systems, including those described below, as reactive intermediates, pollutant precursors, or platform molecule targets (Figure 21).

#### 3.1.3.1 Morpholine

Biomass combustion can lead to the formation of nitrogen-containing compounds.[229] The presence of a second heteroatom in a model species, as well as the role of the nitrogen atom, has been explored via studies of morpholine (1-oxa-4-aza-cyclohexane), a common fuel additive.[11] Noting in particular the role that fuel-bound nitrogen can play in harmful $NO_x$ emissions, Lucassen et al.[230] explored the flame chemistry of morpholine at 40 mbar and 298 K. They saw that the combustion of morpholine differed from that of cyclohexane and oxygenated fuels, leading to less HC buildup and soot potential, forming comparable amounts of aldehyde intermediates, and resulting in the formation of $N_2$ and NO from the fuel-bound nitrogen. Altarawneh and Dlugogorski[231] used G3MP2B3 calculations along with RRKM methods to model morpholine decomposition. Starting from each of multiple initiation pathways (Figure 22), they modeled the resulting decomposition pathways, providing mechanistic rationales for previously seen experimental products such as vinyloxyethene, etheneamine, and ethenol. They cited a 1,3-H atom transfer as the dominant early step in the ring opening of morpholine (this pathway yields species M5 in Figure 22). They

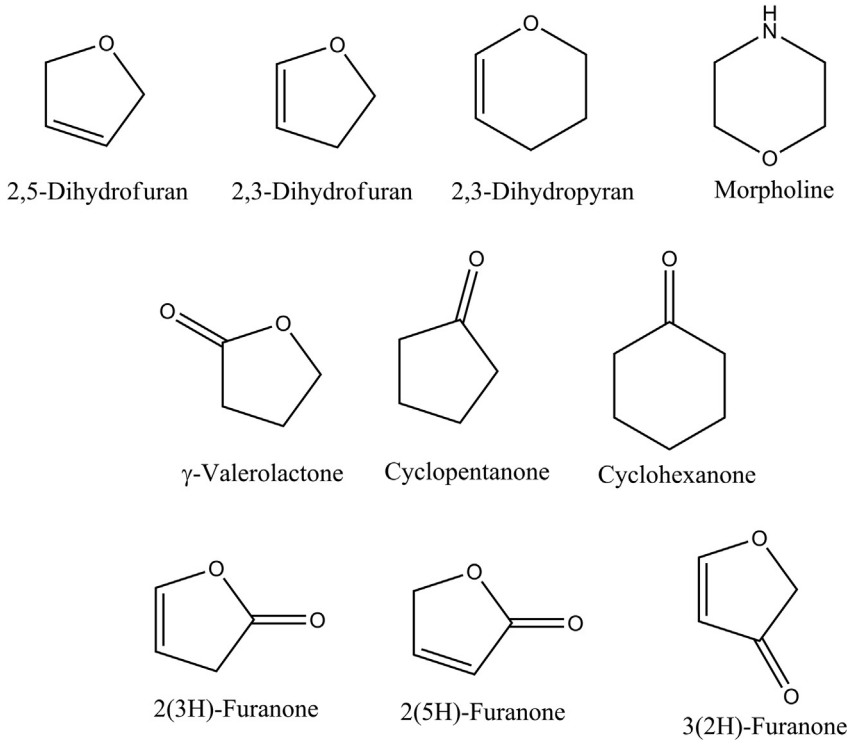


**Figure 21** Other cyclic ethers, esters, and functionalized compounds of interest to modeling biomass combustion.

noted that the decomposition pathways would result in several highly functionalized radicals and alkenes.

Li et al.[232] recently refined the existing reaction set for morpholine[230] while modeling high-pressure oxidation and pyrolysis pathways of that species. They achieved the best agreement between mechanism and experiment by treating reactions analogous to the ring opening of cyclohexane to 1-hexene as the dominant pathways and accounting for the difference between C—N and C—C bond strengths in the energy terms, noting the two fastest pathways shown in Figure 23.

### 3.1.3.2 Glucose and Fructose

The reactions of glucose and fructose (Figure 9) have been of interest from a wide variety of perspectives, including the development of catalytic pathways for conversion of biomass to platform chemicals.[169,177,178] These reactions overlap to an extent with the decomposition pathways available to

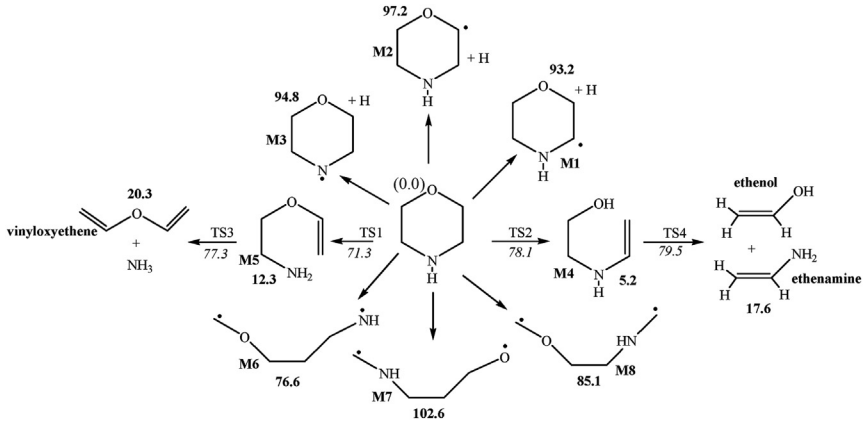


**Figure 22** Potential energy surface for the initial decomposition of morpholine. Values in bold are reaction enthalpies and values in italics are activation enthalpies. All values (in kilocalories per mole) are relative to the parent morpholine calculated at 298.15 K. *Reprinted with permission from: Altarawneh and Dlugogorski.[231] Copyright 2012 American Chemical Society.*

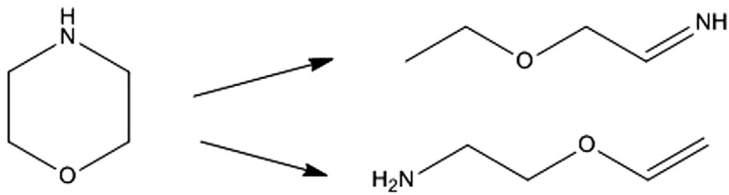


**Figure 23** Key reaction pathways for morpholine identified in Ref. 232.

monocyclic compounds used to model cellulose chemistry. Sanders et al.[233] proposed mechanisms for the pyrolysis of several monosaccharides, including glucose and fructose. Paine et al.[234] used $^{13}C$ labeling studies to track the decomposition of glucose to several carbonyl compounds. Assary and Curtiss[235] used G4 calculations to investigate reactions available to glucose and fructose, including dehydrations, tautomerizations, and isomerizations. Seshadri and Westmoreland[236] examined several concerted reactions of interest to glucose decomposition using CBS-QB3 calculations. They highlighted reaction paths involving dehydrations, keto-enol tautomerizations, and retroaldol reactions. Mayes et al.[237] recently examined the reaction pathways of α- and β-glucose via an experimental and computational study, to determine whether both anomers would play a role in cellulose pyrolysis, since only the β-anomer is present in cellulose itself. They completed an exhaustive study of pathways between glucose and

the key products 5-HMF and levoglucosan and recommended that both anomers of glucose be considered with respect to their impact on cellulose decomposition.

#### 3.1.3.3 Other Cyclic Oxygenates

Unsaturated cyclic ethers have been proposed as intermediates in the decomposition of THF and derivatives,[223] but studies on their chemistry are limited. Alwe et al.[238,239] examined the reactions of THF, THP, 2,5-dihydrofuran, 2,3-dihydrofuran, and 3,4-dihydropyran with common atmospheric species (OH, $O_3$, and Cl), noting that the rate coefficients for the ethers differed from those of their HC analogs and exploring the effects of double-bond position and ring strain on reactivity. Enthalpies of formation of olefinic ethers have been calculated by Taskinen et al. via experiment and DFT[240] and via G3MP2B3 calculations.[241] Boot et al.[242] highlighted the combustion behavior of several oxygenated species, including cyclohexanone. Cyclic esters have likewise been seen as important species in biomass pyrolysis but have undergone relatively little exploration. Vasiliu et al. have used G3MP2 calculations to explore thermodynamic properties of molecules highlighted by the Department of Energy[243] as integral to biomass chemistry, including several cyclic esters, namely, 5-hydroxymethylfurfural, γ-valerolactone, and 3-hydroxybuyrolactone.[244,245] Lucius et al. have examined C—H bond dissociation enthalpies in a wide variety of alkyl-substituted and functionalized THF, THP, cyclohexanone, and cyclopentanone derivatives.[246] Wurmel and Simmie[247] studied the thermodynamic and kinetic properties of 2(3H)-, 2(5H)-, and 3(2H)-furanones, along with several methyl derivatives, via several high-level composite methods. They also explored the kinetics of reactions of these species with hydrogen atom and methyl radical.

## 3.2 Lignin Model Compounds

### *3.2.1 Phenethyl Phenyl Ether*

Most mechanistic studies used to explore the complex system of lignin have focused on PPE, which provides a simplified version of the most prevalent linkage in lignin, guaiacyl-glycerol-β-ether (Figure 24).

Klein and Virk[248] proposed four possible pathways for PPE decomposition: homolytic C—C bond dissociation, homolytic C—O bond dissociation, a retro-ene reaction, and the Maccoll elimination (Figure 25). They noted that pyrolysis of PPE (both neat and in the presence of the H donor tetralin) at temperatures from 573 to 773 K yielded phenol and styrene and

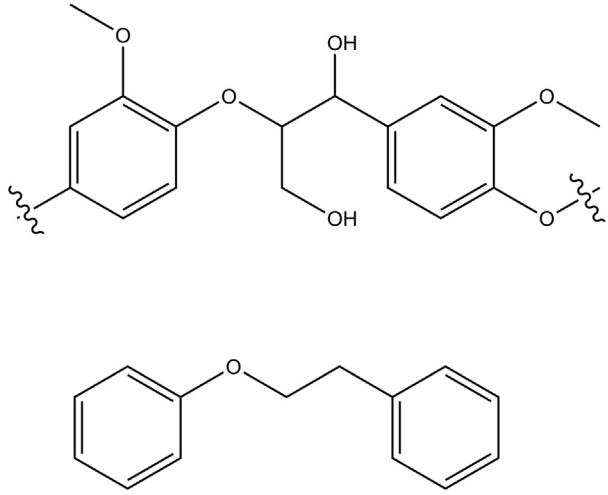


**Figure 24** Representative guaiacyl-glycerol-β-ether linkage found in lignin (top) and model compound PPE (bottom). *Adapted with permission from Klein and Virk.*[248] *Copyright 1983 American Chemical Society.*

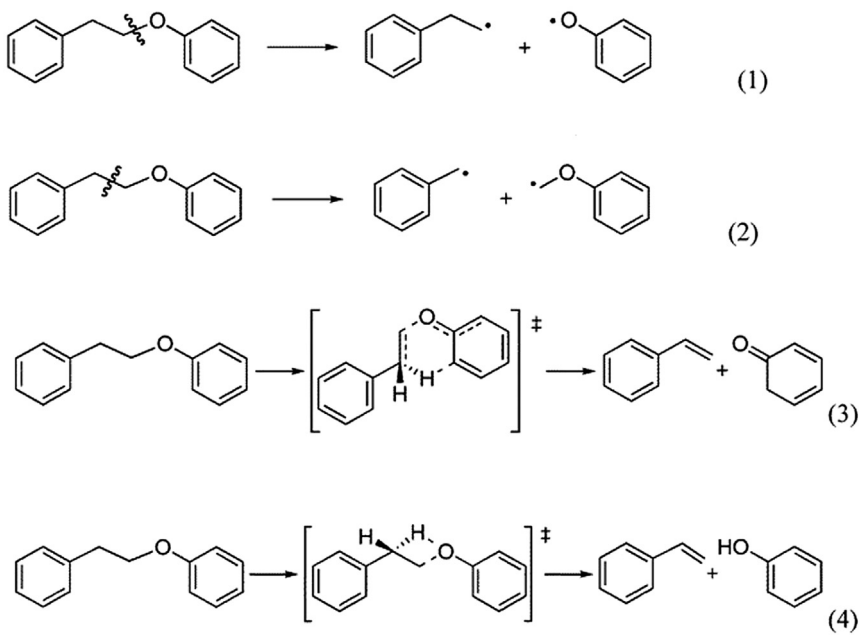


**Figure 25** Initiation pathways possible in the decomposition of PPE: homolytic bond dissociation of the C—O bond (reaction 1), homolytic bond dissociation of the C—C bond (reaction 2), the retro-ene reaction (reaction 3), and the Maccoll elimination (reaction 4). *Adapted with permission from Jarvis et al.*[251] *Copyright 2011 American Chemical Society.*

proposed that the retro-ene reaction was most likely under these conditions, while radical reactions played minor roles. Conversely, Gilbert and Gajewski[249] studied PPE thermolysis in both the liquid and gas phase over a temperature range of 623–663 K and proposed that a free radical mechanism was responsible.

Britt et al.[250] examined the pyrolysis of PPE over the 603–698 K temperature range, in both the liquid and gas phases, to better understand this discrepancy. They observed styrene and phenol, as seen in previous work, but they also observed the formation of benzaldehyde and toluene. They traced these two sets of products to two reaction pathways beginning with hydrogen atom abstraction from either the α- or β-position of PPE (Figure 26), defining this parameter as α/β-selectivity. Abstraction from the α-position led to styrene and phenol as the major products, while abstraction from the β-position led to benzaldehyde and toluene. The authors saw data consistent with a radical chain mechanism and suggested that bond dissociation at the α-position was more likely, following an investigation of isotope effects.

Jarvis et al.[251] used a hyperthermal nozzle with short residence times and low substrate concentrations, over a temperature range of 573–1623 K, to better explore the initial reaction steps of PPE decomposition, along with the corresponding steps in phenyl ethyl ether, in which homolysis of the C–O bond was less likely. They also completed CBS-QB3 calculations of the reaction pathways, ultimately concluding that the concerted reactions are likely at low temperatures and C–O bond-breaking pathways become a factor above 1273 K. Huang et al.[252] completed a DFT study on 10 possible PPE decomposition pathways, two of which were concerted mechanisms and eight of which were free-radical mechanisms; they saw that the concerted mechanisms were the preferred reaction channels and that these mechanisms overlapped with the retro-ene and Maccoll pathways explored previously.

Studies of substituent effects on the PPE decomposition mechanisms have been instructive. Kawamoto et al. have explored the effect of

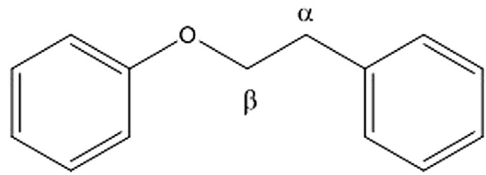


**Figure 26** Positions for possible hydrogen atom abstractions in PPE.

functional group substitution on a variety of model dimers, including those with β-O-4 linkages.[253,254] Elder and Beste[255] modeled the decomposition reaction pathways available to a variety of substituted PPE derivatives using M06-2X calculations, examining the pathways of guaiacyl, syringyl, and *p*-hydroxy models, noting similar preferences for the retro-ene reaction but higher reaction barriers compared with unsubstituted PPE.

Several other aspects of the reactivity of PPE have been examined. Beste et al. have investigated α/β-selectivities,[256,257] bond dissociation enthalpies,[258,259] and product selectivities[260] in PPE and its derivatives and have completed a wide variety of kinetic studies on its reaction pathways, such as hydrogen atom abstractions[261] and phenyl shifts.[262]

### 3.2.2 Other Lignin Models

In addition to PPE, studies of other lignin model systems have been reported in the literature. In addition to the model monomeric lignols shown in Figure 8, some other common lignin linkages and model systems are shown in Figure 27.

Asmadi et al.[263] examined the thermal reaction of guaiacol and syringol via a closed ampoule reactor, noting that decomposition of each species begins with the cleavage of the O—$CH_3$ bonds and identifying differences between their subsequent reactivity; they have also examined[264] the reactivity of multiple species arising from lignin pyrolysis, namely, catechols/pyrogallols and cresols/xylenols. Elder calculated bond dissociation enthalpies in dibenzodioxocin[265] and pinoresinol,[266] models for other common linkages in lignin, using DFT calculations. Also via DFT, Parthasarathi et al.[267] examined 65 different lignin model compounds encompassing several different linkages: β-O-4, α-O-4, β-1, α-1, β-5,

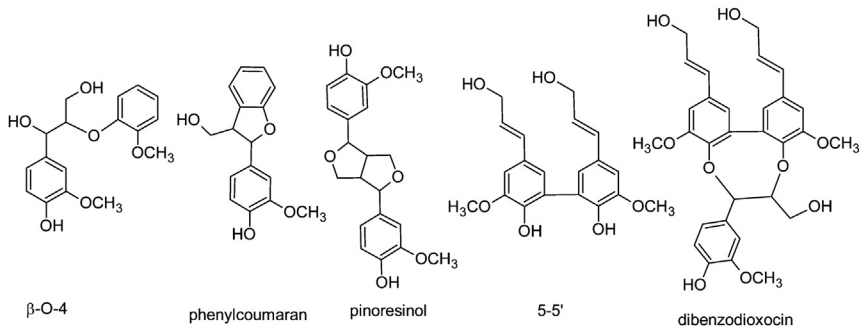


**Figure 27** Principal interunit linkages in lignin. *Figure reprinted with permission from Elder.[266] Copyright 2014 American Chemical Society.*

and 5-5; they have reported bond dissociation enthalpies for both the C−C and O−C linkages in all these compounds, identifying the strongest and weakest bonds for each group. Kim et al.[268] completed another wide-ranging DFT study of bond dissociation enthalpies in lignin dimers and their oxidized derivatives; they highlighted the importance of conformational analysis with these functionalized species. Holmelid et al.[269] looked at the degradation reactivity of several lignin model dimers, exploring α-O-4, β-O-4, α-hydroxy-β-O-4, and aryl-protected glycerol type linkages. Huang et al.[270] examined the breakdown of guaiacol via B3LYP calculations, considering homolytic cleavage of the O−$CH_3$ bond, homolytic cleavage of the O−H bond, and H atom addition to the benzene ring. Gardrat et al.[271] studied the thermal degradation of a dibenzodioxocin model compound via mass spectrometry, differential scanning calorimetry, and thermogravimetry, along with supporting calculations. Custodis et al.[272] recently reported a pyrolysis microreactor study on diphenylether and guaiacol as models for lignin.

## 3.3 General Challenges in Modeling Lignocellulosic Biofuels

Overall, developing detailed chemical kinetic mechanisms for cellulose- and lignin-derived biofuels is more complicated than developing models for biofuels derived from animal fats and plant oils, which consist of relatively simple saturated and unsaturated alkyl esters. Converting cellulose or hemicellulose to a fuel requires that the biomass first undergo various processes (e.g., gasification, pyrolysis, hydrolysis) breaking it down into sugars (e.g., glucose, xylose), then transforming these sugars into furan derivatives (e.g., 5-HMF, furfural).[273] These platform molecules are then converted to useable acid/esters, glycerols, ethers, alcohols, etc. in order to produce liquid HC fuels.[274] Similar processes are required to convert lignins (wood material) to biofuels; a fundamental difference is that lignin is a phenolic polymer. Thus, in order to be converted into HC fuels (or pyrolysis oils), the phenol derivatives must undergo hydrodeoxygenation, eliminating oxygen and introducing hydrogen.[275]

Mechanisms related to cellulose-derived biofuels focus on the chemistry of furan derivatives. Beyond the unimolecular decompositions and oxidative reactions discussed previously in this section, furan derivatives can undergo a wide variety of other reactions. They are transformed by pyrolytic, hydrolytic, and other chemical processes to longer chain ethers ($R_1OR_2$) and aldols (hydroxyaldehydes and hydroxyketones, $R_1(OH)R_2C(O)R_3$). These oxygenated species are then converted through hydrogenation and deoxygenation processes to liquid HC fuels (alkanes).

Multiple detailed chemical kinetic mechanisms have recently been developed for the combustion of furan and its derivatives.[198,215–219,276] Moreover, reaction pathways unique to the second-generation biofuels can be identified. A primary decomposition pathway for the furans involves H atom transfer leading to the formation of a carbene intermediate and ring opening to form a conjugated alkadienylketone[222]; decomposition of furanylmethyl species through ring opening can lead to the formation of cyclohexadienone species[215] and hydroxyl (OH) addition to furan rings leads to the production of alkenyl ketones and aldehydes. An important class of reactions for furans and furfurals are Diels–Alder cycloadditions: reactions with unsaturated species to form larger cyclic structures. The simplest reaction of this class would be furan reacting with ethene to form a bicyclic compound, 7-oxabicyclo[2.2.1]hept-2-ene (Figure 28); furan can also react with itself in a Diels–Alder cycloaddition to form a tricylic compound. Furthermore, a host of different oxygenated cyclic compounds can be produced from the reaction of furan (and derivatives) with different hydroxyaldehydes and ketones.[277] The pyrolytic decomposition of MF can lead to a wide range of products. In addition to producing simple HCs such as methane, ethyne, and propyne, as well as CO (the primary oxygenated product), it is observed that 1,3-butadienes, cyclopentadienes, phenols, and aromatics are formed. The simple aromatics such as benzene, toluene, indene, and naphthalene are likely produced through reactions involving cyclopentadienes, and at high temperatures, this leads to the formation of polyaromatics (soot precursors).[278] Soot formation from furan derivatives is a hindrance for use of these platform molecules as clean-burning biofuels.

As described above, models for lignin-derived biofuels typically utilize derivatives of PPEs ($PhCH_2CH_2OPh$)[255,279,280] or similar molecules as surrogates for the more complicated units in lignin (Figure 7). The mechanistic studies in this area focus on the complicated pyrolytic decomposition pathways for the surrogate ethers. A strong temperature dependence to the reaction channels is observed with a competition between homolytic bond fission reactions and a concerted retro-ene reaction.[251] β-Scissions following H atom abstractions, H atom transfer reactions, and the influence of substituents[261] are only a few examples of chemistry that needs to be better

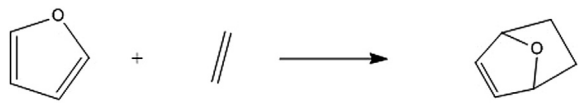

**Figure 28** Diels–Alder reaction possible for furan and ethene.

understood in order to develop detailed chemical kinetic mechanisms for lignin-derived biofuels.[267]

## 4. OVERVIEW OF THIRD- AND FOURTH-GENERATION BIOFUELS

Beyond first- and second-generation biofuels are third-generation and fourth-generation fuels, which are biofuels of interest derived from, respectively, algal biomass and bioengineered microorganisms.[281–284] (Challenges in using these latter biofuels are primarily engineering related; the identities of the fuels themselves overlap with the chemical compounds discussed previously.)

First-generation biofuels are derived from plants that are also potentially used for food, including feedstocks such as corn and sugarcane.[285] The sugars from these feedstocks are fermented to produce mainly ethanol as the fuel, although other fuels, such as butanol, can also be produced. Non-sugar-based feedstocks include animal fats, as well as soybean, palm, and rapeseed oils, which can all be converted to biodiesel fuel using a transesterification process.[286–288] The transesterification process reacts the oil triglycerides with alcohols to produce glycerol, a byproduct, and monoalkyl esters, which serve as the fuel. In first-generation biofuels, the sugar/starches or lipids are somewhat directly extracted from the plants. Second-generation biofuels and biodiesel come from more diverse feedstocks, utilizing sugars and oils from largely nonedible plant matter (or nonfood crops).[289] Cellulosic ethanol, for instance, is produced from lignocellulose from wood chips, switch grasses, and other plants, rather than edible sugars. First- and second-generation biofuels have drawbacks. The competition of first-generation fuel feedstocks with food crops has been noted. They also require significant fresh water and fertilizers, and scarce high-quality cropland. While second-generation biofuels do not compete with the food cycle, more processing steps (extraction, thermal, chemical, biochemical, purification, etc.) are needed: lignins and cellulose are first extracted, and then converted into alcohols and other fuels. These additional steps require added energy and thus negatively impact the full-cycle $CO_2$ budget. Regardless of the source, changes in the fuel combustion chemistry can also be problematic: a particular disadvantage of ethanol, for example, is that it can damage internal combustion engines, increasing exhaust temperatures, causing deterioration of emission control systems, and causing failure of various components through chemical action. As a result it cannot yet be used in large proportions in unmodified engines.

Similarly, unmodified biodiesels are not suitable as jet fuels, mainly as a result of physical properties such as viscosity and a high freezing point.

Third-generation biofuels provide a way to bypass these challenges; these fuels are those derived from algal biomass. The term algae (or macroalgae) refers to photosynthetic plants such as seaweed, while microalgae refers to microscopic cellular organisms. Algae are responsible for processing or capture of much of the $CO_2$ in the world, as well as generation of significant $O_2$. Microalgae can produce oils with very high yields, much more efficiently than terrestrial plants.[290–293] C3 terrestrial plants are plants using three-carbon fixation pathways; these have maximum potential photoefficiencies (converting solar energy into biomass energy) of about 5%, but a practical maximum about half that (2.5%). Microalgae, on the other hand, likely have practical maximum efficiencies several times that (8–10%).[294]

Microalgae are extremely adaptable to changes in conditions; this property is termed metabolic plasticity.[295] These microorganisms have the potential for producing diverse biomass, in diverse and harsh environments. Algal-based systems can be used on land unsuited for agricultural and can use non-fresh water sources such as remediated municipal wastewater[296–301] and even brackish water.[302,303] Microalgae can fixate carbon via photosynthesis, sequestering $CO_2$ from industrial sources and power plants, bioconverting $CO_2$ and recycling it back to raw materials (fuels).[304–306] This process has been termed "sunlight to biomass."[307–310]

There are several different reactor systems and variations for cultivating algae. The simplest and least expensive of these is the use of natural waters such as open ponds, lagoons, and raceway ponds.[311,312] The drawbacks include the potential for contamination by other species, losses due to evaporation, and slow uptake of atmospheric $CO_2$. A solution to some of these issues is employing closed ponds, where use of a transparent cover eliminates contamination and evaporation, and creates a greenhouse effect, extending the season for cultivation. Closed tubular photobioreactors (and other geometries) provide the ability to highly control the production of algal biofuels and obtain high yields. These systems are, however, more complicated and have much higher capital costs.[313,314]

Algal-based bioconversion processes are simplified conceptually compared to second-generation biofuel processes, since in this case, the primary reactor is a cellular organism that can bypass other processing steps that would otherwise require physical reactors (such as for separation, thermal processing, chemical transformations, etc.). This makes the overall process more efficient.

Much more research is needed, however, in order to fully understand and optimize the mechanisms of algae-based fuel production.[315,316] Metabolic engineering will be required. In assessing the feasibility of scaling up the algae-to-biofuel conversion on a commercial scale, one must consider many factors, including a full life cycle assessment of the overall process and the energy budget to manage water consumption and extraction processes.[317–320] Light is an important element in the equation. Sources of energy losses in light harvesting need to be identified and minimized, photosynthesis efficiency needs to be increased, and the problem of light penetration into dense cultures needs to be addressed. A second important element is the source of carbon: ideally, algal biofuel production would be collocated with power plants that generate $CO_2$ and mechanisms for concentrating the $CO_2$ would be developed. The third element in the algae-to-biofuel equation is the source of fertilizers (nitrogen- and phosphorous-containing fertilizers); economic and readily available sources must be established, as must be the ability to recycle the fertilizers.[313]

Finally, as described in the referenced work, bioengineered algae, also referred to as fourth-generation biofuels, could potentially produce a plethora of fuels including ethanol,[282,321] butanol,[322] methane, hydrogen,[323,324] isoprene,[325,326] vegetable oil, biodiesel, gasoline, and jet fuel.[327] There is great potential for producing fuels simply from solar energy, water, and $CO_2$: all in great abundance; the combustion behavior of these fuels can again be modeled through the use of detailed chemical kinetic mechanisms.

## 5. CHALLENGES IN BIOFUEL COMBUSTION ENGINEERING

On a global scale, interest in biofuels is related to the desire to reduce dependence on petroleum products used for transportation and heating fuels by supplementing these fuels with energy generated from biomass. The major goals are to develop sustainable (and economical) sources of renewable energy, to develop fuels that are clean burning, and to reduce greenhouse gases and toxic emissions. In considering the efficacy of various types of biomass as fuels, one must look at each potential fuel in a full life cycle assessment considering economic, environmental, and even social impacts. Similarly, when considering a life cycle assessment of particular biofuels, one must evaluate the complete impact on carbon neutrality. The combustion of biomass is theoretically carbon neutral, since the $CO_2$ generated (and released into the atmosphere) during combustion is being recycled from

$CO_2$, which was extracted from the atmosphere by the plants and used through the process of photosynthesis (light, water, and $CO_2$) to generate biomass. In a full life cycle assessment, one must also consider a wide range of other factors including health, environment, natural resources, land use changes, geographic variability, agricultural policies, and economic impacts.[328] For example, with regard to land use changes, the clearing of pasture land and rainforests to use for growing sugarcane (or palm) impacts the food supply, reduces natural $CO_2$ sequestration, and decreases biodiversity.[329–332]

From an engineering perspective, in assessing the required characteristics of the biofuels themselves, one must consider a variety of chemical, physical, and environmental properties. These include factors such as total energy content, ease of ignition (quantified by octane and cetane numbers), heat release rates, evaporative spray characteristics (vapor pressures), flammability safety (flash point), flow properties (viscosity), density, miscibility, fuel toxicity, emissions, impact on engine parts, and stability in storage.

With respect to factors pertaining to the use of biofuels, the blending of biofuels with HC fuels poses challenges.[155] For example, ethanol is hygroscopic, absorbing moisture, leading to contamination in storage tanks and phase separation of an ethanol–water layer particularly in cold weather (condensation).[333] Ethanol blends are also problematic in transportation through pipelines; ethanol can cause corrosion and also scrubs water from the walls of the pipelines.

Butanol blends are superior to ethanol in most regards. Compared to ethanol, butanol has energy content comparable to HC fuels, and lower temperature ignition characteristics; it can be used at higher concentration blends (without modification to engines), and it is a safer fuel (higher flash point and lower volatility).[334,335] In general, it lowers unfavorable emissions (HCs, CO, $NO_x$, soot) compared to HC fuels, although this depends upon engine characteristics, conditions, and other factors. The cost of production of butanol is much higher than that for ethanol, as it requires more processing steps to convert raw material (e.g., switchgrass) to useful fuel. In particular, butanol/gasoline blends have an improved emission profile (decreasing HCs, CO, and $NO_x$ emissions) and lower vapor pressures; furthermore, these blends do not damage engines like ethanol, they have heat content similar to gasoline alone (while ethanol has a limited energy density), and they are safer to transport.

The shelf life of biofuels is also a practical issue. Biodiesel is composed of oxygenated HCs and thus oxidized more quickly than pure HC fuels,

particularly for biodiesel with unsaturated compounds.[336] A nitrogen blanket can be used to prevent oxidation of biodiesel in storage tanks. Additives can be used to minimize degradation of the fuel. Biodiesel is more likely to gel in cold weather, which can be effectively solved with additives. Some biofuel blends may also cause problems by degrading fuel lines, seals, and other components. Some modifications to engines may be necessary with higher biofuel content: replacement of incompatible seals and gaskets, replacing fuel injectors to optimize fuel spray characteristics, adjusting of timing, and changes in emission control (to minimize $NO_x$).

Relative to HC fuels, biodiesel has less energy content ($\sim$10%), thereby reducing power and fuel economy. However, biodiesel used as a heating fuel has better performance, results in lower $NO_x$ emissions, and produces less $SO_2$ (because of the high sulfur content in petroleum-based heating oil).[337,338] Biodiesel fuel has higher cetane values, resulting in better ignition.[339] Biofuels are also beneficial when blended because of increased lubrication in diesel fuels; their high viscosity makes them better lubricants, increasing engine life. However, unrefined vegetable oils used as fuels can cause engine deposits, gelling, valve sticking, and other problems due to greater viscosity of the oils.

Biodiesel is a good solvent and consequently can keep an engine cleaner. However, alkyl esters (the components in biodiesel) can dissolve sediments in tanks, pipes, and engines; soften rubber compounds in hoses and gaskets; and react with plastic, brass, bronze, and galvanized metals. Moreover, biodiesel gelling can clog filters.[340]

Biodiesel fuels (composed typically of methyl, ethyl, and isopropyl esters) generally reduce particulate matter (PM), HC, and carbon monoxide (CO) emissions, because of greater oxygen content in the fuel.[341,342] The reduction in PM and HC emissions makes diesel less toxic. $NO_x$ emissions, however, are observed to increase.[343]

Exhaust emissions from biofuel blends are an important concern.[344] The oxygenated HCs naturally can lead to increased emission of carbonyl-containing compounds: aldehydes and ketones. Common undesirable emissions include formaldehyde [$CH_2O$], acetaldehyde [$CH_3CH(O)$], and acrolein, also called propenal [$CH_2{=}CHCH(O)$].[345] These are irritants that impact humans (eyes, nose, throat, lungs), particularly of those with asthma and allergies.[346] Acrolein decomposes in water and hence adversely impacts aquatic plants[347]; this decomposition is accelerated by sunlight. These carbonyl compounds and other volatile organic compounds also impact air quality as precursors to photochemical smog.[348–350]

While the above challenges represent areas that need further work and consideration, none of the difficulties appear to be insurmountable, and biofuels continue to be a promising solution in the quest to develop renewable and sustainable energy sources.

## 6. CONCLUSION

In this chapter, we have provided an overview of the development of detailed chemical kinetic mechanisms. We have addressed recent experimental and computational work of interest in developing detailed chemical kinetic mechanisms for first- and second-generation biofuels. We have also provided an overview of third- and fourth-generation biofuels and current challenges facing the combustion chemistry community.

With respect to first-generation biofuels, at this point, a general picture of the combustion chemistry of ethanol has been established. The remaining kinetic questions revolve around details concerning branching ratios, correct descriptions of the pressure dependence of reactions, and the quantitative importance of chemically activated reactions. That is certainly not to say that a fully validated model for all conditions is currently available. Even for well-studied reactions, it is often the case that different levels of theory yield different answers with respect to both the branching of competing pathways and the impact of pressure and temperature on the rate constants. Such differences translate into different predictions for global properties of interest, a particular problem when models are extrapolated outside of experimentally studied conditions. A current difficulty is the absence of reliable reference data that can be used to test theoretical predictions of elementary processes and establish which methods are most reliable.

The past decade has seen rapid progress in the development of detailed chemical kinetic models of biodiesel fuels. While there is now a general understanding of much of the chemistry, there remain various difficulties with quantitative predictions and the ability to match all experimental results over a wide range of conditions. Many of the issues have to do with the kinetics of specific elementary reactions, and there are an increasing number of publications that attempt to directly study these processes and obtain more accurate kinetics. These recent works give greater insight into combustion chemistry of methyl butanoate (MB) and other esters, both in the ignition region and in the high-temperature regime. Many of the results, however, have not yet been incorporated into the detailed kinetic models, and it remains to be seen to what extent the new data will resolve the various discrepancies

between experiment and simulation. At this point it is clear from the available work that the branching ratios for competing elementary reactions are a key determinant of behavior. It is also seen that different values are obtained at different levels of theory. Reducing the uncertainty in the relative rates, either by experiment or improved theory, is one of the future challenges in this field.

Studies of lignocellulosic biofuel model compounds have likewise increased significantly in the past decade. Reaction pathways with implications for soot, aldehydic, and $NO_x$ emissions from oxygenated and otherwise-functionalized fuels have been examined. Several key intermediates in pyrolytic pathways have been identified, including furanic carbenes, furanylmethyl radicals, dihydrofurans, and unsaturated ketones and aldehydes. Low-temperature combustion reactions available to these compounds are largely unexplored and, where modeled, involve highly functionalized peroxy radicals with the capacity for novel reactions. As cyclic oxygenated species break down into smaller acyclic species, some potential arises for overlap with extant mechanisms for HC combustion. Composite ab initio and DFT calculations have been proved to be particularly useful in recent computational explorations of these compounds and their reaction pathways.

Third- and fourth-generation biofuels employ algae and bioengineered algae, respectively, to generate a wide variety of useful fuels. These innovative techniques for fuel production are only beginning to be explored. The increasing focus on alternative fuels presents a wide variety of interesting experimental targets and challenges, from both molecular and macroscopic standpoints.

In preparing this chapter, we have focused on experiments and computational studies completed over the past few decades, regarding the complex chemistry of biofuels and their model compounds, and we have highlighted reactive intermediates likely to be of future interest, in the development of detailed chemical kinetic mechanisms for biofuels. We anticipate that the thermodynamic properties and kinetic parameters of these oxygenated fuels and their reaction pathways will continue to provide interesting targets for physical organic chemists in the years ahead.

## REFERENCES

1. Tilman D, Socolow R, Foley JA, et al. Beneficial biofuels: the food, energy, and environment trilemma. *Science*. 2009;325:270–271.
2. Bryan P. The four horsemen of the biofuels apocalypse: sustainability, technology, profitability, and politics. In: *Denver ACS National Meeting (March 22–26, 2015)*; Spring 2015. Online. Internet. Available: http://presentations.acs.org/common/presentation-detail.aspx/Spring2015/MPPG/MPPG001a/2145106. Accessed 16.06.15.

3. MacLean HL, Lave LB. Evaluating automobile fuel/propulsions system technologies. *Prog Energy Combust Sci*. 2003;29:1–69.
4. Conti JJ, Holtberg PD, Diefenderfer JR, et al. *Annual Energy Outlook 2015 with Projections to 2040*. Washington, DC: Energy Information Administration, U.S. Department of Energy; April 2015, 20585. DOE/EIA-0383.
5. Westbrook CK. Biofuels combustion. *Annu Rev Phys Chem*. 2013;64:201–219.
6. Curran HJ, Gaffuri P, Pitz WJ, Westbrook CK. A comprehensive modeling study of *n*-heptane oxidation. *Combust Flame*. 1998;114:149–177.
7. Curran HJ, Gaffuri P, Pitz WJ, Westbrook CK. A comprehensive modeling study of iso-octane oxidation. *Combust Flame*. 2002;129:253–280.
8. Graboski MS, McCormick RL. Combustion of fat and vegetable oil derived fuels in diesel engines. *Prog Energy Combust Sci*. 1998;24:125–164.
9. Huber GW, Iborra S, Corma A. Synthesis of transportation fuels from biomass: chemistry, catalysts, and engineering. *Chem Rev*. 2006;106:4044–4098.
10. Naik SN, Goud VV, Rout PK, Dalai AK. Production of first and second generation biofuels: a comprehensive review. *Renew Sustain Energy Rev*. 2010;14:578–597.
11. Kohse-Höinghaus K, Oßwald P, Cool TA, et al. Biofuel combustion chemistry: from ethanol to biodiesel. *Angew Chem Int Ed*. 2010;49:3572–3597.
12. Lai JYW, Lin KC, Violi A. Biodiesel combustion: advances in chemical kinetic modeling. *Prog Energ Combust Sci*. 2011;37:1–14.
13. Tran LS, Sirjean B, Glaude P-A, Fournet R, Battin-Leclerc F. Progress in detailed kinetic modeling of the combustion of oxygenated components of biofuels. *Energy*. 2012;43:4–18.
14. Nigam PS, Singh A. Production of liquid biofuels from renewable resources. *Prog Energ Combust Sci*. 2011;37:52–68.
15. Battin-Leclerc F, Blurock E, Bounaceur R, et al. Towards cleaner combustion engines through groundbreaking detailed chemical kinetic models. *Chem Soc Rev*. 2011;40:4762–4782.
16. Bergthorson JM, Thomson MJ. A review of the combustion and emissions properties of advanced transportation biofuels and their impact on existing and future engines. *Renew Sustain Energy Rev*. 2015;42:1393–1417.
17. Dryer FL. Chemical kinetic and combustion characteristics of transportation fuels. *Proc Combust Inst*. 2015;35:117–144.
18. Senkan SM. Detailed chemical kinetic modeling: chemical reaction engineering of the future. *Adv Chem Eng*. 1992;18:95–192.
19. Frenklach M. Transforming data into knowledge—Process informatics for combustion chemistry. *Proc Comb Inst*. 2007;31:125–140.
20. Such software packages include
    a. CHEMKIN 10131. *Reaction Design*. 2013. San Diego;
    b. Goodwin D. *Cantera: An Object-Oriented Software Toolkit for Chemical Kinetics, Thermodynamics, and Transport Processes*. Pasadena: Caltech; 2009. Online. Available: http://www.cantera.org/docs/doxygen/html/index.html;
    c. Deminsky M, Chorkov V, Belov G, et al. Chemical workbench: integrated environment for materials science. *Comp Mater Sci*. 2003;28:169–178.
21. a. Lawrence Livermore National Laboratory. Combustion Mechanisms. https://combustion.llnl.gov/mechanisms Accessed 26.06.15.
    b. UC-San Diego Combustion Research Group. http://web.eng.ucsd.edu/mae/groups/combustion/mechanism.html Accessed 26.06.15.
    c. Law Combustion Group. Princeton University. http://lcg.princeton.edu/research/chemical-kinetic-mechanisms.aspx Accessed 26.06.15.
    d. The Master Chemical Mechanism. Leeds University. http://mcm.leeds.ac.uk/MCM/home.htt Accessed 26.06.15.

e. Other such mechanisms are compiled via Reaction Design. Chemical mechanisms data. http://www.reactiondesign.com/support/chemical-mechanisms-data/ Accessed 26.06.15.
22. Green WH, Allen JW, Bhoorasingh P, et al. *Reaction Mechanism Generator*; 2013. http://rmg.mit.edu/.
23. IUPAC Task Group on Atmospheric Chemical Kinetic Data Evaluation. http://iupac.pole-ether.fr/ Retrieved 26.06.15.
24. Manion JA, Huie RE, Levin RD, et al. *NIST Chemical Kinetics Database, NIST Standard Reference Database 17, Version 7.0 (Web Version), Release 1.6.8, Data Version 2015.09*. Gaithersburg, Maryland: National Institute of Standards and Technology; 20899–28320. Available: http://kinetics.nist.gov/ Retrieved 26.06.15.
25. NIST Real Fuels Project Resources. Available: http://kinetics.nist.gov/RealFuels/ Retrieved 26.06.15.
26. In one multi-institute collaboration, the Department of Energy's Joint BioEnergy Institute (http://www.jbei.org/) Coordinates Research from Lawrence Berkeley National Laboratory, Sandia National Laboratory, Pacific Northwest Laboratory, Lawrence Livermore National Laboratory, University of California-Berkeley, University of California-Davis, and the Carnegie Institution for Science. Other such collaborations are described in Reference 5.
27. a. Stein SE, Heller SR, Tchekhovskoi D. Proc 2003 Intl Chem Info Conf (Nimes). *Infonortics*. 2003:131–143;
b. Rovner SL. Chemical 'naming' method unveiled. *Chem Eng News*. 2005;83:39–40;
c. http://www.iupac.org/inchi/ The IUPAC International Chemical Identifier (InChI). Accessed 26.06.15.
d. http://www.inchi-trust.org/ InChI Trust. Accessed 26.06.15.
28. Burgess Jr DR, Manion JA, Hayes CJ. Data formats for elementary gas phase kinetics, part 1: unique representations of species at the molecular level. *Int J Chem Kinet*. 2014;46:640–650.
29. Burgess Jr DR, Manion JA, Hayes CJ. Data formats for elementary gas-phase kinetics: part 2. Unique representations of reactions. *Int J Chem Kinet*. 2015;47:334–350.
30. Burgess Jr DR, Manion JA, Hayes CJ. Data formats for elementary gas-phase kinetics, part 3: reaction classification. *Int J Chem Kinet*. 2015;47:361–378.
31. Kee RJ, Coltrin ME, Glarborg P. *Chemically Reacting Flow: Theory and Practice*. Hoboken, NJ: John Wiley and Sons; 2003.
32. Egolfopoulos FN, Hansen N, Ju Y, Kohse-Höinghaus K, Law CK, Qi F. Advances and challenges in laminar flame experiments and implications for combustion chemistry. *Prog Energy Combust Sci*. 2014;43:36–67.
33. Herbinet O, Guillaume D. Jet-stirred reactors. In: Battin-Leclerc F, Simmie JM, Blurock E, eds. *Cleaner Combustion: Developing Detailed Chemical Kinetic Models*. London: Springer-Verlag. Green Energy and Technology; 2013:183–210. ISBN: 978-1-4471-5306-1.
34. Sung C-J, Curran HJ. Using rapid compression machines for chemical kinetics studies. *Prog Energ Combust Sci*. 2014;44:1–18.
35. Steinfeld JI, Francisco JS, Hase WL. *Chemical Kinetics and Dynamics*. 2nd ed. Upper Saddle River, NJ: Prentice Hall; 1999.
36. a. Cool TA, McIlroy A, Qi F, et al. Photoionization mass spectrometer for studies of flame chemistry with a synchrotron light source. *Rev Sci Instrum*. 2005;76(094102):1–7;
b. Cool TA, Nakajima K, Mostefaoui TA, et al. Selective detection of isomers with photoionization mass spectrometry for studies of hydrocarbon flame chemistry. *J Chem Phys*. 2003;119:8356–8365.
37. Lewars EG. *Computational Chemistry: Introduction to the Theory and Applications of Molecular and Quantum Mechanics*. 2nd ed. New York: Springer; 2011.

38. Cramer CJ. *Essentials of Computational Chemistry: Theories and Models*. 2nd ed. Hoboken, NJ: Wiley; 2004.
39. NIST. In: Russell D, Johnson III, eds. *Computational Chemistry Comparison and Benchmark Database. NIST Standard Reference Database Number 101. Release 16a*; August 2013. Available: http://cccbdb.nist.gov/.
40. Hehre WJ, Radom L, Schleyer PVR, Pople JA. *Ab Initio Molecular Orbital Theory*. New York: John Wiley and Sons; 1986.
41. Parr RG, Yang W. *Density Functional Theory of Atoms and Molecules*. New York: Oxford University Press; 1989.
42. Laidler KJ. *Chemical Kinetics*. New York: Harper & Row; 1987.
43. Wigner EPZ. *Phys Chem Abst B*. 1932;19:203.
44. a. Marcus RA. Unimolecular dissociations and free radical recombination reactions. *J Chem Phys*. 1952;20:359–363;
b. Wardlaw DM, Marcus RA. RRKM reaction rate theory for transition states of any looseness. *Chem Phys Lett*. 1984;110:230–234.
45. Tsang W, Hudgens JW, Allison TC, Burgess Jr DR, Manion JA, Matheu DM. In: *Workshop on Combustion Simulation Databases for Real Transportation Fuels*. Gaithersburg, MD 20899: National Institute of Standards and Technology; September 4–5, 2003. NISTIR 7155. Online. Available: http://kinetics.nist.gov/RealFuels/content/RealFuelsReport_NISTIR7155.pdf. Retrieved 25.06.15.
46. Westbrook CK, Dryer FL. Chemical kinetic modeling of hydrocarbon combustion. *Prog Energy Combust Sci*. 1984;10:1–57.
47. Merle JK, Hayes CJ, Zalyubovsky SJ, Glover BG, Miller TA, Hadad CM. Theoretical determinations of the ambient conformational distribution and unimolecular decomposition of n-propylperoxy radical. *J Phys Chem A*. 2005;109:3637–3646.
48. Vereecken L, Peeters J. The 1,5-shift in 1-butoxy: a case study in the rigorous implementation of transition state theory for a multirotamer system. *J Chem Phys*. 2003;119:5159–5170.
49. Jitariu LC, Jones LD, Robertson SH, Pilling MJ, Hillier IH. Thermal rate coefficients via variational transition state theory for the unimolecular decomposition/isomerization of 1-pentyl radical: ab initio and direct dynamics calculations. *J Phys Chem A*. 2003;107:8607–8617.
50. a. Awan IA, Burgess Jr DR, Manion JA. Pressure dependence and branching ratios in the decomposition of 1-pentyl radicals: shock tube experiments and master equation modeling. *J Phys Chem A*. 2012;116:2895–2910;
b. Comandini A, Awan IA, Manion JA. Thermal decomposition of 1-pentyl radicals at high pressures and temperatures. *Chem Phys Lett*. 2012;552:20–26.
51. Marinov NM. A detailed chemical kinetic model for high temperature ethanol oxidation. *Int J Chem Kinet*. March 1999;31:183–220.
52. Villano SM, Huynh LK, Carstensen HH, Dean AM. High-pressure rate rules for alkyl + $O_2$ reactions. 2. The isomerization, cyclic ether formation, and beta-scission reactions of hydroperoxy alkyl radicals. *J Phys Chem A*. 2012;116:5068–5089.
53. Villano SM, Huynh LK, Carstensen HH, Dean AM. High-pressure rate rules for alkyl + O2 reactions. 1. the dissociation, concerted elimination, and isomerization channels of the alkylperoxy radical. *J Phys Chem A*. 2012;115:13425–13442.
54. We can understand this by more closely examining a few key pathways represented in Figure 3. Most directly, the propagation steps by which the alkyl hydroperoxide (QOOH) dissociates are crucial for moving the overall reaction rate forward. However, the formation of QOOH in the first place relies on via isomerization of the peroxy radical ROO, which is itself formed by the addition of molecular oxygen to the radical R. Considering these low-T pathways, we can thus see that as temperature increases, the reactants in peroxy radical formation (R + $O_2$) are increasingly favored, shifting the

equilibrium left. Thus, ROO formation and thus QOOH formation will decrease, slowing the overall reaction. This phenomenon is eventually bypassed as a fuel mixture achieves temperatures > 1000 K, at which high-temperature combustion pathways dominate. For further discussion, see References 5, 31, and 55; also see: Hayes CJ, Merle JK, Hadad CM. Chemistry of reactive radical intermediates in combustion and the atmosphere. *Adv Phys Org Chem*. 2009;43:79–134.

55. Glassman I, Yetter RA, Glumac NG. *Combustion*. 5th ed. Academic Press; 2014.
56. Monks PS. Gas radical chemistry in the troposphere. *Chem Soc Rev*. 2005;34:376–395.
57. Atkinson R, Arey J. Atmospheric degradation of volatile organic compounds. *Chem Rev*. 2003;103:4605–4638.
58. Finlayson-Pitts BJ, Pitts Jr JN. *Chemistry of the Upper and Lower Atmosphere: Theory, Experiments, and Applications*. New York: Academic Press; 2000.
59. Sander SP, Abbatt J, Barker JR, et al. *Chemical Kinetics and Photochemical Data for Use in Atmospheric Studies*. Evaluation No. 17. JPL Publication 10-6. Pasadena: Jet Propulsion Laboratory; 2011. http://jpldataeval.jpl.nasa.gov.
60. IUPAC task group on atmospheric chemical kinetic data evaluation. Online. Internet. Available: http://iupac.pole-ether.fr Accessed 10.09.15.
61. Master chemical mechanism, MCM v3.3. Online. Internet. Available: http://mcm.leeds.ac.uk/MCM. Accessed 10.09.15.
62. Haynes BS, Wagner HG. Soot formation. *Prog Energy Combust Sci*. 1981;7:229–273.
63. Glassman I. Soot formation in combustion processes. *Proc Combust Inst*. 1988; 22:295.
64. Westbrook CK, Pitz WJ, Curran HJ. Chemical kinetic modeling study of the effects of oxygenated hydrocarbons on soot emissions from diesel engines. *J Phys Chem A*. 2006; 110:6912–6922.
65. Omidvarborna H, Kumar A, Kim D-S. Recent studies on soot modeling for diesel combustion. *Renew Sustain Energy Rev*. 2015;48:635–647.
66. Mueller CJ, Boehman AL, Martin GC. An experimental investigation of the origin of increased $NO_x$ emissions when fueling a heavy-duty compression-ignition engine with soy biodiesel. *SAE Int J Fuels Lubr*. 2009;2:789–816.
67. Jacobson MZ. Effects of ethanol (E85) versus gasoline vehicles on cancer and mortality in the United States. *Environ Sci Technol*. 2007;41:4150–4157.
68. Sarathy SM, Osswald P, Hansen N, Kohse-Hoinghaus K. Alcohol combustion chemistry. *Prog Energy Combust Sci*. October 2014;44:40–102.
69. Coniglio L, Bennadji H, Glaude PA, Herbinet O, Billaud F. Combustion chemical kinetics of biodiesel and related compounds (methyl and ethyl esters): experiments and modeling – advances and future refinements. *Prog Energy Combust Sci*. August 2013;39:340–382.
70. Park J, Xu ZF, Lin MC. Thermal decomposition of ethanol. II. A computational study of the kinetics and mechanism for the $H+C_2H_5OH$ reaction. *J Chem Phys*. June 2003; 118:9990–9996.
71. Li J, Kazakov A, Dryer FL. Experimental and numerical studies of ethanol decomposition reactions. *J Phys Chem A*. September 2004;108:7671–7680.
72. Tsang W. Energy transfer effects during the multichannel decomposition of ethanol. *Int J Chem Kinet*. August 2004;36:456–465.
73. Baulch DL, Bowman CT, Cobos CJ, et al. Evaluated kinetic data for combustion modeling: supplement II. *J Phys Chem Ref Data*. 2005;34:757–1397.
74. Egolfopoulos FN, Du DX, Law CK. A study on ethanol oxidation kinetics in laminar premixed flames, flow reactors, and shock tubes. *Proc Combust Inst*. 1992; 24:833–841.
75. Saxena P, Williams FA. Numerical and experimental studies of ethanol flames. *Proc Combust Inst*. 2007;31:1149–1156.

76. Haas FM, Chaos M, Dryer FL. Low and intermediate temperature oxidation of ethanol and ethanol-PRF blends: an experimental and modeling study. *Combust Flame*. December 2009;156:2346–2350.
77. Leplat N, Dagaut P, Togbe C, Vandooren J. Numerical and experimental study of ethanol combustion and oxidation in laminar premixed flames and in jet-stirred reactor. *Combust Flame*. April 2011;158:705–725.
78. Lee C, Vranckx S, Heufer KA, et al. On the chemical kinetics of ethanol oxidation: shock tube, rapid compression machine and detailed modeling study. *Z Phys Chemie-Int J Res Phys Chem Chem Phys*. 2012;226:1–27.
79. Metcalfe WK, Burke SM, Ahmed SS, Curran HJ. A hierarchical and comparative kinetic modeling study of $C_1 - C_2$ hydrocarbon and oxygenated fuels. *Int J Chem Kinet*. October 2013;45:638–675.
80. Meier U, Grotheer HH, Riekert G, Just T. Temperature dependence and branching ratio of the $C_2H_5OH$ +OH reaction. *Chem Phys Lett*. 1985;115:221–225.
81. Xu S, Lin MC. Theoretical study on the kinetics for OH reactions with $CH_3OH$ and $C_2H_5OH$. *Proc Combust Inst*. 2007;31:159–166.
82. Sivaramakrishnan R, Su MC, Michael JV, Klippenstein SJ, Harding LB, Ruscic B. Rate constants for the thermal decomposition of ethanol and its bimolecular reactions with OH and D: reflected shock tube and theoretical studies. *J Phys Chem A*. September 2010;114:9425–9439.
83. Carr SA, Blitz MA, Seakins PW. Site-specific rate coefficients for reaction of OH with ethanol from 298 to 900 K. *J Phys Chem A*. April 2011;115:3335–3345.
84. Zheng JJ, Truhlar DG. Multi-path variational transition state theory for chemical reaction rates of complex polyatomic species: ethanol plus OH reactions. *Faraday Discuss*. 2012;157:59–88.
85. Aders WK, Wagner HG. Studies on reaction of hydrogen atoms with ethanol and *tert*-butanol. *Ber Bunsen-Ges Phys Chem Chem Phys*. 1973;77:712–718.
86. Wu CW, Lee YP, Xu SC, Lin MC. Experimental and theoretical studies of rate coefficients for the reaction $O(^3P)$ plus $C_2H_5OH$ at high temperatures. *J Phys Chem A*. July 2007;111:6693–6703.
87. Carr SA, Blitz MA, Seakins PW. Product branching fractions for the reaction of $O(^3P)$ atoms with methanol and ethanol. *Chem Phys Lett*. August 2011;511:207–212.
88. Xu ZF, Park J, Lin MC. Thermal decomposition of ethanol. III. A computational study of the kinetics and mechanism for the $CH_3+C_2H_5OH$ reaction. *J Chem Phys*. April 2004;120:6593–6599.
89. Curran HJ. Rate constant estimation for $C_1$ to $C_4$ alkyl and alkoxyl radical decomposition. *Int J Chem Kinet*. April 2006;38:250–275.
90. Matus MH, Nguyen MT, Dixon DA. Theoretical prediction of the heats of formation of $C_2H_5O$• radicals derived from ethanol and of the kinetics of $\beta$-C-C scission in the ethoxy radical. *J Phys Chem A*. January 2007;111:113–126.
91. Shao Y, Yao L, Mao YC, Zhong JJ. Anharmonic effect of dissociation rate constant of the ethoxy radical. *Chem Phys Lett*. December 2010;501:134–139.
92. Xu ZF, Xu K, Lin MC. Ab initio kinetics for Decomposition/isomerization reactions of $C_2H_5O$ radicals. *Chemphyschem*. April 2009;10:972–982.
93. Dames EE. Master equation modeling of the unimolecular decompositions of $\alpha$-hydroxyethyl ($CH_3CHOH$) and ethoxy ($CH_3CH_2O$) Radicals. *Int J Chem Kinet*. March 2014;46:176–188.
94. Zador J, Fernandes RX, Georgievskii Y, Meloni G, Taatjes CA, Miller JA. The reaction of hydroxyethyl radicals with $O_2$: a theoretical analysis and experimental product study. *Proc Combust Inst*. 2009;32:271–277.
95. Labbe NJ, Sivaramakrishnan R, Klippenstein SJ. The role of radical plus fuel-radical well-skipping reactions in ethanol and methylformate low-pressure flames. *Proc Combust Inst*. 2015;35:447–455.

96. Van Gerpen J, Shanks B, Pruszko R, Clements D, Knothe G. *Biodiesel Production Technology*. Golden, Colorado 80401: National Renewable Energy Laboratory; 2004. NREL Subcontractor Report NREL/SR-510−36244.
97. Simmie JM. Detailed chemical kinetic models for the combustion of hydrocarbon fuels. *Prog Energy Combust Sci*. 2003;29:599−634.
98. Battin-Leclerc F. Detailed chemical kinetic models for the low-temperature combustion of hydrocarbons with application to gasoline and diesel fuel surrogates. *Prog Energy Combust Sci*. August 2008;34:440−498.
99. Fisher EM, Pitz WJ, Curran HJ, Westbrook CK. Detailed chemical kinetic mechanisms for combustion of oxygenated fuels. *Proc Combust Inst*. 2000;28:1579−1586.
100. Marchese AJ, Angioletti M, Dryer FL. Flow reactor studies of surrogate biodiesel fuels. Work-in progress poster 1F1−03. In: *Thirtieth International Symposium on Combustion*. 2004. Chicago, IL, USA.
101. Gail S, Thomson MJ, Sarathy SM, et al. A wide-ranging kinetic modeling study of methyl butanoate combustion. *Proc Combust Inst*. 2007;31:305−311.
102. El-Nahas AM, Navarro MV, Simmie JM, et al. Enthalpies of formation, bond dissociation energies and reaction paths for the decomposition of model biofuels: ethyl propanoate and methyl butanoate. *J Phys Chem A*. May 2007;111:3727−3739.
103. Metcalfe WK, Dooley S, Curran HJ, Simmie JM, El-Nahas AM, Navarro MV. Experimental and modeling study of $C_5H_{10}O_2$ ethyl and methyl esters. *J Phys Chem A*. May 2007;111:4001−4014.
104. O' Conaire M, Curran HJ, Simmie JM, Pitz WJ, Westbrook CK. A comprehensive modeling study of hydrogen oxidation. *Int J Chem Kinet*. November 2004;36:603−622.
105. Dooley S, Curran HJ, Simmie JM. Autoignition measurements and a validated kinetic model for the biodiesel surrogate, methyl butanoate. *Combust Flame*. April 2008;153:2−32.
106. Petersen EL, Kalitan DM, Simmons S, Bourque G, Curran HJ, Simmie JM. Methane/propane oxidation at high pressures: experimental and detailed chemical kinetic modeling. *Proc Combust Inst*. 2007;31:447−454.
107. Walton SM, Wooldridge MS, Westbrook CK. An experimental investigation of structural effects on the auto-ignition properties of two C5 esters. *Proc Combust Inst*. 2009;32:255−262.
108. Huynh LK, Violi A. Thermal decomposition of methyl butanoate: ab initio study of a biodiesel fuel surrogate. *J Org Chem*. January 2008;73:94−101.
109. Huynh LK, Lin KC, Violi A. Kinetic modeling of methyl butanoate in shock tube. *J Phys Chem A*. December 2008;112:13470−13480.
110. Farooq A, Davidson DF, Hanson RK, Huynh LK, Violi A. An experimental and computational study of methyl ester decomposition pathways using shock tubes. *Proc Combust Inst*. 2009;32:247−253.
111. Farooq A, Ren W, Lam KY, Davidson DF, Hanson RK, Westbrook CK. Shock tube studies of methyl butanoate pyrolysis with relevance to biodiesel. *Combust Flame*. November 2012;159:3235−3241.
112. Warth V, Battin-Leclerc F, Fournet R, Glaude PA, Come GM, Scacchi G. Computer based generation of reaction mechanisms for gas-phase oxidation. *Comput Chem*. July 2000;24:541−560.
113. Warth V, Stef N, Glaude PA, Battin-Leclerc F, Scacchi G, Come GM. Computer-aided derivation of gas-phase oxidation mechanisms: application to the modeling of the oxidation of *n*-butane. *Combust Flame*. July 1998;114:81−102.
114. Glaude PA, Battin-Leclerc F, Judenherc B, et al. Experimental and modeling study of the gas-phase oxidation of methyl and ethyl tertiary butyl ethers. *Combust Flame*. April 2000;121:345−355.

115. Westbrook CK, Pitz WJ, Westmoreland PR, et al. A detailed chemical kinetic reaction mechanism for oxidation of four small alkyl esters in laminar premixed flames. *Proc Combust Inst*. 2009;32:221–228.
116. Yang B, Westbrook CK, Cool TA, Hansen N, Kohse-Hoinghaus K. Fuel-specific influences on the composition of reaction intermediates in premixed flames of three $C_5H_{10}O_2$ ester isomers. *Phys Chem Chem Phys*. 2011;13:6901–6913.
117. Wang YL, Lee DJ, Westbrook CK, Egolfopoulos FN, Tsotsis TT. Oxidation of small alkyl esters in flames. *Combust Flame*. March 2014;161:810–817.
118. Dayma G, Gail S, Dagaut P. Experimental and kinetic modeling study of the oxidation of methyl hexanoate. *Energy Fuels*. May-Jun 2008;22:1469–1479.
119. Dayma G, Togbe C, Dagaut P. Detailed kinetic mechanism for the oxidation of vegetable oil methyl esters: new evidence from methyl heptanoate. *Energy Fuels*. September 2009;23:4254–4268.
120. HadjAli K, Crochet M, Vanhove G, Ribaucour M, Minetti R. A study of the low temperature autoignition of methyl esters. *Proc Combust Inst*. 2009;32:239–246.
121. Dayma G, Halter F, Foucher F, Togbe C, Mounaim-Rousselle C, Dagaut P. Experimental and detailed kinetic modeling study of ethyl pentanoate (ethyl valerate) oxidation in a jet stirred reactor and laminar burning velocities in a spherical combustion chamber. *Energy Fuels*. August 2012;26:4735–4748.
122. Dayma G, Halter F, Foucher F, Mounaim-Rousselle C, Dagaut P. Laminar burning velocities of $C_4$-$C_7$ ethyl esters in a spherical combustion chamber: experimental and detailed kinetic modeling. *Energy Fuels*. November 2012;26:6669–6677.
123. Herbinet O, Pitz WJ, Westbrook CK. Detailed chemical kinetic oxidation mechanism for a biodiesel surrogate. *Combust Flame*. August 2008;154:507–528.
124. Seshadri K, Lu TF, Herbinet O, et al. Experimental and kinetic modeling study of extinction and ignition of methyl decanoate in laminar non-premixed flows. *Proc Combust Inst*. 2009;32:1067–1074.
125. Sarathy SM, Thomson MJ, Pitz WJ, Lu T. An experimental and kinetic modeling study of methyl decanoate combustion. *Proc Combust Inst*. 2011;33:399–405.
126. Glaude PA, Herbinet O, Bax S, Biet J, Warth V, Battin-Leclerc F. Modeling of the oxidation of methyl esters-Validation for methyl hexanoate, methyl heptanoate, and methyl decanoate in a jet-stirred reactor. *Combust Flame*. 2010;157:2035–2050.
127. Herbinet O, Biet J, Hakka MH, et al. Modeling study of the low-temperature oxidation of large methyl esters from $C_{11}$ to $C_{19}$. *Proc Combust Inst*. 2011;33:391–398.
128. Sarathy SM, Gail S, Syed SA, Thomson MJ, Dagaut P. A comparison of saturated and unsaturated C-4 fatty acid methyl esters in an opposed flow diffusion flame and a jet stirred reactor. *Proc Combust Inst*. 2007;31:1015–1022.
129. Gail S, Sarathy SM, Thomson MJ, Dievart P, Dagaut P. Experimental and chemical kinetic modeling study of small methyl esters oxidation: methyl (*E*)-2-butenoate and methyl butanoate. *Combust Flame*. December 2008;155:635–650.
130. Dagaut P, Gail S, Sahasrabudhe M. Rapeseed oil methyl ester oxidation over extended ranges of pressure, temperature, and equivalence ratio: experimental and modeling kinetic study. *Proc Combust Inst*. 2007;31:2955–2961.
131. Herbinet O, Pitz WJ, Westbrook CK. Detailed chemical kinetic mechanism for the oxidation of biodiesel fuels blend surrogate. *Combust Flame*. May 2010;157:893–908.
132. Westbrook CK, Naik CV, Herbinet O, et al. Detailed chemical kinetic reaction mechanisms for soy and rapeseed biodiesel fuels. *Combust Flame*. April 2011;158:742–755.
133. Westbrook CK, Pitz WJ, Sarathy SM, Mehl M. Detailed chemical kinetic modeling of the effects of C=C double bonds on the ignition of biodiesel fuels. *Proc Combust Inst*. 2013;34:3049–3056.
134. Ali MA, Violi A. Reaction pathways for the thermal decomposition of methyl butanoate. *J Org Chem*. June 2013;78:5898–5908.

135. Akih-Kumgeh B, Bergthorson JM. Structure-reactivity trends of C1-C4 alkanoic acid methyl esters. *Combust Flame*. June 2011;158:1037–1048.
136. Liu W, Sivaramakrishnan R, Davis MJ, Som S, Longman DE, Lu TF. Development of a reduced biodiesel surrogate model for compression ignition engine modeling. *Proc Combust Inst*. 2013;34:401–409.
137. Zhang LD, Chen QX, Zhang P. A theoretical kinetics study of the reactions of methylbutanoate with hydrogen and hydroxyl radicals. *Proc Combust Inst*. 2015;35:481–489.
138. Le Calve S, Le Bras G, Mellouki A. Kinetic studies of OH reactions with a series of methyl esters. *J Phys Chem A*. November 1997;101:9137–9141.
139. Schutze N, Zhong XY, Kirschbaum S, Bejan I, Barnes I, Benter T. Relative kinetic measurements of rate coefficients for the gas-phase reactions of Cl atoms and OH radicals with a series of methyl alkyl esters. *Atmos Environ*. December 2010;44:5407–5414.
140. Wallington TJ, Dagaut P, Liu RH, Kurylo MJ. The gas-phase reactions of hydroxyl radicals with a series of esters over the temperature range 240–440-K. *Int J Chem Kinet*. February 1988;20:177–186.
141. Lam KY, Davidson DF, Hanson RK. High-temperature measurements of the reactions of OH with small methyl esters: methyl formate, methyl acetate, methyl propanoate, and methyl butanoate. *J Phys Chem A*. December 2012;116:12229–12241.
142. Zador J, Taatjes CA, Fernandes RX. Kinetics of elementary reactions in low-temperature autoignition chemistry. *Prog Energy Combust Sci*. August 2011;37:371–421.
143. Villano SM, Carstensen HH, Dean AM. Rate rules, branching ratios, and pressure dependence of the $HO_2$ + olefin addition channels. *J Phys Chem A*. 2013;117:6458–6473.
144. Hayes CJ, Burgess DR. Exploring the oxidative decompositions of methyl esters: methyl butanoate and methyl pentanoate as model compounds for biodiesel. *Proc Combust Inst*. 2009;32:263–270.
145. Tao HR, Lin KC. Pathways, kinetics and thermochemistry of methyl-ester peroxy radical decomposition in the low-temperature oxidation of methyl butanoate: a computational study of a biodiesel fuel surrogate. *Combust Flame*. September 2014;161:2270–2287.
146. Jiao Y, Zhang F, Dibble TS. Quantum chemical study of autoignition of methyl butanoate. *J Phys Chem A*. 2015;119:7282–7292.
147. Mai TVT, Le XT, Huynh LK. Mechanism and kinetics of low-temperature oxidation of a biodiesel surrogate-methyl acetate radicals with molecular oxygen. *Struct Chem*. April 2015;26:431–444.
148. Le XT, Mai TVT, Ratkiewicz A, Huynh LK. Mechanism and kinetics of low-temperature oxidation of a biodiesel surrogate: methyl propanoate radicals with oxygen molecule. *J Phys Chem A*. April 2015;119:3689–3703.
149. Zhang LD, Zhang P. Towards high-level theoretical studies of large biodiesel molecules: an ONIOM QCISD(T)/CBS: DFT study of hydrogen abstraction reactions of $C_nH_{2n+1}COOC_mH_{2m+1}$ + H. *Phys Chem Chem Phys*. 2015;17:200–208.
150. Svensson M, Humbel S, Froese RDJ, Matsubara T, Sieber S, Morokuma K. ONIOM: a multilayered integrated MO+MM method for geometry optimizations and single point energy predictions. A test for Diels-Alder reactions and $Pt(P(t\text{-}Bu)_3)_2+H_2$ oxidative addition. *J Phys Chem*. December 1996;100:19357–19363.
151. Knothe G. A comprehensive evaluation of the cetane numbers of fatty acid methyl esters. *Fuel*. 2014;119:6–13.
152. Koivisto E, Ladommatos N, Gold M. Systematic study of the effect of the hydroxyl functional group in alcohol molecules on compression ignition and exhaust gas emissions. *Fuel*. 2015;153:650–663.

153. Knothe G. Cetane numbers of branched and straight-chain fatty esters determined in an ignition quality tester. *Fuel*. 2003;82:971–975.
154. Koekman SK, Broch A, Robbins C, Ceniceros E, Natarajan M. Review of biodiesel composition, properties, and specifications. *Renew Sustain Energy Rev*. 2012;16:143–169.
155. Refaat AA. Correlation between the chemical structure of biodiesel and its physical properties. *Int J Environ Sci Technol*. 2009;6:677–694.
156. Knothe G. Dependence of biodiesel fuel properties on the structure of fatty acid alkyl esters. *Fuel Process Technol*. 2005;86:1059–1070.
157. Lin KC, Lai KYW, Violi A. The role of the methyl ester moiety in biodiesel combustion: a kinetic modeling comparison of methyl butanoate and *n*-butane. *Fuel*. 2012;92:16–26.
158. Hoffman SR, Abraham J. A comparative study of n-heptane, methyl decanoate, and dimethyl ether combustion characteristics under homogeneous-charge compression-ignition engine conditions. *Fuel*. 2009;88:1099–1108.
159. Naik CV, Westbrook CK, Herbinet O, Pitz WJ, Mehl M. Detailed chemical kinetic reaction mechanism for biodiesel components methyl stearate and methyl oleate. *Proc Combust Inst*. 2011;33:383–389.
160. Tang CL, Wei LJ, Man XJ, Zhang JX, Huang ZH, Law CK. High temperature ignition delay times of C5 primary alcohols. *Combust Flame*. 2013;160:520–529.
161. Serinyel Z, Togbe C, Dayma G, Daguat P. An experimental and modeling study of 2-methyl-1-butanol oxidation in a jet-stirred reactor. *Combust Flame*. 2014;161:3003–3013.
162. Sarathy SM, Park S, Weber BW, et al. A comprehensive experimental and modeling study of iso-pentanol combustion. *Combust Flame*. 2013;160:2712–2728.
163. Welz O, Savee JD, Eskola AJ, Sheps L, Osborn DL, Taatjes CA. Low-temperature combustion chemistry of biofuels: pathways in the low-temperature (550–700 K) oxidation chemistry of isobutanol and tert-butanol. *Proc Combust Inst*. 2013;34:493–500.
164. Vranckx S, Heufer KA, Lee C, et al. Role of peroxy chemistry in the high-pressure ignition of n-butanol. Experiments and detailed kinetic modelling. *Combust Flame*. 2011;158:1444–1455.
165. Karwat DMA, Wooldridge MS, Klippenstein SJ, Davis MJ. Effects of new ab initio rate coefficients on predictions of species formed during *n*-butanol ignition and pyrolysis. *J Phys Chem A*. 2015;119:543–551.
166. Zheng J, Truhlar DG. Quantum thermochemistry: multistructural method with torsional anharmonicity based on a coupled torsional potential. *J Chem Theory Comput*. 2013;9:1356–1367.
167. Lange JP. Lignocellulose conversion: an introduction to chemistry, process and economics. *Biofuels Bioprod Bioref*. 2007;1:39–48.
168. The Water-Sustainable Management of Biofuels. Mission 2017. Available: http://12.000.scripts.mit.edu/mission2017/biofuels-overview/ Retrieved 22.06.15.
169. Resasco DE, Sitthisa S, Faria J, Prasomsri T, Ruiz MP. Furfurals as chemical platform for biofuels production. In: Kubicka D, Kubickova I, eds. *Heterogeneous Catalysis in Biomass to Chemicals and Fuels*. 2011.
170. Klemm D, Heublein B, Fink HP, Bohn A. Cellulose: fascinating biopolymer and sustainable raw material. *Angew Chem Int Ed*. 2005;44:3358–3393.
171. Scheller HV, Ulvskov P. Hemicelluloses. *Annu Rev Plant Biol*. 2010;61:263–289.
172. Vollhardt KPC, Schore NE. *Organic Chemistry, Structure and Function*. 4th ed. New York: W. H. Freeman; 2003.
173. Lupoi JS, Singh S, Parthasarathi R, Simmons BA, Henry RJ. Recent innovations in analytical methods for the qualitative and quantitative assessment of lignin. *Renew Sustain Energ Rev*. 2015;49:871–906.

174. Freudenberg K, Neish AC. In: Springer GF, Kleinzeller A, eds. *Constitution and Biosynthesis of Lignin*. New York: Springer-Verlag; 1968.
175. Evans RJ, Milne TA. Molecular characterization of the pyrolysis of biomass. 1. Fundamentals. *Energy Fuels*. 1987;1:123–137.
176. Diebold JP. A unified, global model for the pyrolysis of cellulose. *Biomass Bioenergy*. 1994;7:75–85.
177. Farmer TJ, Mascal M. Platform molecules. In: Clark J, Deswarte F, eds. *Introduction to Chemicals from Biomass*. 2nd ed. John Wiley & Sons, Ltd; 2015.
178. Nimlos MR, Qian X, Davis M, Himmel ME, Johnson DK. Energetics of xylose decomposition as determined using quantum mechanics modeling. *J Phys Chem A*. 2006;110:11824–11838.
179. Caratzoulas S, Davis ME, Gorte RJ, et al. Challenges of and insights into acid-catalyzed transformations of sugars. *J Phys Chem C*. 2014;118:22815–22833.
180. Lange JP, Van Der Heide E, Van Buijtenen J, Price R. Furfural-a promising platform for lignocellulosic biofuels. *ChemSusChem*. 2012;5(1):150–166.
181. Yan K, Wu G, Lafleur T, Jarvis C. Production, properties and catalytic hydrogenation of furfural to fuel additives and value-added chemicals. *Renew Sustain Energy Rev*. 2014;38:663–676.
182. Huber GW, Chheda JN, Barrett CJ, Dumesic JA. Production of liquid alkanes by aqueous-phase processing of biomass-derived carbohydrates. *Science*. 2005;308:1446–1450.
183. Corma A, Iborra S, Velty A. Chemical routes for the transformation of biomass into chemicals. *Chem Rev*. 2007;107:2411–2502.
184. Chheda JN, Huber GW, Dumesic JA. Liquid-phase catalytic processing of biomass-derived oxygenated hydrocarbons to fuels and chemicals. *Angew Chem Int Ed*. 2007;46:7164–7183.
185. Lin Y-C, Huber GW. The critical role of heterogeneous catalysis in lignocellulosic biomass conversion. *Energy Environ Sci*. 2009;2:68–80.
186. Bohre A, Dutta S, Saha B, Abu-Omar MM. Upgrading furfurals to drop-in biofuels: an overview. *ACS Sustain Chem Eng*. 2015;3:1263–1277.
187. Roman-Leshkov Y, Barrett CJ, Liu ZY, Dumesic JA. Production of dimethylfuran for liquid fuels from biomass-derived carbohydrates. *Nature*. 2007;447:982–985.
188. Yang W, Sen A. One-step catalytic transformation of carbohydrates and cellulosic biomass to 2,5-dimethyltetrahydrofuran for liquid fuels. *ChemSusChem*. 2010;3:597–603.
189. Phuong J, Kim S, Thomas R, Zhang L. Predicted toxicity of the biofuel candidate 2,5-dimethylfuran in environmental and biological systems. *Environ Mol Mutagen*. 2012;53:478–487.
190. Simmie JM, Wurmel J. Harmonising production, properties and environmental consequences of liquid transport fuels from biomass—2,5-dimethylfuran as a case study. *ChemSusChem*. 2013;6:36–41.
191. Amen-Chen C, Pakdel H, Roy C. Production of monomeric phenols by thermochemical conversion of biomass: a review. *Bioresour Technol*. 2001;79:277–299.
192. Elder T, Fort Jr RC. Reactivity of lignin- correlation with molecular orbital calculations. In: *Lignin and Lignans: Advances in Chemistry*. CRC Press; 2010.
193. Zakzeski J, Bruijnincx PCA, Jongerius AL, Weckhuysen BM. The catalytic valorization of lignin for the production of renewable chemicals. *Chem Rev*. 2010;110:3552–3599.
194. Grela MA, Amorebieta VT, Colussi AJ. Very low pressure pyrolysis of furan, 2-methylfuran, and 2,5-dimethylfuran. The stability of the furan ring. *J Phys Chem*. 1985;89:38–41.
195. Lifshitz A, Bidani M, Bidani S. Thermal reactions of cyclic ethers at high temperatures. 3. Pyrolysis of furan behind reflected shocks. *J Phys Chem*. 1986;90:5373–5377.

196. Organ PP, Mackie JC. Kinetics of pyrolysis of furan. *J Chem Soc Faraday Trans*. 1991; 87:815–823.
197. Lifshitz A, Tamburu C, Shashua R. Decomposition of 2-methylfuran. Experimental and modeling study. *J Phys Chem A*. 1997;101:1018–1029.
198. Lifshitz A, Tamburu C, Shashua R. Thermal decomposition of 2,5-dimethylfuran. Experimental results and computer modeling. *J Phys Chem A*. 1998;102:10655–10670.
199. Sendt K, Bacskay GB, Mackie JC. Pyrolysis of furan: ab initio quantum chemical and kinetic modeling studies. *J Phys Chem A*. 2000;104:1861–1875.
200. a. Liu R, Zhou X, Zuo T. The pyrolysis of furan revisited. *Chem Phys Lett*. 2000;325: 457–464;
b. Liu R, Zhou X, Zhai L. Theoretical investigation of unimolecular decomposition channels of furan. *J Comp Chem*. 1998;19:240–249.
201. Vasiliou A, Nimlos MR, Daily JW, Ellison GB. Thermal decomposition of furan generates propargyl radicals. *J Phys Chem A*. 2009;113:8540–8547.
202. Simmie JM, Curran HJ. Formation enthalpies and bond dissociation energies of alkylfurans. The strongest C–X bonds known? *J Phys Chem A*. 2009;113: 5128–5137.
203. Vogulhuber KM, Wren SW, Sheps L, Lineberger WC. The C–H bond dissociation energy of furan: photoelectron spectroscopy of the furanide anion. *J Chem Phys*. 2011; 134, 064302.1-8.
204. Simmie JM, Metcalfe WK. Ab initio study of the decomposition of 2,5-dimethylfuran. *J Phys Chem A*. 2011;115:8877–8888.
205. Feller D, Simmie JM. High-level ab initio enthalpies of formation of 2,5-dimethylfuran, 2-methylfuran, and furan. *J Phys Chem A*. 2012;116:11768–11775.
206. Simmie JM, Somers KP, Metcalfe WK, Curran HJ. Substituent effects in the thermochemistry of furans: a theoretical (CBS-QB3, CBS-APNO, and G3) study. *J Chem Thermodyn*. 2013;58:117–128.
207. a. Sirjean B, Fournet R. Theoretical study of the thermal decomposition of the 5-methyl-2-furanylmethyl radical. *J Phys Chem A*. 2012;116:6675–6684;
b. Sirjean B, Fournet R. Unimolecular decomposition of 2,5-dimethylfuran: a theoretical chemical kinetic study. *Phys Chem Chem Phys*. 2013;15:596–611.
208. Fadden MJ, Hadad CM. Rearrangement pathways of arylperoxy radicals. 1. The azabenzenes. *J Phys Chem A*. 2000;104:6324–6331.
209. Fadden MJ, Hadad CM. Rearrangement pathways of arylperoxy radicals. 2. Five-membered heterocycles. *J Phys Chem A*. 2000;104:6324–6331.
210. Davis AC, Sarathy SM. Computational study of the combustion and atmospheric decomposition of 2-methylfuran. *J Phys Chem A*. 2013;117:7670–7685.
211. Somers KP, Simmie JM, Metcalfe WK, Curran HJ. The pyrolysis of 2-methylfuran: a quantum chemical, statistical rate theory and kinetic modeling study. *Phys Chem Chem Phys*. 2014;16:5349–5367.
212. Bruinsma OSL, Tromp PJJ, de Sauvage Nolting HJJ, Mouljin JA. Gas-phase pyrolysis of coal-related aromatic compounds in a coiled tube flow reactor. *Fuel*. 1988; 67:334–340.
213. Hudzik JM, Bozzelli JW. Structure and thermochemical properties of 2-methoxyfuran, 3-methoxyfuran, and their carbon-centered radicals using computational chemistry. *J Phys Chem A*. 2010;114:7984–7995.
214. Simmie JM, Somers KP, Yasunaga K, Curran HJ. A quantum chemical study of the abnormal reactivity of 2-methoxyfuran. *Int J Chem Kinet*. 2013;45:531–541.
215. Somers KP, Simmie JM, Gillespie F, et al. A comprehensive experimental and detailed chemical kinetic modeling study of 2,5-dimethyl furan pyrolysis and oxidation. *Combust Flame*. 2013;160:2291–2318.

216. Somers KP, Simmie JM, Gillespie F, et al. A high temperature and atmospheric pressure experimental and detailed chemical kinetic modelling study of 2-methylfuran oxidation. *Proc Combust Inst*. 2013;34:225–232.
217. Liu D, Togbé C, Tran L-S, et al. Combustion chemistry and flame structure of furan group biofuels using molecular-beam mass spectrometry and gas chromatography – part I: furan. *Combust Flame*. 2014;161:748–765.
218. Tran L-S, Togbé C, Liu D, et al. Combustion chemistry and flame structure of furan group biofuels using molecular-beam mass spectrometry and gas chromatography – part II: 2-methylfuran. *Combust Flame*. 2014;161:766–779.
219. Togbé C, Tran L-S, Liu D, et al. Combustion chemistry and flame structure of furan group biofuels using molecular-beam mass spectrometry and gas chromatography – part III: 2,5-dimethylfuran. *Combust Flame*. 2014;161:780–797.
220. Klute CH, Walters W. The thermal decomposition of tetrahydrofuran. *J Am Chem Soc*. 1946;68:506–511.
221. Lifshitz A, Bidani M, Bidani S. Thermal reactions of cyclic ethers at high temperatures. 2. Pyrolysis of tetrahydrofuran behind reflected shocks. *J Phys Chem*. 1986;90:3422–3429.
222. Verdicchio M, Sirjean B, Tran LS, Glaude P-A, Battin-Leclerc F. Unimolecular decomposition of tetrahydrofuran: carbene vs. diradical pathways. *Proc Combust Inst*. 2015;35:533–541.
223. Simmie JM. Kinetics and thermochemistry of 2,5-dimethyltetrahydrofuran and related oxolanes: next next-generation biofuels. *J Phys Chem A*. 2012;116:4528–4538.
224. Pedley JB, Naylor RD, Kirby SP. *Thermochemical Data of Organic Compounds*. 2nd ed. London: Chapman & Hall; 1986.
225. Moshammer K, Vranckx S, Chakravarty HK, Parab P, Fernandes RX, Kohse-Höinghaus K. An experimental and kinetic modeling study of 2-methyltetrahydrofuran flames. *Combust Flame*. 2013;160:2729–2743.
226. Chakravarty HK, Fernandes RX. Reaction kinetics of hydrogen abstraction reactions by hydroperoxyl radical from 2-methyltetrahydrofuran and 2,5-dimethyltetrahydrofuran. *J Phys Chem A*. 2013;117:5028–5041.
227. Labbe NJ, Seshadri V, Kasper T, Hansen N, Oßwald P, Westmoreland PR. Flame chemistry of tetrahydropyran as a model heteroatomic biofuel. *Proc Combust Inst*. 2013;34:259–267.
228. Li W, Law ME, Westmoreland PR, Kasper T, Hansen N, Kohse-Höinghaus K. Multiple benzene-formation paths in a fuel-rich cyclohexane flame. *Combust Flame*. 2011;158:2077–2089.
229. Hansson KM, Samuelsson J, Tullin C, Åmand LE. Formation of HNCO, HCN, and NH3 from the pyrolysis of bark and nitrogen-containing model compounds. *Combust Flame*. 2004;137:265–277.
230. Lucassen A, Labbe N, Westmoreland PR, Kohse-Höinghaus K. Combustion chemistry and fuel-nitrogen conversion in a laminar premixed flame of morpholine as a model biofuel. *Combust Flame*. 2011;158:1647–1666.
231. Altarawneh M, Dlugogorski BZ. A mechanistic and kinetic study on the decomposition of morpholine. *J Phys Chem A*. 2012;116:7703–7711.
232. Li S, Davidson DF, Hanson RK, et al. Shock tube measurements and model development for morpholine pyrolysis and oxidation at high pressures. *Combust Flame*. 2013;160(9):1559–1571.
233. Sanders EB, Goldsmith AI, Seeman JI. A model that distinguishes the pyrolysis of D-glucose, D-fructose, and sucrose from that of cellulose. Application to the understanding of cigarette smoke formation. *J Anal Appl Pyrol*. 2003;66:29–50.
234. Paine JB, Pithawalla YB, Naworal JD. Carbohydrate pyrolysis mechanisms from isotopic labeling. *J Anal Appl Pyrol*. 2008;82:42–69.

235. Assary RS, Curtiss LA. Comparison of sugar molecule decomposition through glucose and fructose: a high-level quantum chemical study. *Energy Fuels*. 2012;26:1344–1352.
236. Seshadri V, Westmoreland PR. Concerted reactions and mechanism of glucose pyrolysis and implications for cellulose kinetics. *J Phys Chem A*. 2012;116:11997–12013.
237. Mayes HB, Nolte MW, Beckham GT, Shanks BH, Broadbelt LJ. The alpha-bet(a) of glucose pyrolysis: computational and experimental investigations of 5-hydroxymethylfurfural and levoglucosan formation reveal implications for cellulose pyrolysis. *ACS Sustain Chem Eng*. 2014;2:1461–1473.
238. Alwe HD, Walawalkar M, Sharma A, Pushpa KK, Dhanya S, Naik PD. Rate coefficients for the gas-phase reactions of chlorine atoms with cyclic ethers at 298 K. *Int J Chem Kinet*. 2013;45(5):295–305.
239. Alwe HD, Walavalkar MP, Sharma A, Dhanya S, Naik PD. Tropospheric oxidation of cyclic unsaturated ethers in the day-time: comparison of the reactions with Cl, OH and $O_3$ based on the determination of their rate coefficients at 298 K. *Atmos Environ*. 2014;82:113–120.
240. Taskinen E, Alanko T, Liebman JF. Relative thermodynamic stabilities of the isomeric dihydrofurans and isomeric dihydropyrans. An experimental and DFT study. *Struct Chem*. 2006;17:323–326.
241. Taskinen E. Enthalpies of formation of olefinic ethers by G3(MP2)//B3LYP calculations. *J Phys Org Chem*. 2009;22:42–51.
242. Boot M, Frijters P, Luijten C, et al. Cyclic oxygenates: a new class of second-generation biofuels for diesel engines? *Energy Fuels*. 2009;23:1808–1817.
243. Werpy T, Peterson GW. *Top Value Added Chemicals from Biomass, Volume I — Results of Screening for Potential Candidates from Sugars and Synthesis Gas*. U.S. Department of Energy; 2004. Online. Internet. Available: http://www.nrel.gov/docs/fy04osti/35523.pdf. Accessed 05.06.15.
244. Vasiliu M, Jones AJ, Guynn K, Dixon DA. Prediction of the thermodynamic properties of key products and intermediates from biomass. *J Phys Chem C*. 2011;115:15686–15702.
245. Vasiliu M, Jones AJ, Guynn K, Dixon DA. Prediction of the thermodynamic properties of key products and intermediates from biomass. II. *J Phys Chem C*. 2012;116:20738–20754.
246. Lucius ME, Taylor CR, Hayes CJ. Exploring the thermochemistry of monocyclic and bicyclic oxygenated species via computational chemistry methods. In: *247th American Chemical Society National Meeting (Poster Session). Dallas, TX*. March 2014.
247. Wurmel J, Simmie JM. Thermochemistry and kinetics of angelica and cognate lactones. *J Phys Chem A*. 2014;118:4172–4183.
248. Klein MT, Virk PS. Model pathways in lignin thermolysis. 1. Phenethyl phenyl ether. *Ind Eng Chem Fundam*. 1983;22:35–45.
249. Gilbert KE, Gajewski JJ. Coal liquefaction model studies: free radical chain decomposition of diphenylpropane, dibenzyl ether, and phenyl ether via β-scission. *J Org Chem*. 1982;47:4899–4902.
250. Britt PF, Buchanan AC, Malcolm EA. Thermolysis of phenethyl phenyl ether: a model for ether linkages in lignin and low rank coal. *J Org Chem*. 2008;60:6523–6536.
251. Jarvis MW, Daily JW, Carstensen HH, et al. Direct detection of products from the pyrolysis of 2-phenethyl phenyl ether. *J Phys Chem A*. 2011;115:428–438.
252. Haung X, Liu C, Huang J, Li H. Theory studies on pyrolysis mechanism of phenethyl phenyl ether. *Comput Theor Chem*. 2011;976:51–59.
253. Nakamura T, Kawamoto H, Saka S. Pyrolysis behavior of Japanese cedar wood lignin studied with various model dimers. *J Anal Appl Pyrol*. 2008;81(2):173–182.

254. Kawamoto H, Ryoritani M, Saka S. Different pyrolytic cleavage mechanisms of β-ether bond depending on the side-chain structure of lignin dimers. *J Anal Appl Pyrol*. 2008;81:88–94.
255. Elder T, Beste A. Density functional theory study of the concerted pyrolysis mechanism for lignin models. *Energy Fuels*. 2014;28:5229–5235.
256. Beste A, Buchanan III AC, Britt PF, Hathorn BC, Harrison RJ. Kinetic analysis of the pyrolysis of phenethyl phenyl ether: computational predictions of α/β selectivities. *J Phys Chem A*. 2007;111:12118–12126.
257. Beste A, Buchanan III AC, Harrison RJ. Computational prediction of α/β selectivities in the pyrolysis of oxygen-substituted phenethyl phenyl ethers. *J Phys Chem A*. 2008; 112:4982–4988.
258. Beste A, Buchanan III AC. Computational study of bond dissociation enthalpies for lignin model compounds: substituent effects in phenethyl phenyl ethers. *J Org Chem*. 2009;74:f-2841.
259. Younker JM, Beste A, Buchanan III AC. Computational study of bond dissociation enthalpies for substituted β-O-4 lignin model compounds. *ChemPhysChem*. 2011; 12:3556–3565.
260. Beste A, Buchanan III AC. Computational investigation of the pyrolysis product selectivity for a-hydroxy phenethyl phenyl ether and phenethyl phenyl ether: analysis of substituent effects and reactant conformer selection. *J Phys Chem A*. 2013;117:3235–3242.
261. Beste A, Buchanan III AC. Substituent effects on the reaction rates of hydrogen abstraction in the pyrolysis of phenethyl phenyl ethers. *Energy Fuels*. 2010;24:2857–2867.
262. Beste A, Buchanan III AC. Kinetic analysis of the phenyl-shift reaction in β-O-4 lignin model compounds: a computational study. *J Org Chem*. 2011;76:2195–2203.
263. Asmadi M, Kawamoto H, Saka S. Thermal reactions of guaiacol and syringol as lignin model aromatic nuclei. *J Anal Appl Pyrol*. 2011;92:88–98.
264. Asmadi M, Kawamoto H, Saka S. Thermal reactivities of catechols/pyrogallols and cresols/xylenols as lignin pyrolysis intermediates. *J Anal Appl Pyrol*. 2011;92(1):76–87.
265. Elder T. Bond dissociation enthalpies of a dibenzodioxocin lignin model compound. *Energy Fuels*. 2013;27:4785–4790.
266. Elder T. Bond dissociation enthalpies of a pinoresinol lignin model compound. *Energy Fuels*. 2014;28:1175–1182.
267. Parthasarathi R, Romero RA, Redondo A, Gnanakaran S. Theoretical study of the remarkably diverse linkages in lignin. *J Phys Chem Lett*. 2011;2:2660–2666.
268. Kim S, Chmely SC, Nimlos MR, et al. Computational study of bond dissociation enthalpies for a large range of native and modified lignins. *J Phys Chem Lett*. 2011: 2846–2852.
269. Holmelid B, Kleinert M, Barth T. Reactivity and reaction pathways in thermochemical treatment of selected lignin-like model compounds under hydrogen rich conditions. *J Anal Appl Pyrol*. 2012;98:37–44.
270. Huang J, Li X, Wu D, Tong H, Li W. Theoretical studies on pyrolysis mechanism of guaiacol as lignin model compound. *J Renew Sustain Energy*. 2013;5:043112.
271. Gardrat C, Ruggiero R, Rayez M, Rayez J, Castellan A. Experimental and theoretical studies of the thermal degradation of a phenolic dibenzodioxocin lignin model. *Wood Sci Technol*. 2013;47:27–41.
272. Custodis VBF, Hemberger P, Van Bokhoven JA. Mechanism of fast pyrolysis of lignin: studying model compounds. *J Phys Chem B*. 2014;118:8524–8531.
273. Climent MJ, Corma A, Iborra S. Conversion of biomass platform molecules into fuel additives and liquid hydrocarbon fuels. *Green Chem*. 2014;16:516–547.
274. Delidovich I, Leonhard K, Palkovits R. Cellulose and hemicellulose valorisation: an integrated challenge of catalysis and reaction engineering. *Energy Environ Sci*. 2014; 7:2803–2830.

275. Henriksson G, Li J, Zhang L, Lindstrom ME. Lignin utilization. In: Crocker M, ed. *Thermochemical Conversion of Biomass to Liquid Fuels and Chemicals*. Cambridge, UK: RSC Publishing; 2010:222–262 [Chapter 9].
276. Cheng ZJ, Xing LL, Zeng MR, et al. Experimental and kinetic modeling study of 2,5-dimethylfuran pyrolysis at various pressures. *Combust Flame*. 2014;161:2496–2511.
277. Liu C, Assary RS, Curtiss LA. Investigation of thermochemistry associated with the carbon-carbon coupling reactions of furan and furfural using ab initio methods. *J Phys Chem A*. 2014;118:4392–4404.
278. Djokic M, Carstensen HH, Van Geem, Marin GB. The thermal decomposition of 2,5-dimethylfuran. *Proc Combust Inst*. 2013;34:251–258.
279. Beste A, Buchanan AC. Role of carbon-carbon phenyl migration in the pyrolysis mechanism of beta-O-4 lignin model compounds: phenethyl phenyl ether and alpha-hydroxy phenethyl phenyl ether. *J Phys Chem A*. 2012;116:12242–12248.
280. Chu S, Subrahmanyam A, Huber GW. The pyrolysis chemistry of a beta-O-4 type oligomeric lignin model compound. *Green Chem*. 2013;154:125–136.
281. Radakovits R, Jinkerson RE, Darzins A, Posewitz MC. Genetic engineering of algae for enhanced biofuel production. *Eukaryot Cell*. 2010;9:486–501.
282. Lue J, Sheahan C, Fu P. Metabolic engineering of algae for fourth generation biofuels production. *Energy Environ Sci*. 2011;4:2451–2466.
283. Georgianna DR, Mayfield SP. Exploiting diversity and synthetic biology for the production of algal biofuels. *Nature*. 2012;488:329–335.
284. Keasling JD, Chou H. Metabolic engineering delivers next-generation biofuels. *Nat Biotechnol*. 2008;36:298–299.
285. Ho DP, Ngo HH, Guo W. A mini review on renewable sources for biofuel. *Bioresour Technol*. 2014;169:742–749.
286. Issariyakul T, Dalai AK. Biodiesel from vegetable oils. *Renew Sustain Energy Rev*. 2014; 31:446–471.
287. Salvi BL, Panwar NL. Biodiesel resources and production technologies – a review. *Renew Sustain Energy Rev*. 2012;16:3680–3689.
288. Meher LC, Sagar DV, Naik SN. Technical aspects of biodiesel production by transesterification – a review. *Renew Sustain Energy Rev*. 2006;10:248–268.
289. Gressel J. Transgenics are imperative for biofuel crops. *Plant Sci*. 2008;1784:246–263.
290. Stephenson PPG, Moore CM, Terry MJ, Zubkov MV, Bibby TS. Improving photosynthesis for algal biofuels: toward a green revolution. *Trends Biotechnol*. 2011;29:615–623.
291. Greenwell HC, Laurens LML, Shields RJ, Lovitt RW, Flynn KJ. Placing microalgae on the biofuels priority list: a review of the technological challenges. *J R Soc Interface*. 2010;7:703–726.
292. Brennan L, Owende P. Biofuels from microalgae – a review of technologies for production, processing, and extractions of biofuels and co-products. *Renew Sustain Energy Rev*. 2010;14:557–577.
293. Williams PJL, Laurens LML. Microalgae as biodiesel & biomass feedstocks: review & analysis of the biochemistry, energetics & economics. *Energy Environ Sci*. 2010;3: 554–590.
294. Zhu XG, Long SP, Ort DR. What is the maximum efficiency with which photosynthesis can convert solar energy into biomass? *Curr Opin Biotechnol*. 2008;19:153–159.
295. Amaro HM, Macedo AC, Malcata FX. Microalgae: an alternative as sustainable source of biofuels? *Energy*. 2012;44:158–166.
296. Bhattacharjee M, Siemann E. Low algal diversity systems are a promising method for biodiesel production in wastewater fed open reactors. *Algae*. 2015;30:67–79.
297. Chen G, Zhao L, Qi Y. Enhancing the productivity of microalgae cultivated in wastewater toward biofuel production: a critical review. *Appl Energy*. 2015;137:282–291.

298. Maity JP, Hou C-P, Majumder D, et al. The production of biofuel and bioelectricity associated with wastewater treatment by green algae. *Energy*. 2014;78:94–103.
299. Pires JCM, Alvim-Ferraz MCM, Martins F, Simoes M. Wastewater treatment to enhance the economic viability of microalgae culture. *Environ Sci Pollut Res*. 2013; 20:5096–5105.
300. Logan BE, Rabaey K. Conversion of wastes into bioelectricity and chemicals by using microbial electrochemical technologies. *Science*. 2012;337:686–690.
301. Pittman JK, Dean AP, Osundeko O. The potential of sustainable algal biofuel production using wastewater resources. *Bioresour Technol*. 2011;102:17–25.
302. Schwenk D, Seppala J, Spoilling K, et al. Lipid content in 19 brackish and marine microalgae: influence of growth phase, salinity and temperature. *Aquat Ecol*. 2013;47:415–424.
303. Markou G, Angelidaki I, Georgakakis D. Microalgal carbohydrates: an overview of the factors influencing carbohydrates production, and of main bioconversion technologies for production of biofuels. *Appl Microbio Biotechnol*. 2012;96:631–645.
304. Cheah WY, Show PL, Chang J-S, Ling TC, Juan JC. Biosequestration of atmospheric $CO_2$ and flue gas-containing $CO_2$ by microalgae. *Bioresour Technol*. 2015;184:190–201.
305. Razzak SA, Hossain MM, Lucky RA, Bassi AS, de Lasa H. Integrated $CO_2$ capture, wastewater treatment and biofuel production by microalgae culturing – a review. *Renew Sustain Energy Rev*. 2013;27:622–654.
306. Pires JCM, Alvim-Ferraz MCM, Martins FG, Simoes M. Carbon dioxide capture from flue gases using microalgae: engineering aspects and biorefinery concept. *Renew Sustain Energy Rev*. 2012;16:3043–3053.
307. Wobbe L, Remacle C. Improving the sunlight-to-biomass conversion efficiency in microalgal biofactories. *J Biotechnol*. 2015;201:28–42.
308. Cazzaniga S, Dall'Osto L, Szaub J, et al. Domestication of the green alga *Chlorella sorokiniana*: reduction of antenna size improves light-use efficiency in a photobioreactor. *Biotechnol Biofuels*. 2014;7:157.
309. Carvalho AP, Silva SO, Baptista JM, Malcata FX. Light requirements in microalgal photobioreactors: an overview of biophotonic aspects. *Appl Microbiol Biotechnol*. 2011;89:1275–1288.
310. Beckmann J, Lehr F, Finazzi G, et al. Improvement of light to biomass conversion by de-regulation of light-harvesting protein translation in *Chlamydomonas reinhardtii*. *J Biotechnol*. 2009;142:70–77.
311. Rogers JN, Rosenberg JN, Guzman BJ, et al. A critical analysis of paddlewheel-driven raceway ponds for algal biofuel production at commercial scales. *Algal Res*. 2014;4:76–88.
312. Chiaramonti D, Prussi M, Casini D, et al. Review of energy balance in raceway ponds for microalgae cultivation: re-thinking a traditional system is possible. *Appl Energy*. 2013;102:101–111.
313. Chisti Y. Constraints to commercialization of algal fuels. *J Biotechnol*. 2013;167:201–214.
314. Droch M, Geng S, Wang G. Recent advances in liquid biofuel production from algal feedstocks. *Appl Energy*. 2013;102:1371–1381.
315. Bahadar A, Khan MB. Progress in energy from microalgae: a review. *Renew Sustain Energy Rev*. 2013;27:128–148.
316. Chisti Y, Yan JY. Energy from algae: current status and future trends algal biofuels – a status report. *Appl Energy*. 2011;88:3277–3279.
317. Quinn JC, Davis R. The potentials and challenges of algae based biofuels: a review of the techno-economic, life cycle, and resource assessment modeling. *Bioresour Technol*. 2015;184:444–452.
318. Venteris ER, Skgags RL, Coleman AM, Wigmosta MS. A GIS cost model to assess the availability of freshwater, seawater, and saline groundwater for algal biofuel production in the United States. *Environ Sci Technol*. 2013;47:4840–4849.

319. De Boer K, Moheimani NR, Borowitzka MA, Bahri PA. Extraction and conversion pathways for microalgae to biodiesel: a review focused on energy consumption. *J Appl Physcol*. 2012;24(6):1681–1698.
320. Murphy CF, Allen DT. Energy-water nexus for mass cultivation of algae. *Environ Sci Technol*. 2011;45:5861–5868.
321. Ho SH, Kondo A, Hasunuma T, Chang JS. Engineering strategies for improving the $CO_2$ fixation and carbohydrate productivity of *Scenedesmus obliquus* CNW-N used for bioethanol fermentation. *Bioresour Technol*. 2013;143:163–171.
322. Ellis JT, Hengge NN, Sims RC, Miller CD. Acetone, butanol, and ethanol production from wastewater algae. *Bioresour Technol*. 2012;111:491–495.
323. Sambusiti C, Bellucci M, Zabaniotou A, Beneducew L, Monlau F. Algae as promising feedstocks for fermentative biohydrogen production according to a biorefinery approach: a comprehensive review. *Renew Sustain Energy Rev*. 2015;44:20–36.
324. Dasgupta CN, Gilbert JJ, Lindblad P, et al. Recent trends on the development of photobiological processes and photobioreactors for the improvement of hydrogen production. *Int J Hydrogen Energy*. 2010;35:10218–10238.
325. Melis A. Photosynthesis-to-fuels: from sunlight to hydrogen, isoprene, and botryococcene production. *Energy Environ Sci*. 2012;5:5531–5539.
326. Razeghifard R. Algal biofuels. *Photosynth Res*. 2013;117:207–209.
327. Lestari S, Maki-Arvela P, Beltramini J, Max Lu GQ, Murzin DY. Transforming triglycerides and fatty acids into biofuels. *ChemSusChem*. 2009;2:1109–1119.
328. a. Curran MA. *A Review of Life-Cycle Based Tools used to Assess the Environmental Sustainability of Biofuels in the United States*. Washington, DC: U.S. Environmental Protection Agency; 2013. EPA/600/R/12/709;
b. *RSB principles & Criteria for Sustainable Biofuel Production. RSB-STD-01–001 (Vers. 2.1)*. Geneva, Switzerland: Roundtable on Sustainable Biomaterials; November 2011.
329. Brienen RJW, Phillips OL, Feldpausch TR, et al. Long term decline of the Amazon carbon sink. *Nature*. 2015;519:344–348.
330. Carlson KM, Curran LM, Asner GP, Pittman AM, Trigg SN, Adeney JM. Carbon emissions from forest conversion by Kalimantan oil palm plantations. *Nat Clim Change*. 2013;3:283–287.
331. Baccini A, Goetz SJ, Walker WS, et al. Estimated carbon dioxide emissions from tropical deforestation improved by carbon-density maps. *Nat Clim Change*. 2012;2:182–185.
332. Koh LP, Wilcove DS. Is oil palm agriculture really destroying tropical biodiversity? *Conserv Lett*. 2008;1:60–64.
333. Leung DYC, Koo BCP, Guo Y. Degradation of biodiesel under different storage conditions. *Bioresour Technol*. 2006;97:250–256.
334. Yilmaz N, Vigil FM, Benalil K, Davis SM, Calva A. Effect of biodiesel-butanol fuel blends on emissions and performance characteristics of a diesel engine. *Fuel*. 2014;135:46–50.
335. Jin C, Yao MF, Liu HF, Lee CFF, Ji J. Progress in the production and application of n-butanol as a biofuel. *Renew Sustain Energy Rev*. 2011;15:4080–4106.
336. Knothe G. Some aspects of biodiesel oxidative stability. *Fuel Process Technol*. 2007;88:669–677.
337. Ghorbani A, Bazooyar B, Shariati A, Jokar SM, Ajami H, Naderi A. A comparative study of combustion performance and emission of biodiesel blends and diesel in an experimental boiler. *Appl Energy*. 2011;88:4725–4732.
338. Macor A, Pavanello P. Performance and emissions of biodiesel in a boiler for residential heating. *Energy*. 2009;34:2025–2032.
339. Gill SS, Tsolakis A, Dearn KD, Rodriquez-Fernandez J. Combustion characteristics and emissions of Fischer–Tropsch diesel fuels in IC engines. *Prog Energy Combust Sci*. 2011;37:503–523.

340. National Biodiesel Board. Materials Compatibility. http://biodiesel.org/docs/ffs-performace_usage/materials-compatibility.pdf Accessed 23.06.15.
341. Shahir VK, Jawahar CP, Suresh PR. Comparative study of diesel and biodiesel on CI engine with emphasis to emissions – a review. *Renew Sustain Energy Rev*. 2015;45:686–697.
342. Basha SA, Gopa KR, Jebaraj S. A review on biodiesel production, combustion, emissions and performance. *Renew Sustain Energy Rev*. 2009;13:1628–1634.
343. Hoekman SK, Robbins C. Review of the effects of biodiesel on $NO_x$ emissions. *Fuel Process Technol*. 2012;96:237–249.
344. Gaffney JS, Marley NA. The impacts of combustion emissions on air quality and climate – from coal to biofuels and beyond. *Atmos Environ*. 2009;43:23–36.
345. Faroon O, Roney N, Taylor J, Ashizawa A, Lumpkin MH, Plewak DJ. Acrolein environmental levels and potential for human exposure. *Toxicol Ind Health*. 2008;2:543–564.
346. deCastro BR. Acrolein and asthma attack prevalence in a representative sample of the United States adult population 2000–2009. *PLoS One*. 2014;9:e96926.
347. Peterson HG, Boutin C, Martin PA, Freemark KE, Ruecker NJ. Moody. Aquatic phyto-toxicity of 23 pesticides applied at expected environmental concentrations. *Aquat Toxicol*. 1994;28:275–292.
348. Bateman AP, Nizkorodov SA, Laskin J, Laskin A. Photolytic processing of secondary organic aerosols dissolved in cloud droplets. *Phys Chem Chem Phys*. 2011;13:12199–12212.
349. Ervens B, Turpin BJ, Weber RJ. Secondary organic aerosol formation in cloud droplets and aqueous particles (aqSOA): a review of laboratory, field and model studies. *Atmos Chem Phys*. 2011;11:11069–11102.
350. Fiore AM, Naik V, Spracklen DV, et al. Global air quality and climate. *Chem Soc Rev*. 2012;41:6663–6683.
351. (a) Cheskis S, Goldman A. Laser diagnostics of trace species in low-pressure flat flame. *Prog Energy Combust Sci*. 2009;35:365–382.
(b) Kohler M, Kathrotia T, Osswald P, Fischer-Tammer ML, Mosharnmer K, Riedel U. 1-, 2-and 3-Pentanol combustion in laminar hydrogen flames - a comparative experimental and modeling study. *Combust Flame*. 2015;162:3197–3209.
(c) Seidel L, Moshammer K, Wang XX, Zeuch T, Kohse-Hoinghaus K, Mauss F. Comprehensive kinetic modeling and experimental study of a fuel-rich, premixed n-heptane flame. *Combust Flame*. 2015;162:2045–2058.